Tropospheric ozone assessment report: Present-day tropospheric ozone distribution and trends relevant to vegetation

ELEMENTA
Science of the Anthropocene

Mills, G, et al. 2018. Tropospheric Ozone Assessment Report: Present-day tropospheric ozone distribution and trends relevant to vegetation. *Elem Sci Anth,* 6: 47. DOI: https://doi.org/10.1525/elementa.302

RESEARCH ARTICLE

Tropospheric Ozone Assessment Report: Present-day tropospheric ozone distribution and trends relevant to vegetation

Gina Mills[*,†], Håkan Pleijel[†], Christopher S. Malley[‡,§,‖], Baerbel Sinha[¶], Owen R. Cooper[**], Martin G. Schultz[††], Howard S. Neufeld[‡‡], David Simpson[§§,‖‖], Katrina Sharps[*], Zhaozhong Feng[¶¶], Giacomo Gerosa[***], Harry Harmens[*], Kazuhiko Kobayashi[†††], Pallavi Saxena[‡‡‡], Elena Paoletti[§§§], Vinayak Sinha[¶] and Xiaobin Xu[‖‖‖‖]

This Tropospheric Ozone Assessment Report (TOAR) on the current state of knowledge of ozone metrics of relevance to vegetation (*TOAR-Vegetation*) reports on present-day global distribution of ozone at over 3300 vegetated sites and the long-term trends at nearly 1200 sites. *TOAR-Vegetation* focusses on three metrics over vegetation-relevant time-periods across major world climatic zones: M12, the mean ozone during 08:00–19:59; AOT40, the accumulation of hourly mean ozone values over 40 ppb during daylight hours, and W126 with stronger weighting to higher hourly mean values, accumulated during 08:00–19:59.

Although the density of measurement stations is highly variable across regions, in general, the highest ozone values (mean, 2010–14) are in mid-latitudes of the northern hemisphere, including southern USA, the Mediterranean basin, northern India, north, north-west and east China, the Republic of Korea and Japan. The lowest metric values reported are in Australia, New Zealand, southern parts of South America and some northern parts of Europe, Canada and the USA. Regional-scale assessments showed, for example, significantly higher AOT40 and W126 values in East Asia (EAS) than Europe (EUR) in wheat growing areas ($p < 0.05$), but not in rice growing areas. In NAM, the dominant trend during 1995–2014 was a significant decrease in ozone, whilst in EUR it was no change and in EAS it was a significant increase.

TOAR-Vegetation provides recommendations to facilitate a more complete global assessment of ozone impacts on vegetation in the future, including: an increase in monitoring of ozone and collation of field evidence of the damaging effects on vegetation; an investigation of the effects on peri-urban agriculture and in mountain/upland areas; inclusion of additional pollutant, meteorological and inlet height data in the TOAR dataset; where not already in existence, establishing new region-specific thresholds for vegetation damage and an innovative integration of observations and modelling including stomatal uptake of the pollutant.

Keywords: Ozone; vegetation; metrics; crops; perennials; global

* NERC Centre for Ecology and Hydrology, Environment Centre Wales, Bangor, UK
† Biological and Environmental Sciences, University of Gothenburg, Gothenburg, SE
‡ Stockholm Environment Institute, Environment Department, University of York, York, UK
§ NERC Centre for Ecology and Hydrology, Penicuik, UK
‖ School of Chemistry, University of Edinburgh, Edinburgh, UK
¶ Indian Institute of Science Education and Research Mohali, Sector 81, S. A. S Nagar, Manauli PO, Punjab, 140306, IN
** Cooperative Institute for Research in Environmental Sciences, University of Colorado/NOAA Earth System Research Laboratory, Boulder, US
†† Forschungszentrum Jülich GmbH, Jülich, DE
‡‡ Department of Biology, Appalachian State University, Boone, NC, US
§§ EMEP MSC-W, Norwegian Meteorological Institute, Oslo, NO
‖‖ Department of Space, Earth and Environment, Chalmers University of Technology, Gothenburg, SE
¶¶ Research Center for Eco-Environmental Sciences, Chinese Academy of Sciences, Beijing, CN
*** Dipartimento di Matematica e Fisica, Università Cattolica del Sacro Cuore, Brescia, IT
††† Graduate School of Agricultural and Life Sciences, The University of Tokyo, Tokyo, JP
‡‡‡ School of Environmental Sciences, Jawaharlal Nehru University, New Delhi, IN
§§§ Institute for Sustainable Plant Protection, National Research Council, Florence, IT
‖‖‖‖ Key Laboratory for Atmospheric Chemistry, Institute of Atmospheric Composition, Chinese Academy of Meteorological Sciences, Beijing, CN
Corresponding author: Gina Mills (gmi@ceh.ac.uk)

1. Introduction

Tropospheric ozone is a greenhouse gas and pollutant detrimental to human health and crop and ecosystem productivity (CLRTAP, 2016; Mills and Harmens, 2011; Mills et al., 2013; Monks et al., 2015; REVIHAAP, 2013; US EPA, 2013). Since 1990, a large portion of the anthropogenic emissions that react in the atmosphere to produce ozone have shifted from North America and Europe to Asia (Cooper et al., 2014; Granier et al., 2011; Zhang et al., 2016). This rapid shift, coupled with limited ozone monitoring in developing nations, has left scientists unable to answer the most basic questions: Which regions of the world have the greatest human and plant exposure to ozone pollution? Is ozone continuing to decline in nations with strong emission controls? To what extent is ozone increasing in the developing world? How can the atmospheric sciences community facilitate access to ozone metrics necessary for quantifying ozone impacts on climate, human health and crop/ecosystem productivity?

To answer these questions, the International Global Atmospheric Chemistry Project (IGAC) developed the *Tropospheric Ozone Assessment Report (TOAR): Global metrics for climate change, human health and crop/ecosystem research* (www.igacproject.org/TOAR). Initiated in 2014, TOAR's mission is to provide the research community with an up-to-date scientific assessment of the global distribution and trends for tropospheric ozone, from the surface to the tropopause. TOAR's primary goals are: i) produce the first tropospheric ozone assessment report based on all available surface observations, the peer-reviewed literature and new analyses, and ii) generate easily accessible, ozone exposure metrics at thousands of measurement sites worldwide. Through the TOAR Surface Ozone Database (https://join.fz-juelich.de), these ozone metrics are freely accessible for research on the global-scale impact of ozone on climate, human health and crop/ecosystem productivity (Schultz et al., 2017, hereinafter referred to as *TOAR-Surface Ozone Database*). The assessment report is organized as a series of papers in a Special Feature of *Elementa: Science of the Anthropocene.* In this paper, *TOAR-Vegetation*, we provide an overview of the vegetation metrics available through the TOAR database, focussing on global and regional distributions and trends for three widely used metrics.

Ozone levels can be high in rural and semi-rural areas where ecosystems provide essential services such as agricultural production, forest production and water supply (Mills et al., 2013). Here, ozone impacts on ecosystems will include direct plant toxicity and cell damage, indirect effects mediated by changes in individual organisms and their ecological interactions, and changes in the rate and nature of chemical and biological processes (Ainsworth, 2016; Ainsworth et al., 2012; Ashmore, 2005). Ozone effects on vegetation are species- and cultivar-specific (Büker et al., 2015; Hayes et al., 2007; Mills et al., 2007a, b). Excessive ozone uptake can cause altered physiology (photosynthesis, respiration, carbon allocation, stomatal functioning and emissions of volatile organic compounds), reduced growth (both above– and below-ground), reduced seed production, altered phenology, increased senescence and/or altered sensitivity to other biotic and abiotic stresses (e.g. Ainsworth, 2016; Ainsworth et al., 2012; Hoshika et al., 2015). Prolonged ozone uptake by vegetation may lead to changes in gene expression and species composition, the functioning of ecosystems, water economy and carbon sequestration (Bassin et al., 2007; Harmens and Mills, 2012; McLaughlin et al., 2007; Sitch et al., 2007; Sun et al., 2012). Therefore, ozone pollution has the potential to affect the main services provided by terrestrial plant ecosystems, such as biodiversity conservation, production of food and forest-based products, carbon sequestration and water regulation.

Plants are vulnerable to ozone episodes where levels are high on several consecutive days as well as to long-term cumulative effects of absorbed ozone over one or several growing seasons (Ainsworth, 2016). Ozone exposure can result in visible leaf injury (leaf stipple, pale yellow or bronze lesions), which can alter the economic value of leafy vegetables (Fumagalli et al., 2001), whilst long-term exposure tends to be associated with growth or yield reductions and altered sensitivity to other abiotic and biotic stresses. Local controls on precursor emissions have partially reduced peak ozone levels in regions such as the USA and Europe in the last two decades (CLRTAP, 2016; Cooper et al., 2012; Derwent et al., 2010; Simon et al., 2015). However, trends in daytime average ozone values are more varied with general decreases across North America during the growing season, weaker decreases across Europe and increases across Asia (see Gaudel et al., 2017, hereinafter referred to as *TOAR-Climate* for more details, and Chang et al., 2017).

Developing scientifically justified strategies for protecting vegetation from ozone and maximizing the provision of plant ecosystem services under ozone-polluted environments requires a sound knowledge of how vegetation responds to ozone, how vegetation-relevant metrics are distributed in different ecosystems and how they vary over time. In this paper, we consider the risk posed to vegetation by ozone by assuming that the greater the ozone levels or exceedance of national or international standards, then the greater the likelihood of negative effects such as yield or growth reduction. We do not include here any quantification of the amount of damage. We acknowledge that ideally, risk assessments for vegetation should be based on the temporal changes in the amount of ozone absorbed through the stomatal pores on the leaf surface (stomatal uptake or flux), taking into account the detoxification capacity of the plant (Mills et al., 2011b; Musselman et al., 2006). Such a method has been developed and adopted by the United Nations Convention on Long-Range Transboundary Air Pollution (UN CLRTAP) and was included in the 2016 amendment of the European Union's National Emissions Ceiling Directive (NECD) (CLRTAP, 2017; EC, 2016). The stomatal flux of ozone is calculated at the leaf level at the top of the canopy using the DO_3SE (Deposition of Ozone for Stomatal Exchange) model which considers the varying effects of plant phenology, climate and soil moisture on stomatal aperture (Emberson et al., 2000; Mills et al., 2011a, b). The flux method is considered to be more biologically relevant

than concentration-based methods (CLRTAP, 2017; Mills et al., 2011a, b), and provides a better fit to field evidence of effects (Braun et al., 2014; Mills et al., 2011a). Currently, the TOAR database only contains ozone metrics based on ambient observations, and thus it is not possible to include global maps of the stomatal uptake of ozone in this paper. Instead, we present a first global analysis of the distribution of ozone metrics based on ambient observations to give an indication of the potential damaging effects of ozone. These results are presented for different global regions and climatic zones on the understanding that data coverage varies and in some of the driest areas, there may be substantial stomatal limitation of ozone uptake in C3 plants such as wheat, rice and many perennial species, as plants reduce stomatal apertures to lower water loss. In such areas, the effects on vegetation may not be as high as expected based solely on the magnitude of an ozone metric based on ambient observations.

An extensive range of ozone metrics relevant to effects on vegetation has been collated in the TOAR database (see **Table 1**), including those averaged or accumulated over a range of time-periods. In this paper, we focus on three vegetation metrics that are used in national and international standards for protecting vegetation and/or in global or regional impact modelling. The units for each metric are those cited in regulatory documents or those most commonly used by scientists in the field. As described below, the distribution and trends of each metric are considered for perennial vegetation (tree and grassland species and perennial crops) and two annual crops, wheat and rice. We use vegetation and climatic zone-specific time intervals for accumulation or averaging of each metric, reflecting the differing optimum growth periods around the world.

The first metric included here is AOT40, the only concentration-based metric applied at the international scale. Adopted by the 51 signatory countries of the UN CLRTAP (including EU countries, the USA and Canada), AOT40 (defined fully in Section 2.1) is the accumulation of hourly mean ozone values over 40 ppb (parts per billion (10^9), equivalent to nmol mol^{-1}) during daylight hours for vegetation-specific time intervals (units ppb h). AOT40 is also used by the EU Directive on Ambient Air Quality and Cleaner Air (EC, 2008), where it is calculated during the hours 08:00 to 20:00, presented in units of $\mu g\ m^{-3}\ h$ with a target and long-term objective defined (**Table 2**). In this paper, AOT40 results are based on the CLRTAP definition, being the most commonly applied in global studies. TOAR data are discussed in relation to exceedance of the CLRTAP's AOT40-based critical levels (CLs) for crops and perennial species (**Table 2**), ozone exposures "above which, direct adverse effects on sensitive vegetation may occur according to present knowledge" (CLRTAP, 2017). These CLs were first established by CLRTAP in 2007, and have been retained in the most recent revision of the Convention's Modelling and Mapping Manual.

We also include an assessment of the global distribution of W126, an ozone metric extensively used in the USA to assess vegetation impacts of ozone (see Lefohn et al., 1988, and Lefohn et al., 2018, hereinafter referred to as *TOAR-Metrics*). W126 is calculated at ozone monitor inlet height and includes a sigmoidal weighting function, with the highest weighting to hourly mean values $\geq$ 100 ppb, and is accumulated over 12h (08:00–19:59, local time) by the US Environmental Protection Agency (EPA) for vegetation-specific time intervals (units ppb-hrs). The US EPA reviewed the National Ambient Air Quality Standards (NAAQS) for ozone in 2015, and determined that a 3-month W126 index level of 17000 ppb-hrs is sufficient to protect the public welfare based on the latest science on effects of ozone on vegetation (**Table 2** and US Federal Register, 2015). Analyses of data from air quality monitors showed that attainment of an 8-hour standard of 70 ppb (0.07 ppm) would keep cumulative, maximum 3-month exposures below a W126 index level of 17000 ppb-hrs, averaged over three years. On reviewing the presented evidence, the US EPA established a secondary ozone standard at the 70 ppb level to protect human welfare by improving protection for trees, plants, and ecosystems. This is the same as the primary standard for protection of human health (see US Federal Register, 2015 and Fleming et al., 2017, hereinafter referred to as *TOAR-Health*).

AOT40 and W126 have three aspects in common: (i) They are vegetation type/species-specific, recognizing the varying sensitivity to ozone; (ii) Higher ozone levels have greater impact on vegetation; and (iii) The metrics are accumulated over specific time intervals and at specific times of the day to reflect the time-period when plants are most likely to absorb ozone. In contrast to

Table 1: TOAR-Vegetation metrics available in the TOAR Surface Ozone Database. Bold font indicates metrics selected for use in this paper. DOI: https://doi.org/10.1525/elementa.302.t1

- W126 (24-h), accumulated over 3, 6, 7 and 12 months;
- **W126 (12-h, 08:00–19:59), accumulated over 3, 6**, 7 and 12 months;
- AOT40 (08:00–19:59), accumulated over 3, 6, 7 and 12 months;
- **AOT40 (daylight hours, see Note 3), accumulated over 3,** 6, and 7 months;
- AOT40 (night-time over the period when clear sky radiation < 5 W/m^2) accumulated over 3, 6, and 7 months;
- **M12, the daily 12-h (08:00–19:59) average, averaged over 3, 6**, 7 or 12 months;
- Seasonal percentiles of hourly average ozone values (March–May, June–August, September–November, December–February) (median, 5^{th}, 25^{th}, 75^{th} and 95^{th}, 98^{th}, and 99^{th}).

Note 1: The timing of monthly periods are specified by climatic zone for each metric (see Section 2.3).

Note 2: Information on how to access the TOAR database is provided in the Data Accessibility Statement.

Note 3: Whilst CLRTAP (2017) defines daylight hours as the period when clear sky radiation > 50 W m^{-2}, TOAR uses a threshold of 5° solar elevation angle as a surrogate for defining daylight hours.

Table 2: Overview of vegetation-based critical levels and standards for ozone in Europe, the USA and Parties to the UN Convention on Long-Range Transboundary Air Pollution. Note: All units provided here are as used by the regulatory bodies. DOI: https://doi.org/10.1525/elementa.302.t2

Regulatory body, Reference	Vegetation type, Abbreviation used in this paper	Effect	Metric and accumulation period	Standard
LRTAP Convention CLRTAP, 2017	Agricultural crops CLRTAP_CL_Crops	Grain yield (5%; based on wheat)	AOT40, 3-months	Critical level of 3000 ppb h
	Horticultural crops CLRTAP_CL_Hortic	Fruit yield (5%; based on tomato)	AOT40, 3-months	Critical level of 8000 ppb h
	Forest trees CLRTAP_CL_Perennials	Total biomass (5%; based on beech and birch)	AOT40, 6-months	Critical level of 5000 ppb h
	(Semi-)natural vegetation dominated by annuals CLRTAP_CL_Annual_ Nat-Veg	Above ground biomass (10%)	AOT40, 3-months	Critical level of 3000 ppb h
	(Semi-)natural vegetation dominated by perennials CLRTAP_CL_Perennials	Above ground biomass (10%)	AOT40, 6-months	Critical level of 5000 ppb h
EU[a] EC (2008)	Protection of vegetation EU_Target	Vegetation effects	AOT40[b], 3-months (May to July)	Target value: 18000 μg m^{-3} h
	Protection of vegetation EU_LT_Objective	Vegetation effects	AOT40[b], 3-months (May to July)	Long-term objective 6000 μg m^{-3} h
US National Ambient Air Quality "values of concern" for vegetation US Federal Register, 2015	Support for Secondary (public welfare) standard to improve protection for trees, plants and ecosystems NAAQS_Ecosystems	Protection of trees, plants and ecosystems	W126, highest consecutive three months	17000 ppb-hrs
	Support for Secondary (public welfare) standard to improve protection for trees, plants and ecosystems NAAQS_Crops	To prevent median crop loss from exceeding 5%	W126, highest consecutive three months	15000 ppb-hrs
	Support for Secondary (public welfare) standard to improve protection for trees, plants and ecosystems NAAQS_Injury	To reduce foliar injury prevalence	W126, highest consecutive three months	10000 ppb-hrs
	Support for Secondary (public welfare) standard to improve protection for trees, plants and ecosystems NAAQS_Trees	To limit tree relative biomass loss to no greater than 2%	W126, highest consecutive three months	7000 ppb-hrs

[a]As defined in EC (2008). In December 2016, the EU Parliament approved a revision of the National Emissions Ceilings Directive (EC, 2016), which includes use of methodologies of the LRTAP Convention such as reporting on exceedances of flux-based critical levels.
[b]Accumulated over the hours between 08:00 and 20:00.

the cumulative indices AOT40 and W126, the third metric included in *TOAR-Vegetation* is M12, the mean ozone value for the hours 08:00–19:59 (local time), averaged over 3- or 6-months. M12 is not included in air quality standards but was selected for inclusion here for other reasons. Firstly, M12 has been used in global and regional model-based assessments of crop losses (e.g. Avnery et al., 2011; Hollaway et al., 2012; Van Dingenen et al., 2009).

Secondly, M12 is a potential indicator of changing ozone profiles during the hours when plants are most likely to take up ozone (for further information, see *TOAR-Metrics*). Lastly, inclusion of M12 allows for quantification of ozone at sites where levels are never or rarely high enough to be captured by AOT40 or W126, resulting in an M12 that is below 40 ppb, the cut-off value for AOT40, and the value below which accumulation of W126 is negligible.

Until now, global-scale ozone impact assessments for vegetation have been based on modelling of ambient ozone levels and have mainly been conducted for crop yield. For example, modelling studies have suggested that current ozone levels cause economic losses to the staple food crops wheat, soybean and maize in the range $10–20 billion (Avnery et al., 2011; Van Dingenen et al., 2009). Other modelling studies have quantified regional impacts of ozone on vegetation, including Europe (e.g. Mills and Harmens, 2011), SE Asia (e.g. Tang et al., 2013) and the USA (e.g. Fishman et al., 2010; Yue and Unger, 2014). To date, studies that report observed ozone values tend to be based on local sites (e.g. Malley et al., 2015), and are either country-specific (e.g. Karlsson et al., 2007b; Lal et al., 2017) or region-specific (e.g. Karlsson et al., 2017; Lefohn et al., 2017). TOAR's collation of ozone data provides the first opportunity to understand present-day distribution and trends relevant to vegetation on a global scale. By including data from over 3300 sites representing 12 geographical regions and 10 climatic zones, *TOAR-Vegetation* allows for the first time, identification of world regions likely to be susceptible to impacts of ozone on vegetation, based on measurements rather than modelling.

The main aims of this paper are to:

- Summarize the present-day global distribution of ozone using vegetation metrics of interest to researchers and policy makers, including identifying areas where current ambient ozone standards are exceeded and vegetation is likely to be at risk of damage;
- Inform the vegetation research and policy community of the regions of the world where ozone air quality is improving and where it is declining;
- Identify areas of the world where there is limited or no ozone data currently available for assessing risk to vegetation;
- Consider sources of uncertainty in the *TOAR-Vegetation* data and make recommendations for further development of the TOAR database.

2. Materials and methods

2.1. Definition of vegetation metrics

To facilitate comparison of published studies with the new analyses in *TOAR-Vegetation*, based on the ozone metrics in the TOAR Surface Ozone Database, we briefly describe the choice of ozone units reported in this paper. When referencing an observation in ambient air, TOAR follows World Meteorological Organization guidelines (Galbally et al., 2013) and uses the mole fraction of ozone in air, expressed in SI units of nmol mol^{-1}. Ozone metrics for vegetation (e.g. AOT40 and W126) have typically been developed using the mixing ratio unit of parts per million (ppm) or parts per billion (ppb) which, in the case of ozone, refers to the number of ozone molecules per million or billion moist, ambient air molecules in a fixed volume. In reference to units of nmol mol^{-1} and ppb, Galbally et al. (2013) state: "For all practical purposes the two quantities can be used interchangeably and without distinction". To maintain consistency with the human health and vegetation research community, TOAR uses units of ppb or ppm (or ppb h or ppb-hrs for cumulative indices) when discussing ozone in terms of an exposure metric. Although the usage of the word "concentration" without specifying atmospheric conditions when referring to mole fraction (nmol mol^{-1}) and mixing ratios (ppb) is technically incorrect, the vast amount of literature on ozone health and vegetation effects uses the conventional term "concentration" when referring to an ozone level. This common usage does not distinguish between mixing ratio metrics or true concentrations metrics such as g m^{-3}. To enhance the link to the health and vegetation effects literature and national and international policy, as well as to facilitate the understanding of this paper by vegetation effects scientists, the word "concentration" is used when appropriate.

Many vegetation metrics are included in the TOAR database (**Table 1**), covering a range of time-periods. Results presented in this paper are restricted to the following three metrics:

M12 is the 12-h mean at ozone monitor inlet height, averaged over the period 08:00–19:59h (local time) for 3-months (wheat, rice) or 6-months (perennial vegetation), unit: ppb.

AOT40 presented here uses the CLRTAP definition and is the sum of the difference between the hourly mean ozone value and 40 ppb for all daylight hours over a specified time-period (3-months for wheat and rice, 6-months for perennial vegetation), unit: ppb h. Furthermore, the ozone value should be representative of the top of the plant canopy, usually considered to be 1 m for crops and grassland, and 20 m for trees (CLRTAP, 2017). As TOAR does not include information on the height at which ozone is measured, AOT40 has been calculated in TOAR from the ozone observations at the height of the ozone monitor inlet and not from the canopy height.

W126 is the sigmoidally-weighted sum of all hourly ozone values observed during a specified daily and seasonal time window, where each hourly ozone value is given a weight that increases from zero to one with increasing values, units: ppb-hrs (*TOAR-Metrics*, US Federal Register, 2015). The strongest weight is given to values over 80 ppb. W126 is calculated using hourly mean ozone values at ozone monitor inlet height. In this paper, W126 is accumulated over the hours 08:00–19:59 (local time) for 3-months for wheat and rice, and 6-months for perennial vegetation. The algorithm for calculating W126 is provided in *TOAR-Metrics.*

Specification of the ozone monitor inlet height was not requested when populating the TOAR database with hourly ozone observations. As the ozone monitor inlet height at monitoring stations varies globally, this variation will provide some uncertainty in comparisons of M12, AOT40 and W126. Even within a country, measurement height can vary, for example in the USA, the proportions of monitoring sites with various measurement heights are: 60% at <5 m, 11% at 5–10 m, 12% at ≥10 m, and 16% with no specified height (Lefohn et al., pers. comm.). The implications for vegetation metrics of inconsistencies in measurement height are shown for sample data in the results section and considered in the discussion.

2.2. Choice of vegetation types

We have selected two crops to represent the major food producing areas of the world: wheat and rice. The selection of the highly ozone sensitive crop, wheat, is based upon (i) an assessment of data from exposure experiments conducted around the world (Mills et al., 2007a; Mills and Harmens, 2011) and (ii) evidence that current ambient ozone levels significantly affect the quantity and quality of wheat grain yield (Pleijel, 2011; Pleijel et al., 2018). Wheat is grown in many climatic zones of the world, including cool and warm temperate climates as well as boreal and tropical climates (Supplemental Material (SM), Figure S-1a), and thus its use provides good global coverage for TOAR metrics. The second crop selected is rice which is considered to be "moderately sensitive" to ozone (Mills et al., 2007a; Mills and Harmens, 2011). Although less sensitive to ozone than wheat, rice is an equally important staple food crop. Its inclusion in TOAR together with wheat, allows wide representation of the agricultural areas of the world and extends coverage to tropical climates (Figure S-1b). Together, wheat and rice are grown on nearly 400 million hectares globally (year 2016, FAOSTAT), and cover almost all of the non-urban sites that meet the TOAR Vegetation metric inclusion criteria. Other staple food crops such as soybean and maize were considered for inclusion. However, their distribution largely overlaps with that of wheat (particularly for soybean) and/or they are widely grown in areas of Africa or South America that are very sparsely covered by the TOAR dataset.

The third vegetation category is more general and consists of long-living or perennial vegetation, including grasslands, forested areas, wetlands and heaths, and long-lived crops. Such vegetation, described hereafter as "perennial", contains many ozone-sensitive species including, for example, broad-leaved tree species such as beech and birch, grassland clover species and meadow species of conservation value, as well as perennial crops such as citrus and grape (e.g. Büker et al., 2015; Hayes et al., 2007; Mills et al., 2007b). Given the degree of variation in ozone responses among and within perennial species (e.g. Büker et al., 2015; Fuhrer et al., 2016; Hayes et al., 2007), we have related metric values to biomass effects for sensitive species, as this is the basis for the CLRTAP concentration-based CLs and US NAAQS related to perennial vegetation (**Table 2**).

All analysis provided here is specifically focussed on vegetation such as wheat, rice, beech and birch with C3 photosynthetic pathways, as much less is known about the ozone response of C4 and CAM plants, and so far no national or international standards have been derived for these types of plants.

2.3. Timing of averaging and accumulation windows

The three vegetation ozone metrics are accumulated over 3-months (for wheat and rice) or 6-months (for perennial species) during daylight hours (AOT40) or 12 h (08:00–19:59, M12 and W126). These time-periods reflect the main growing seasons or sensitivity windows for the different types of vegetation. Metrics are accumulated or averaged during daylight or 12 h as these are the usual hours in most climate regions when the stomatal pores on the leaf surface are open and taking up ozone. For some vegetation types and climatic regions, there can be some stomatal conductance at night (e.g. Matyssek et al., 1995). Night-time values are also included in the TOAR database but are not considered in this analysis. For the climatic zones in the northern and southern hemispheres (NH and SH, respectively), the 3-month periods when wheat and rice are likely to be actively growing and most sensitive to ozone are identified per climatic zone whilst for perennial species, 6-month growth seasons are identified by hemisphere (**Table 3**).

Several approaches have been considered for the establishment of the 3-month time intervals for wheat and rice. Because of lack of availability of suitable input data on a global scale, timings based on crop growth models or accumulated photo-thermal time are beyond the scope of TOAR. For wheat and rice, the time interval should reflect the period when the crops are most sensitive to ozone, and should also include the anthesis and seed filling growth stages (e.g., Soja et al., 2000). Whilst the pragmatic latitude model used by the CLRTAP (2017) can be applied in Europe to determine accumulation periods for crops, it is not sufficiently robust or relevant for global application. Other sources of crop cycle data (e.g. Sacks et al., 2010) do not provide spatially available data and were patchy for some countries, while the online data source GAEZ (Global Agro-Ecological Zones) provided spatially available harvest dates, but are inconsistent in some regions.

TOAR has taken a climatic zone approach for 3-month metrics, using hemisphere-specific timings for non-polar climatic zones taken from a spatially available (grid size 5 by 5 arc minutes) dataset (EUSOILS, 2015), illustrated in **Figure 1**. This classification has been applied by IPCC (2006), and the gridded data allowed identification of the climatic zone for each TOAR monitoring site. Three-month intervals have been allocated to each climatic zone relevant for wheat and/or rice ending two weeks before the mean harvest date, with the time-period reflecting the most common growth cycle for that climate (e.g. for winter rather than spring wheat in W Europe). The harvest date per climatic zone has been established by overlaying maps produced by the USDA Major World Crop Areas and Climate Profiles (MWCACP) and cross-checking data with Sacks et al. (2010) and web-based national

Table 3: Timing of averaging or accumulation windows by vegetation type, climatic zone and northern hemisphere (NH) and southern hemisphere (SH). The global distribution of these climatic zones is presented in Figure 1, whilst the climatic zones in wheat and rice growing areas are presented in Figures S-1a and S-1b, respectively. DOI: https://doi.org/10.1525/elementa.302.t3

Aggregated climate zone	Climate zones represented	Hemisphere	3-month metrics, wheat	3-month metrics, rice	6-month metrics, perennial vegetation
Boreal, moist/dry	Boreal, moist and Boreal, dry	NH	Jun to Aug	n.a.	Apr to Sep
Cool Temperate	Cool temperate moist and cool temperate, dry	NH	Apr to Jun	May to July	Apr to Sep
Warm temperate	Warm temperate moist and warm temperate, dry	NH	Mar to May	Jun to Aug	Apr to Sep
Tropical, wet/moist/ montane	Tropical, montane; Tropical, wet and Tropical, moist	NH	Jan to Mar	July to Sep	Apr to Sep
Tropical, dry	Tropical, dry	NH	Jan to Mar	Aug to Oct	Apr to Sep
Cool, Temperate, 0–30 degrees south	Cool temperate moist and cool temperate, dry	SH	Feb to Apr	Dec to Feb	Oct to Mar
Cool, Temperate, >30 degrees south	Cool temperate moist and cool temperate, dry	SH	Nov to Jan	Dec to Feb	Oct to Mar
Warm Temperate, dry	Warm temperate dry	SH	Aug to Oct	Jan to March	Oct to Mar
Warm Temperate, moist	Warm temperate moist	SH	Mid-Aug to mid-Nov	Nov to Jan	Oct to Mar
Tropical, wet/moist/ montane	Tropical, montane; Tropical, wet and Tropical, moist	SH	July to Sep	Dec to Feb	Oct to Mar
Tropical, dry	Tropical, dry	SH	Aug to Oct	n.a.	Oct to Mar

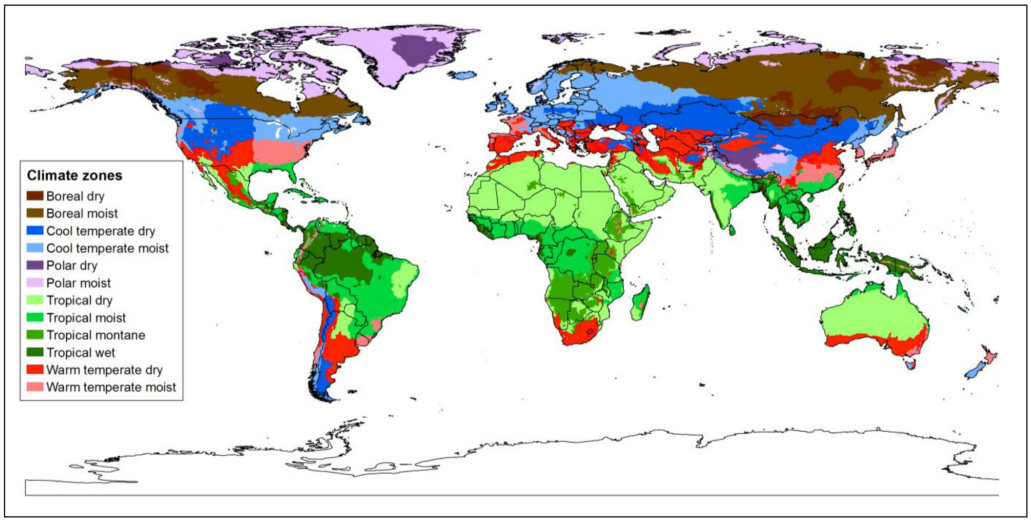

Figure 1: The global distribution of the climatic zones described in Table 3. Reproduced using data from http://eusoils.jrc.ec.europa.eu/projects/RenewableEnergy/. DOI: https://doi.org/10.1525/elementa.302.f1

sources for representative countries per climatic zone. Some climatic zones have been merged for simplification and sub-divisions were added for cool temperate climates 0–30° south and >30° south to account for variations in growth cycles for climates that span such a large geographical area. **Table 3** provides a summary of the specific climatic zones and the time windows defined within each zone, while the global distribution of the climatic zones in wheat and rice growing areas is illustrated in Figure S-1.

The timing interval for perennial vegetation metrics has been fixed at 6-months. Data for 7-months are also available from TOAR for use where earlier starting growth cycles are required. Climatic-zone specific timings were sought for perennial vegetation, but proved difficult to apply given that in some climatic zones, trees may be actively

growing and taking up ozone for the entire year, while in others such as Mediterranean areas, ozone uptake is substantially reduced during the summer (e.g. Anav et al., 2017). The TOAR community has agreed to use hemisphere-specific rather than climatic-zone specific periods for this vegetation type ensuring that metrics are accumulated or averaged over a fixed month range in all areas. The 6-month growth seasons selected are April–September for the NH, and October-March for the SH, with these time intervals described as "summer" in the TOAR database. Although the "summer" period represents a compromise, it is expected that these 6-month time intervals would capture the main growing period for long-living vegetation and trees in most areas of the world.

2.4. CLRTAP critical levels and US standards for vegetation

Of the many vegetation metrics available within the TOAR database (**Table 1**), the three metrics (M12, AOT40, W126), vegetation types (wheat, rice, perennials) and two time intervals (3- or 6-months) analysed here are specifically chosen for their policy relevance.

2.4.1. AOT40-based critical levels

For AOT40, the TOAR data are described in relation to CLs established by CLRTAP (CLRTAP, 2017) and published in the peer-reviewed literature (Grünhage et al., 2012; Karlsson et al., 2007a; Mills et al., 2007a). The AOT40-based CLs discussed here are for wheat (3000 ppb h accumulated over 3-months, hereinafter assigned as CLRTAP_CL_Crops), sensitive tree species represented by beech and birch and (semi-)natural vegetation dominated by perennials (5000 ppb h, 6-months, hereinafter assigned as CLRTAP_CL_Perennials) (**Table 1**). Although a CL has not been adopted by CLRTAP for rice, results presented here are discussed in relation to the AOT40 required for a 5% reduction in rice yield (12800 ppb h, 3-months, Mills et al., 2007a, hereinafter assigned as CL_Rice).

2.4.2. W126-based vegetation values of concern

As discussed above, the 2015 revision of the US EPA NAAQS for ozone concluded that the secondary standard based on an 8h mean ozone level of 70 ppb would protect human welfare by protecting against impacts on vegetation (US Federal Register, 2015). Since this is the same as the primary health standard, presented in detail in *TOAR–Health*, we discuss here the potential for ozone effects on vegetation by referring to W126-based protective levels for vegetation, so-called "values of concern". These provided the underpinning scientific support for the decision to use the 8-h mean-based secondary standard and range from 7000 to 17000 ppb-hrs, applicable for the effects listed in **Table 2**, and hereinafter assigned as NAAQS_Ecosystems, NAAQS_Crops, NAAQS_Injury and NAAQS_Trees. Whilst the US EPA recommends that W126 is calculated for the highest three consecutive months, in this study, W126 metrics are calculated for the same vegetation-specific 3- or 6-month periods used for AOT40 and M12, for consistency across all three metrics.

2.5. Site selection

Full information on the TOAR dataset, including data selection and quality assurance is provided elsewhere in this special feature (*TOAR-Surface Ozone Database*). All data indicating the current or "present-day" values for ozone metrics are a mean of the values per site for 2010–2014, with a minimum inclusion criteria of at least 3 years of data (3 "growing seasons") with data capture > 75%. Trend analysis covers the periods 1995–2014 and 2000–2014, with any site required to have at least 16 or 11 years of data, respectively, and not more than 2 years missing at either end of the interval.

For inclusion in *TOAR-Vegetation*, vegetation-specific site selection has been conducted as follows:

> Perennial species (6-month metrics): Includes all non-polar sites that do not meet the criteria for the TOAR category "urban", including rural-low elevation, rural-high elevation and unclassified sites (see site criteria in *TOAR-Surface Ozone Database*).
>
> Wheat and rice (3-month metrics): Sites where wheat or rice are grown have been identified by first extracting production data in tonnes (t) for irrigated and non-irrigated crops for the year 2000 from the GAEZ data portal v.3. on a 5 × 5 arc minute grid, and then selecting those sites with rice or wheat production >0.099 thousand t year^{-1} (per grid cell). Whilst acknowledging that there will be some inaccuracies introduced by the data being from the year 2000, this is to our knowledge the most recent year for which a sufficiently detailed and suitable spatial dataset on crop distribution is available at the global scale. In some areas of the world, sites classified as urban have a mixture of urban and agricultural areas and meet the inclusion criteria for rice or wheat based on the amount of production.

The regional representation of sites is defined according to the Task Force on Hemispheric Transport of Air Pollutant (HTAP) regions (Dentener and Guizzardi, 2013). The HTAP region abbreviations (**Table 4**) are used throughout this paper.

2.6. Statistical analysis of regional differences in metrics

To investigate differences between the three regions with the most data (EAS, EUR, NAM), general linear mixed models (with normal error) were run using the lme4 package (Bates et al. 2015) of the statistical software R (R Core Team 2018). As there were multiple sites per country per region, 'Country' was included as a random effect in the model. Model residual plots were examined and transformations were carried out where necessary, in order to meet assumptions on normality and heteroscedasticity. Likelihood Ratio Testing (using the 'drop1' command) was used to determine the best model and derive a p-value for the categorical variable 'Region.' Post hoc testing (using a Tukey test) was carried out with the 'multcomp' R package

Table 4: The present-day mean and standard deviation (SD) for M12, AOT40 and W126 for perennial vegetation for the summer 6-month period (2010–2014), presented by HTAP region as defined by Dentener and Guizzardi (2013). Note: The mean, SD and number of sites for each country are provided in Table S-1. DOI: https://doi.org/10.1525/elementa.302.t4

HTAP region	Description	Included in TOAR Vegetation for 6 month metrics	N	M12 (ppb)		AOT40 (ppb h)		W126 (ppb-hrs)	
				Mean	SD	Mean	SD	Mean	SD
NAM	North America (up to 66 N; polar circle)	Canada, USA	1165	41.3	7.0	14183	8518	13832	9755
EUR	W & E Europe plus Turkey	See note 1	1462	40.1	6.2	12758	7731	12295	8552
SAS	South Asia	India, Nepal	4	41.0	13.8	20412	15886	27335	24005
EAS	East Asia	China, Japan, Republic of Korea, Taiwan	612	39.5	4.7	16023	5688	18572	8153
SEA	South East Asia	Indonesia, Thailand	2	20.3	11.3	4379	6107	5767	8003
PAN	Pacific, Australia and New Zealand	Australia, New Zealand	36	24.7	3.3	1663	1221	1917	1312
NAF	North Africa	Algeria	1	41.2		6943		5613	
SAF	Sub Saharan/sub Sahel Africa	Cape Verde, Réunion, South Africa	14	28.4	10.4	5785	6486	6524	7485
MDE	Middle East	Israel	7	54.0	5.2	32644	10822	32937	16058
MCA	Mexico, Central America, Caribbean	Barbados, Bermuda, Guadeloupe, Martinique, Mexico	13	28.0	16.0	7439	10462	7375	10304
SAM	South America	Argentina, Brazil, Chile	6	22.6	12.8	2795	3969	2706	3713
RBU	Russia, Belarussia, Ukraine, central Asia	Armenia, Russia	2	48.8	7.0	22050	12985	17422	12512
Global			**3324**	**40.1**	**6.7**	**13718**	**7959**	**13872**	**9370**

Note 1: Austria, Belgium, Bulgaria, Croatia, Cyprus, Czech Republic, Denmark, Estonia, Finland, France, Germany, Gibraltar, Greece, Hungary, Ireland, Italy, Latvia, Lithuania, Luxembourg, Macedonia, Malta, Netherlands, Norway, Poland, Portugal, Romania, Serbia, Slovakia, Slovenia, Somalia, Spain, Sweden, Switzerland, United Kingdom.

(Hothorn et al., 2008). This analysis was repeated for each metric and vegetation type.

2.7. Trends analysis

Trends were assessed at sites across fixed time-periods of 1995–2014 and 2000–2014. These 20- and 15-year periods were chosen to maximise the number of sites while simultaneously being long enough to characterise long-term trends in the metrics, and to limit the influence of year-to-year variability on the magnitude, direction, and significance of the trends. At each site, the Mann-Kendall statistic has been calculated to determine the significance and direction of change for each metric included here, and the Theil-Sen slope (the median slope between all pairs of points across the time series) has been calculated to determine the magnitude of the trend (see *TOAR-Metrics* for further details).

Analysis of the derived trends in the three vegetation metrics focussed on determining i) the distribution of trends in each metric, ii) the regions where the largest changes in each metric has occurred, and iii) the extent to which the different vegetation metrics provide a consistent picture of change in vegetation-relevant ozone at the suite of sites analysed. The number of sites in different countries and regions with increasing, decreasing and no trend in each metric has been determined. The number of sites with each combination of trends in the three metrics has been calculated (i.e. all metrics significantly increasing, decreasing, or with no significant trend, or a combination of different trends across the metrics).

To ensure comparability between all TOAR papers, for the *TOAR-Vegetation* assessment, the following terminology is used when describing trend results:

- a trend result associated with a *p*-value of 0 to 0.05 is a statistically significant trend;
- a trend result associated with a *p*-value of 0.051 to 0.10 is referred to as indicative of a trend;
- a trend result associated with a *p*-value of 0.101 to 0.34 is described as having a weak indication of change;
- a trend result associated with a *p*-value of 0.341 to 1 is described as no change.

These bounds on *p*-values are based on analysis of the regional average daytime ozone trend across eastern North America by Chang et al. (2017) using a generalized additive mixed model (GAMM). They found that trends at individual sites with *p*-values up to 0.34 consistently

displayed cohesive regional relationships with the pattern of trends where $p < 0.05$. The final two categories listed above are shown for informational purposes only, and researchers are strongly cautioned against associating $p > 0.10$ with statistical significance. An explanation of these choices of *p*-value ranges and descriptive words is provided in *TOAR-Metrics*.

2.8. Quality assurance for the TOAR dataset

A detailed description of data capture processes and associated quality assurance is provided in *TOAR-Surface Ozone Database*.

3. Results

3.1. Data availability

Overall, 3324 global sites met the criteria for inclusion for perennial vegetation for present-day ozone (mean for 2010–2014) (**Table 4**), 2269 sites for wheat (**Table 5**) and 991 for rice (**Table 6**). For the perennial vegetation metrics, 38.5% have a full 5 years of data, 22.6% have 4 years of data and 38.9% have three years of data available for derivation of the mean. The corresponding values for wheat are 29.2% (5 years), 20.5% (4 years) and 50.2% (3 years), whilst data availability for rice is 32.6% (5 years), 34% (4 years) and 33.4% (3 years).

Data representation is greatest for NAM, EUR and EAS (see **Table 4** for region definitions), with sites from these regions making up 97% of the global dataset for the three vegetation metrics. The highest proportion of the metric data for perennial vegetation (43.9%) and wheat (62.5%) are for sites in EUR, with NAM having the next highest representation (35.0% and 23.4% for perennial vegetation and wheat, respectively) whilst rice metric data are most common in EAS (74.1%) reflecting the climatic requirements of this crop. As a consequence, some climatic regions are much better represented than others, with 92% of the data for 6-month metrics being from warm or cool temperate climates. Only 15 sites (0.5%) are in boreal climates, with 236 (7.1%) in tropical climates. Only sparsely distributed sites are available for SAS, SEA, PAN, NAF, SAF, MDE, MCA, SAM, and RBU, making up only 3% of the perennials present day metric (85 sites) and 2.1% of the perennials 1995–2014 trends data (13 sites). Although sites are fewer in number in these regions, they do provide data for many locations for which ozone monitoring data has not previously been publically available.

3.2. Present-day metrics for ozone

3.2.1. Perennial vegetation

By including all non-urban sites with sufficient data, this vegetation type provides the greatest coverage within the TOAR dataset, covering 12 HTAP regions and 60 countries (**Tables 4** and S-1).

3.2.1.1. M12 for Perennial vegetation

Globally, the mean M12 value for perennial vegetation sites is 40.1 ppb (+/– 6.7, N = 3324), which largely reflects the mean values for the three HTAP regions with the most sites: NAM (mean 41.3 +/– 7.0 ppb, N = 1165), EUR (40.1 +/– 6.2 ppb, N = 462) and EAS (39.5 +/– 4.7 ppb, N = 612) (**Table 4**). Despite the similarity in mean values, the highest proportion of sites in EUR and EAS is in the 35–40 ppb range (33.2% and 39.3%, respectively), whilst it is in the 40–45 ppb range for NAM (35.4% of sites, **Figure 2**). EAS also has a high proportion of sites in the 40–45 ppb range (38.1%) and a lower proportion of sites with M12 values < 35 ppb than NAM and EUR. Overall, there are no significant regional differences in the mean M12 values for NAM, EUR and EAS (Text S-1).

In the regions with only a few sites the M12 values are either: (i) higher than the global mean (SAF, 1 site, 57.3 ppb, RBU 2 sites at an altitude > 2000 m with a mean of 49.5 ppb); (ii) close to the global mean (SAS, MDE, MCA, means of 41.4, 41.2, 39.2 ppb for 4, 7 and 13 sites respectively); or (iii) substantially lower than the global mean for SH sites in SAM (11 sites, mean 22.1 ppb) and PAN (16

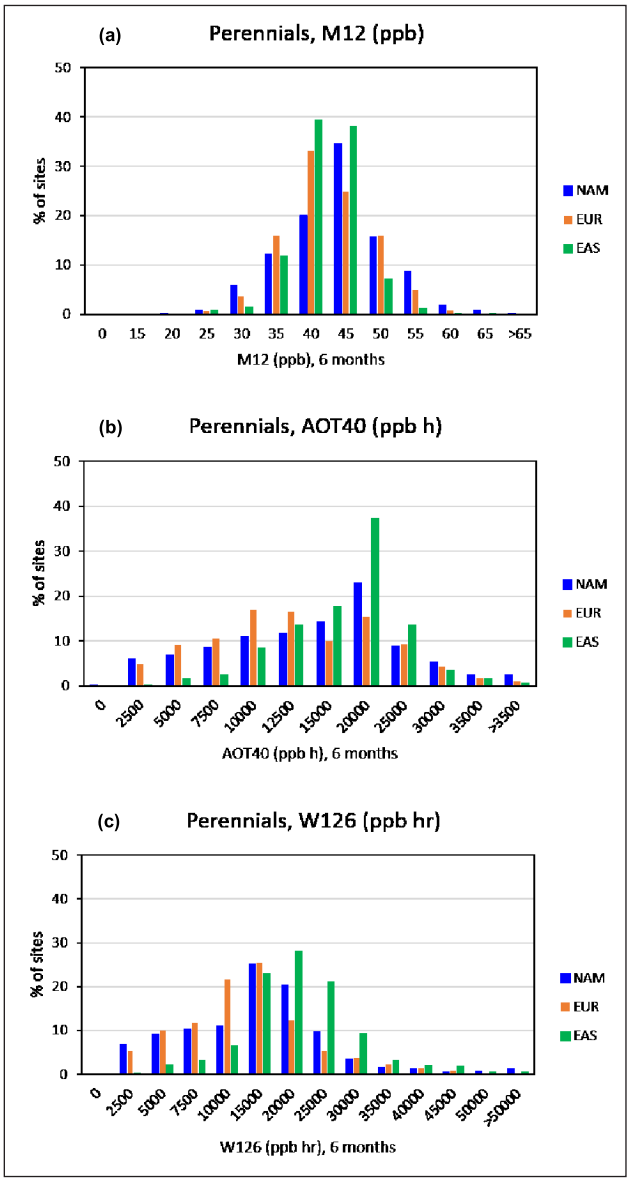

Figure 2: Frequency distributions for mean M12, AOT40 and W126 for the summer 6-month period, 2010–2014. Presented for sites in North America (NAM), Europe (EUR) and East Asia (EAS). DOI: https://doi.org/10.1525/elementa.302.f2

sites, mean 26.4 ppb). In general, the highest M12 values (≥45 ppb) are found in W USA, S EUR, and parts of SAS and EAS, with lower values in the SH (**Figure 3**). Thus, at present, the M12 values considered to be of concern for perennial vegetation (M12 > 36 ppb, Wittig et al., 2009) are concentrated in the northern mid-latitudes, and are not observed in the SH or in subarctic areas. M12 values considered to severely impact angiosperms (M12 > 51 ppb, Wittig et al., 2009) are primarily observed in S EUR, W NAM, the Middle East and East Asia (**Figure 3b**).

Where more than 50 sites were present in a country, the M12 values increase in the order: Canada (32.2 ppb, 146 for the mean and N value respectively) < Germany (36.8 ppb, 231), Japan (39.2 ppb, 476) < Republic of Korea (40.2 ppb, 122) < Austria (40.4 ppb, 96) < France (40.9 ppb, 238) < Spain (41.9 ppb, 255) < USA (42.5 ppb, 1023) <

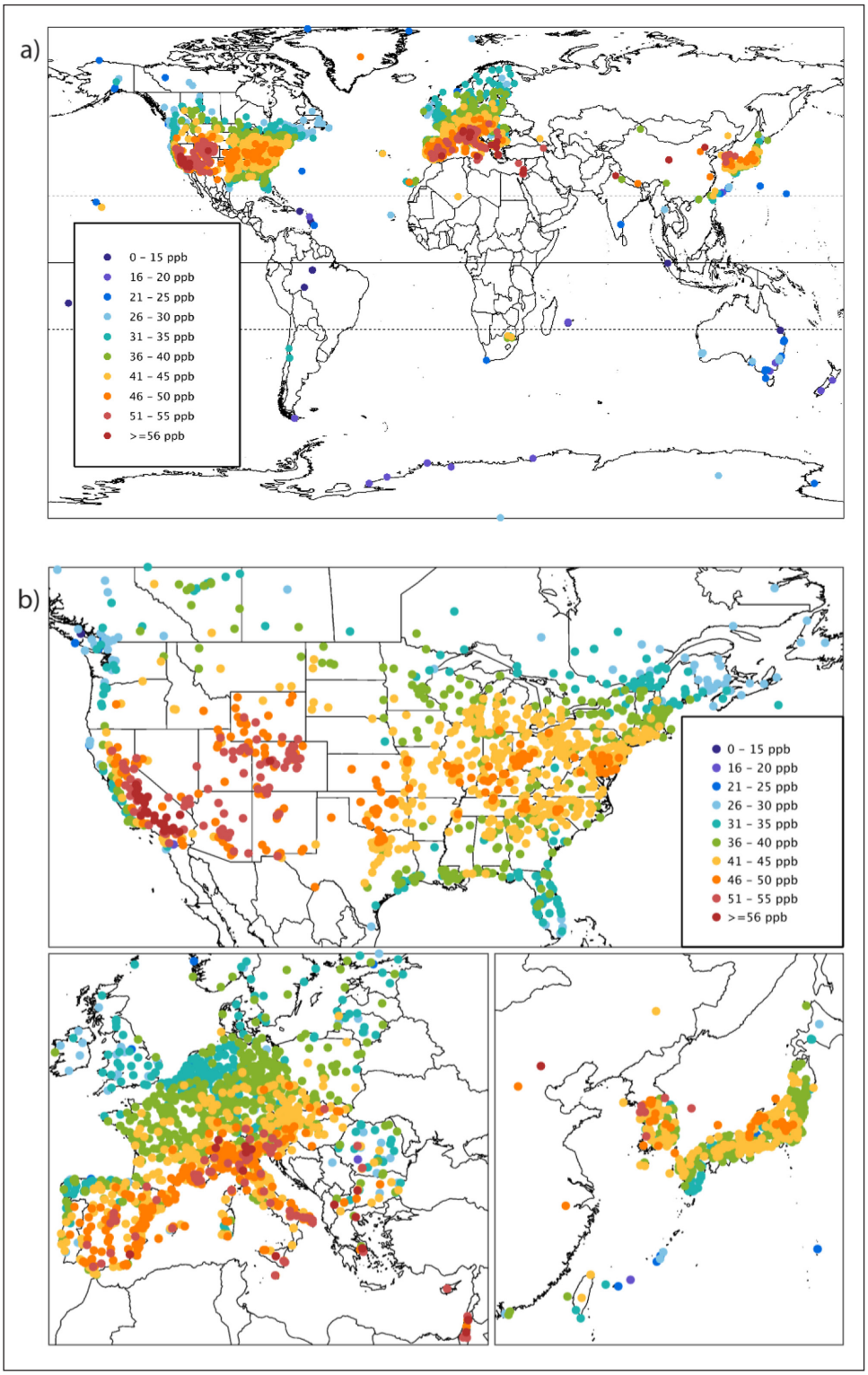

Figure 3: (a) Global and (b) regional distribution of the mean M12, 2010–2014, for perennial vegetation. Data are for 6-month periods, relevant for perennial-vegetation, for non-urban monitoring sites. DOI: https://doi.org/10.1525/elementa.302.f3

Italy (45.2 ppb, 228) (Table S-1). Separation of the data by region and climatic zones indicates that the highest M12 values are in warm temperate dry climates of NAM and EUR (46.9 ppb and 43.5 ppb for 143 and 437 sites, respectively) and tropical dry climates of NAM (47.8 ppb, N = 62). M12 levels are close to the global average in warm temperate moist climates of NAM, EUR and SEA, averaging 42.4, 40.2 and 39.6 ppb for 362, 275 and 572 sites respectively. The lowest M12 values are in cool temperate moist climates of NAM (37.4 ppb, N = 366), EUR (38.0 ppb, N = 605) and tropical moist climates of NAM (35.7 ppb, N = 366, Table S-2).

3.2.1.2. AOT40 for perennial vegetation

The global mean AOT40 across all sites is 13718 ppb h (**Table 4**), more than double the CLRTAP_CL_Perennials of 5000 ppb h, suggesting that globally this vegetation type is likely to be at risk of damage from ozone pollution. Indeed, AOT40 values exceeding the CLRTAP_CL_Perennials are found at 87.3% of sites globally, including most sites in northern mid-latitudes and several sites in southern mid-latitudes (**Figure 4**). In general, the lowest AOT40 values (<2500 ppb h) are reported primarily at coastal sites north of 60°N latitude, at some sites in the tropics and in some SH sites. In all regions, sites further

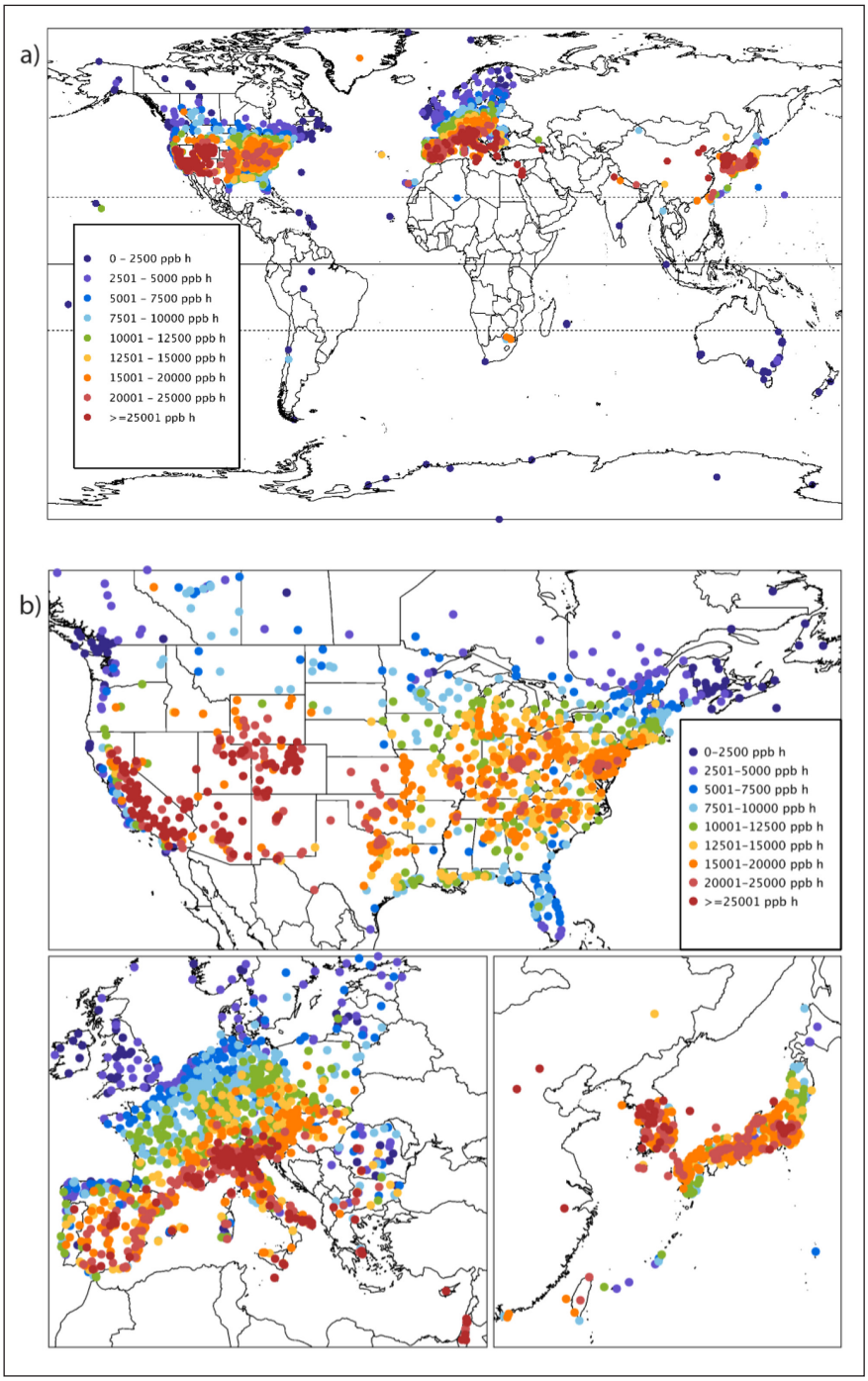

Figure 4: (a) Global and (b) regional distribution of the mean AOT40, 2010–2014, for perennial vegetation. Data are for 6-month periods, relevant for perennial-vegetation, for non-urban monitoring sites. DOI: https://doi.org/10.1525/elementa.302.f4

inland generally report higher AOT40 compared to sites in coastal areas and high altitude sites typically report higher AOT40 compared to low altitude sites within the same region (data not presented).

Of the three HTAP regions with the greatest data representation, AOT40 values are highest in EAS (mean 16023 +/− 5688 ppb h, N = 612) followed by NAM (14183 +/− 8518 ppb h, N = 1165) and EUR (12758 +/− 7731 ppb h, N = 1462, **Table 4**). However, the regional differences are not significant (p = 0.15, Text S-1). In EAS, 17.6% of sites report AOT40 values in the range 12500–15000 ppb h, with 37.3% of sites in the 15000–20000 ppb h category (**Figure 2**). In EUR and NAM, AOT40 values have a much broader frequency distribution. In regions with only a few monitoring sites, the highest regional mean AOT40 values are found in SAS (2 sites, mean 20412 ppb h) and MDE (12 sites, 32644 +/− 10822 ppb h), whilst means are lower in SH regions such as SAM, SEA and SAF, with means of 2795, 4379 and 5785 ppb h for 6, 2 and 7 sites, respectively.

As for M12, for regions/climatic zone combinations with > 50 sites, the highest AOT40 values are in warm temperate dry climates, with means of 21470 ppb h in NAM (N = 143) and 15888 ppb h in EUR (N = 437), and also in NAM tropical dry climates (23073 ppb h, N = 62, Table S-2). Partly reflecting the lower M12 levels in warm and cool temperate moist climates, which are close to or just above 40 ppb, the AOT40 values for these two climatic zones are substantially lower, averaging 15169 (N = 362) and 9529 ppb h (N = 366) respectively for NAM and 13567 (N = 275) and 10486 ppb h (N = 605) respectively for EUR. Warm temperate moist climates of SEA have a mean AOT40 of 16073 ppb h (N = 572). For countries with > 50 sites, the highest mean AOT40 values are in Italy (20043 ppb h, N = 228), Republic of Korea (18273 ppb h, N = 122), the USA (15580 ppb h, N = 1023) and Japan (15281 ppb h, N = 476), whilst the lowest are in Canada (4566 ppb h, N = 146) and Germany (9551 ppb h, N = 231, Table S-1).

3.2.1.3. W126 for perennial vegetation

W126 is similar in concept to AOT40, but provides stronger weighting to the highest ozone values (see *TOAR-Metrics*). As a consequence, the spatial distributions are similar for the two metrics even though the values in ppb h of AOT40 cannot be directly compared with the ppb-hrs of W126 (compare **Figures 4** and **5**, see Section 3.2.5). The higher weighting to the highest ozone levels in W126 results in a larger contrast between areas having higher and lower exposure for W126 than indicated for AOT40. In the three regions with greatest data representation, the mean values of W126 are highest for EAS (18572 +/− 8153 ppb-hrs, N = 612), followed by NAM (13832 +/−9755 ppb-hrs, N = 1165) and then EUR (12295 +/− 8552 ppb-hrs, N = 1462, **Table 4**). These regional differences are significant (p = 0.04, Text S-1), with means for EUR being significantly lower than for EAS (p = 0.04). These regions are ranked in the same order as for AOT40 but with a larger difference between EAS and EUR, even though the mean M12 values are relatively similar in all three regions (39.5–41.3 ppb). Frequency distributions reflect the regional differences in W126, with the highest proportion of occurrences for EAS in the 15000–20000 ppb-hrs class (28.1%) compared to 10000–15000 ppb-hrs for NAM (25.0%) and EUR (23.4% of sites, **Figure 2**). In other regions of the world less well represented in the dataset such as MDE and MCA, W126 is also relatively high (32937 +/− 16058 ppb-hrs, N = 7, and 7375 +/− 10304 ppb-hrs, N = 13 respectively, **Table 4**). The lowest mean W126 values are found in the SH in SEA and PAN (5767 and 1917 ppb-hrs for 2 and 36 sites for the two regions, respectively).

As response functions and standards have not been derived for perennial vegetation for W126 over a 6-month period, the implications for vegetation of the spatial distributions in W126 cannot currently be ascertained. Nevertheless, the global and regional maps presented in **Figure 5** do provide an indication of where perennial vegetation might be at greater risk. The potential implications for perennial vegetation based on the 3-month W126 values based on the maps for wheat are considered separately in Section 3.2.4.

3.2.2. Wheat

Wheat is primarily grown in temperate regions, with some growth in tropical and boreal climates. Overall, there are 2269 TOAR sites that meet the inclusion criteria for wheat, representing 10 HTAP regions and 44 countries (**Table 5** and S-3). *TOAR-Vegetation* includes many sites in major wheat producing countries such as the USA, France, Canada and Germany, but is under-represented in others such as China, India and Russia. Across the wheat sites, the global mean 3-month values are an M12 of 40.2 ppb, an AOT40 of 6066 ppb h and a W126 of 5719 ppb-hrs. The general spatial distribution of wheat metrics was similar to that described for perennial vegetation (Section 3.2), although less common growth of wheat crops in warm dry climates reduced representation of sites in some of the highest ozone areas such as in warm temperate dry climatic zones of the USA, Europe and China (**Figures 7–9**).

3.2.2.1. M12 for wheat

Where data are available, the global distribution of M12 in wheat growing areas (**Figure 7**) indicates that the highest ozone levels are found in EAS, particularly in Japan and parts of China. Values in excess of 50 ppb are also found in the Intermountain West region of the USA and in California, and occasionally in southern Europe. In EUR, M12 declines largely from SE to NW, and in NAM, M12 values are lower in the southernmost and northernmost parts than in the central wheat growing areas. The sparsely located monitoring sites in SAM and PAN regions show much lower M12 than all other regions.

For the three HTAP regions with highest data representation, the regional mean 3-month M12 values at wheat growing sites are higher in EAS than NAM and EUR (45.8 +/− 4.2 ppb, N = 275; 41.0 +/− 4.9 ppb, N = 532; and 39.0 +/− 5.4 ppb, N = 1418, respectively, **Table 5**). Differences between regions are significant (p = 0.048), with values in EUR significantly lower than in EAS (p = 0.04). Over 85% of the wheat M12 values in EAS are in the range 40–50 ppb, with nearly 10% greater than 50 ppb (**Figure 6**). The frequency distribution of

wheat M12 values was similar for NAM and EUR with the highest frequency of sites being in the range 40–45 ppb for NAM and 35–40 ppb for EUR. In contrast, 50% of the M12 values at EAS sites are in the range 45–50 ppb. The lowest regional mean values for M12 for wheat are found at the few monitoring sites in the SH, particularly in PAN (26.4 +/– 3.1 ppb, N = 16) and SAM (22.1 +/– 1.8 ppb, N = 11).

3.2.2.2. AOT40 for wheat

Due to the effect of the 40 ppb threshold in the AOT40 index (Sofiev and Tuovinen, 2001), the discrimination between areas with different ozone pollution levels is much stronger for this metric compared to M12. The global mean AOT40 at the wheat growing sites is 6066 ppb h (**Table 5**), more than double the CLRTAP_CL_Crops (3000 ppb h). The AOT40 for these sites ranges from 320

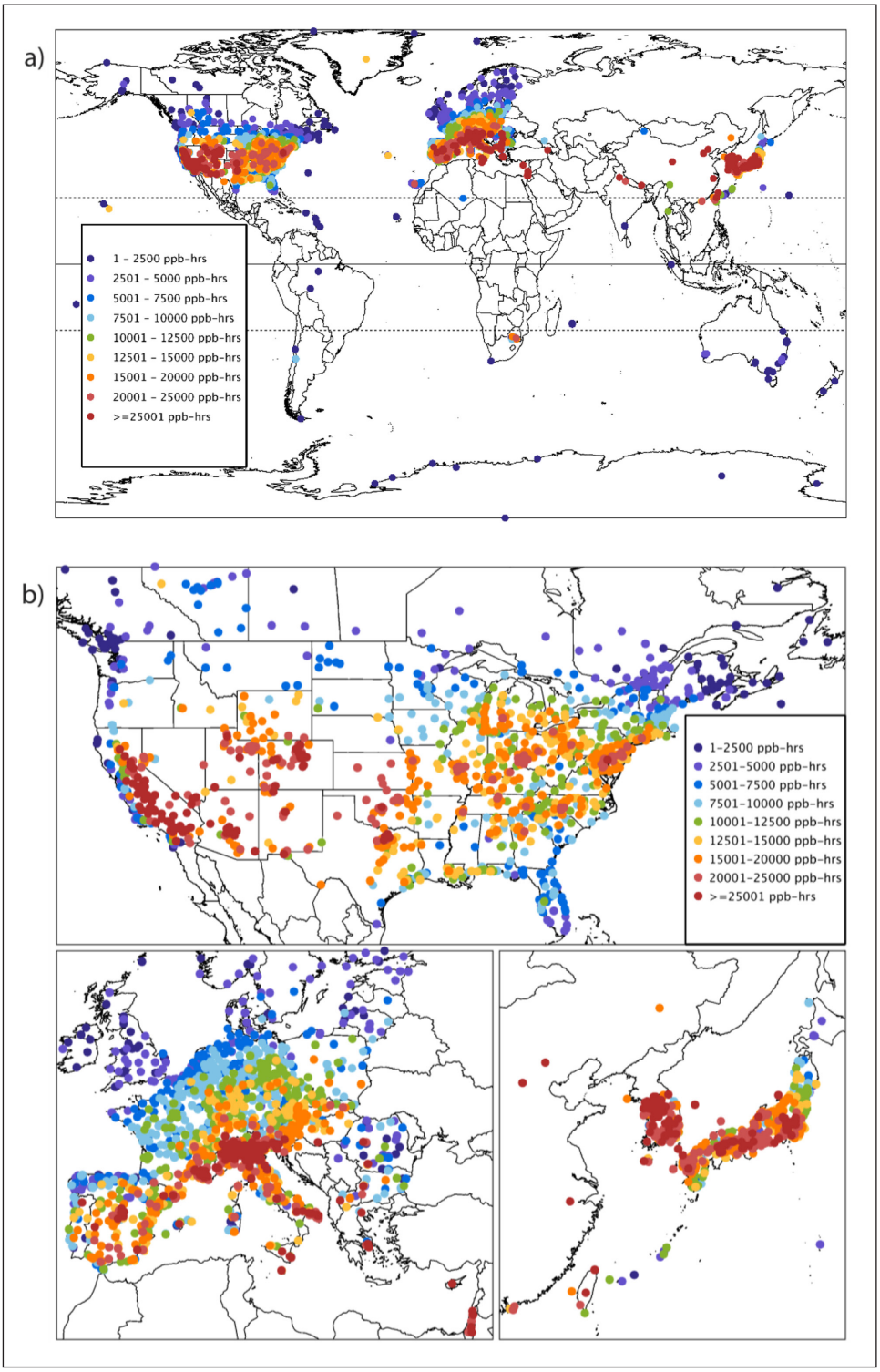

Figure 5: (a) Global and (b) regional distribution of the mean W126, 2010–2014, for perennial vegetation. Data are for 6-month periods, relevant for perennial-vegetation, for non-urban monitoring sites. DOI: https://doi.org/10.1525/elementa.302.f5

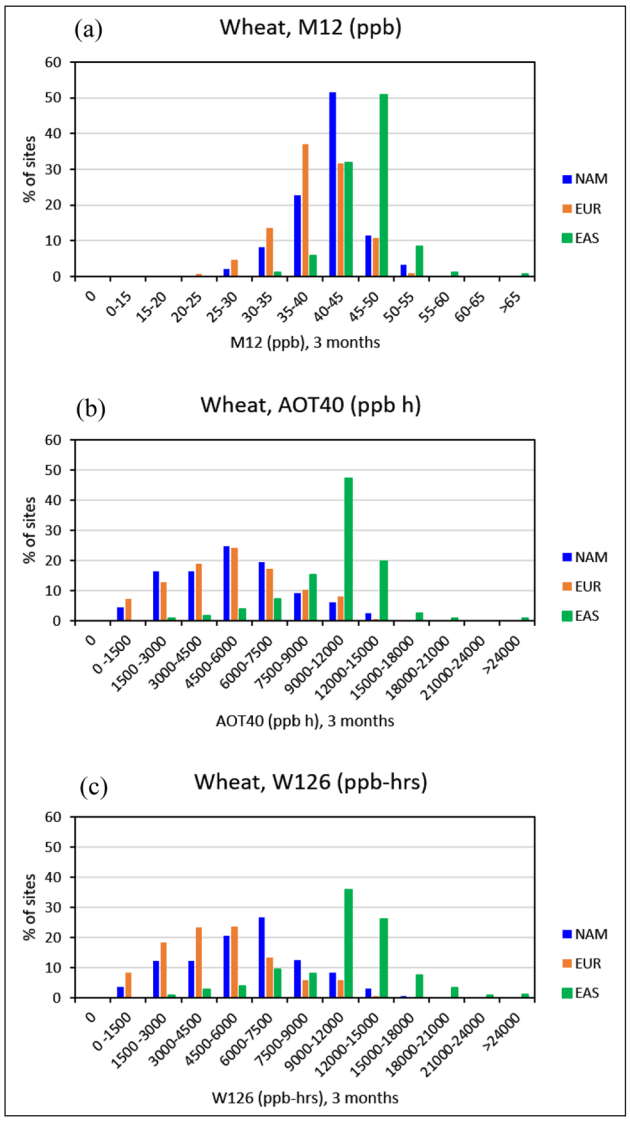

Figure 6: Frequency distributions for mean M12, AOT40 and W126 for the wheat 3-month period, 2010–2014. Presented for sites in North America (NAM), Europe (EUR) and East Asia (EAS). DOI: https://doi.org/10.1525/elementa.302.f6

ppb h in the PAN region (mean of 16 sites) to above 10000 ppb h in EAS (275 sites) and RBU (2 sites, **Table 5**). The mean AOT40 values are similar in NAM (6013 +/– 2821 ppb h, N = 532) and EUR (5324 +/– 2884 ppb h, N = 1418) and significantly lower than in EAS (10373 +/– 3142, N = 275), $p = 0.01$ for EUR v EAS and 0.04 for NAM vs EAS. The frequency distributions indicate that ca. 24% of values in both NAM and EUR are in the range 4500–6000 ppb h and 17–19% of values in the range 6000–7500 ppb h (**Figure 6**). In contrast, 47.2% of the sites in EAS have AOT40 values in the range 9000–12000 ppb h.

The CLRTAP_CL_Crops is exceeded over large parts of the wheat growing area (**Figure 8**). In EAS, southern EUR and certain parts of NAM, AOT40 levels are 3–4 times higher than the CL. The highest mean AOT40 values in countries with > 50 sites are in Japan (10334 +/– 2924 ppb h, N = 269) and are considerably higher than the next highest means of ca. 6400 ppb h in Czech Republic, USA and Italy for 52, 450 and 192 sites, respectively (Table S-3). The lowest mean AOT40 values for well-represented countries are found in Canada, Germany and France (means of 3777, 4671 and 5495 ppb h for 83, 230 and 297 sites, respectively, Table S-3). Nevertheless, these values are above the CLRTAP_CL_Crops, indicating that wheat is also potentially at risk of yield loss in these countries when conditions are conducive to ozone uptake.

Where > 50 sites are present per region and climatic zone combination, the highest AOT40 values in NAM are found in cool temperate dry climates (mean 7778 ppb h, N = 60), followed by warm temperate dry climates (mean 6917 ppb h, N = 81), with similar mean values in warm temperate moist and cool temperate moist sites of 6124 and 5924 ppb h for 180 and 156 sites, respectively (Table S-4). In EUR, the mean AOT40 values ranged from 4893 to 5709 ppb h for the same four climatic zones (N = 132–515), whilst in SEA, 92.7% of sites are in warm temperate moist climates where the mean AOT40 was much higher at 10526 ppb h (N = 255).

3.2.2.3. W126 for wheat

The global mean W126 in the wheat growing areas is 5719 ppb-hrs and is well below the NAAQS_Crops (15000 ppb-hrs, defined in **Table 2**). Indeed, globally, 15000 ppb-hrs is only exceeded in 2.1% of sites. The highest W126 values are found in EAS (mean 11355 +/– 4489 ppb-hrs, N = 275), where 15000 ppb-hrs is exceeded at 33 sites in Japan and 2 sites in China (Table S-3 and **Figure 9**). This value is also exceeded at 7 sites in EUR, 2 sites in NAM and at single sites in SAS, MDE and MCA. The higher weighting given to ozone above 40 ppb in W126, especially to ozone values above 80 ppb, means that W126 tends to be lower in regions where there have been reductions in peak ozone levels (see discussion and *TOAR-Metrics*). This weighting effect is reflected in the lower regional mean W126 values for NAM (5403 +/– 2772 ppb-hrs, N = 532) and EUR (4798 +/– 2886 ppb-hrs, N = 1418) compared to EAS (11355 +/– 4489 ppb-hrs, N = 275, **Table 5**). The regional differences are significant ($p = 0.02$), with differences between EUR and EAS, and NAM and EAS having p values of 0.01 and 0.048, respectively. The frequency distributions for W126 show a stronger shift towards higher value ranges for EAS compared to NAM and EUR than was evident for either the M12 or AOT40 metric (**Figure 6**). In less well represented regions such as SAS, MCA, RBU and MDE (2–7 sites each), mean W126 values are in the range 6306–10582 ppb-hrs, whilst mean values for wheat sites in SAM are 1090 ppb-hrs (N = 11) and PAN are 520 (N = 16) (**Table 5**).

3.2.3. Rice

Of the TOAR sites located in rice growing areas, 97% are in either EUR (21.4%), NAM (11.8%) or EAS (64.2%, comprising data almost exclusively from Japan and the Republic of Korea, **Tables 6** and S-5). Unfortunately, TOAR's data coverage for the world's largest rice producers, China (4 sites), India (1 site), Indonesia (1 site), Bangladesh (0 sites) and Vietnam (0 sites) is very sparse, which limits the conclusions that can be drawn about the global risks posed to this moderately ozone-sensitive crop.

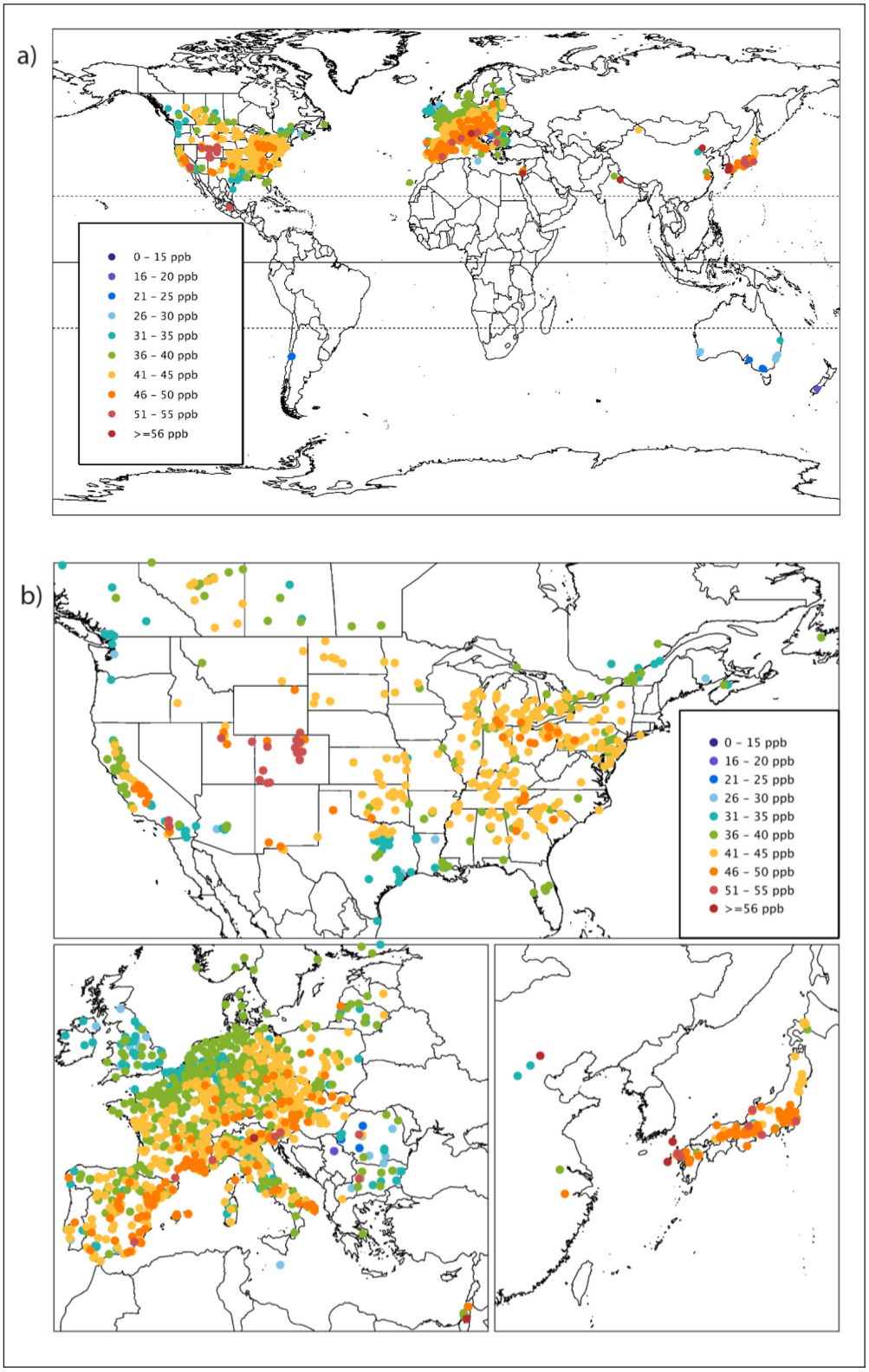

Figure 7: (a) Global and (b) regional distribution of the mean M12, 2010–2014, for wheat (3-months). DOI: https://doi.org/10.1525/elementa.302.f7

3.2.3.1. M12 for rice

In NAM, the M12 values at rice growing sites are in the range 21–35 ppb in Florida, 41–50 ppb in the eastern states and in excess of 51 ppb at several sites in California (**Figure 11**). Overall, the mean M12 value in the rice growing areas of NAM, EUR and EAS are not significantly different from each other. The mean for NAM is 39.3 +/– 9.4 ppb (N = 58), which is lower than that for EUR at 46.3 +/– 6.8 ppb (N = 178), where the highest M12 values are found around the Mediterranean basin, particularly in northern Italy and parts of SW Spain (**Figure 11**, Table S-5). The lowest mean M12 value is for EAS at 36.9 +/– 5.9 ppb (N = 734). The small number of sites providing data for SEA (N = 5), PAN (N = 3) and SAM (N = 9) indicated mean M12

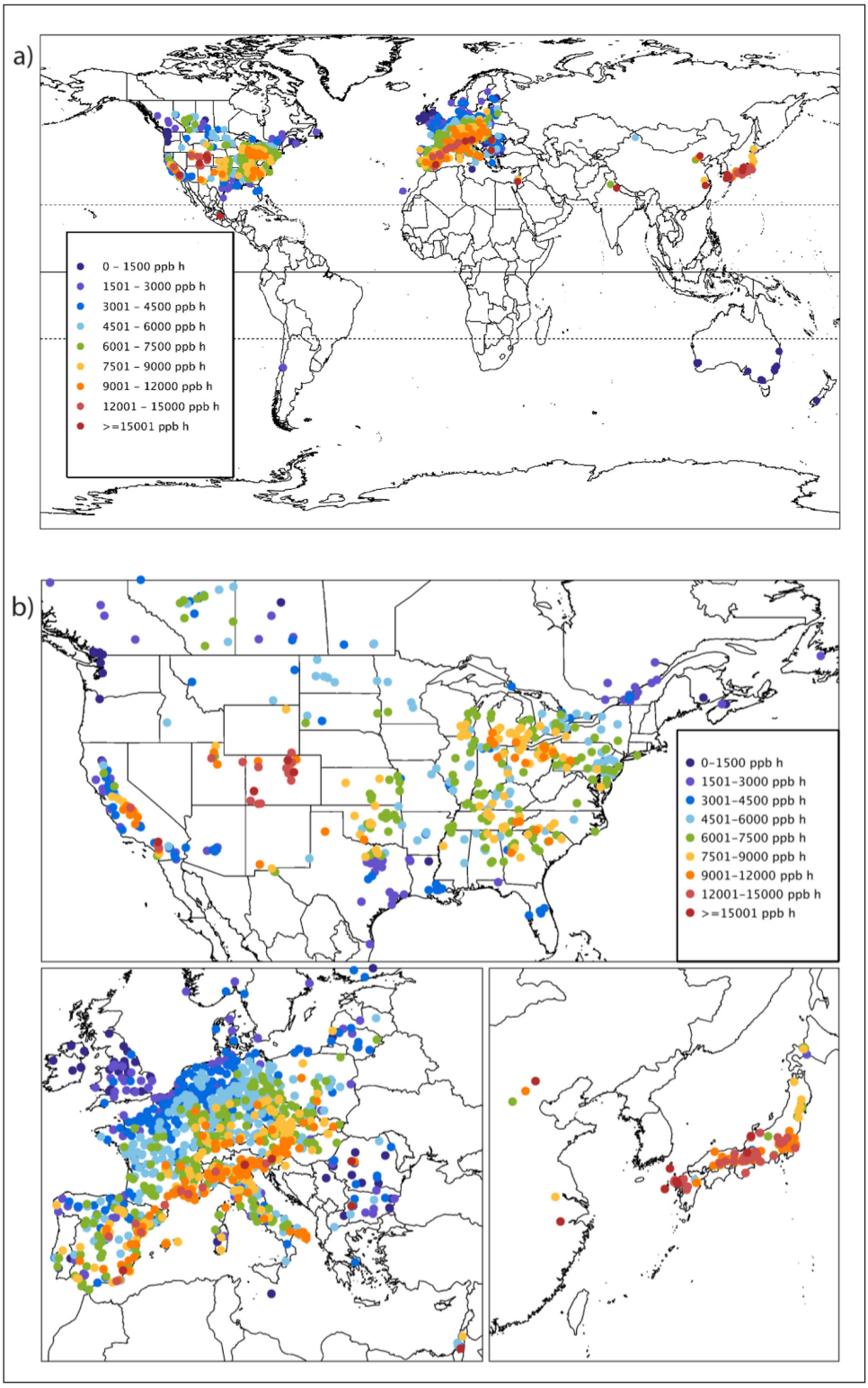

Figure 8: (a) Global and (b) regional distribution of the mean AOT40, 2010–2014, for wheat (3-months). DOI: https://doi.org/10.1525/elementa.302.f8

values in the range 19–29 ppb. The proportion of sites with M12 values in the range 40–55 ppb was 77.5% for EUR, 39.7% for NAM and 27.2% for EAS (**Figure 10**).

3.2.3.2. AOT40 for rice

Globally, 13.3% of sites have AOT40 values above the value of 12800 ppb h, expected to cause a 5% yield reduction (Mills et al., 2007a); of these, 50.8% are in EUR, 6.1% are in NAM and 43.2% are in EAS. AOT40 values in all HTAP regions except EAS are higher, on average by ~30%, for rice than for wheat. These observations mean that part of the difference in sensitivity between the two crops may potentially be counteracted by higher ozone exposure of rice. As with M12, the regional mean AOT40 values (**Table 6**) are not significantly different from each other. The mean values are:

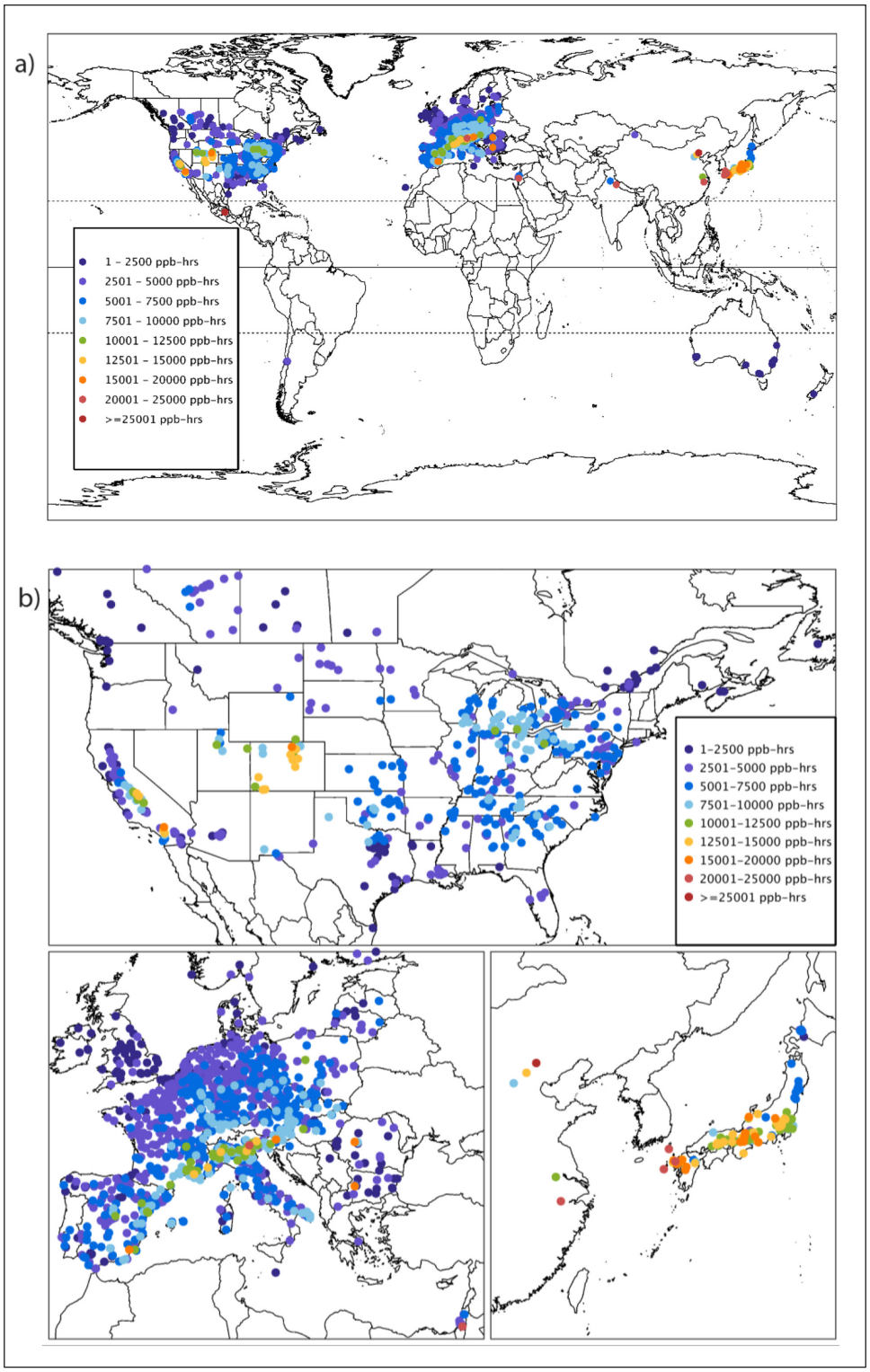

Figure 9: (a) Global and (b) regional distribution of the mean W126, 2010–2014, for wheat (3-months). DOI: https://doi.org/10.1525/elementa.302.f9

EUR (10502 +/– 5780 ppb h, N = 178), NAM (7112 +/– 5954 ppb h, N = 58) and EAS (7454 +/– 3774 ppb h, N = 734). The large SDs of these regional means are indicative of the considerable spatial variation found within each region and are contributing to the lack of statistical significance (Text S-3). For example, parts of the rice growing areas in southern USA and in Japan experience low to moderate ozone exposure, whilst rice production in Europe is located in the south where ozone levels are mostly high (**Figure 12**). The frequency distributions exhibited in **Figure 10**, indicate that the sites with the highest categories of ozone exposure are more common in EUR than in NAM and EAS. Of the regions with very few sites, the highest values are found in SAS (mean 4920 +/– 6041 ppb h, N = 3) and MCA (6985 ppb h, 1 site, **Table 6**). Values are lower in SAM (mean of 3357 +/– 1488 ppb h, N = 9) and PAN (mean of 705 +/– 467 ppb h, N = 3).

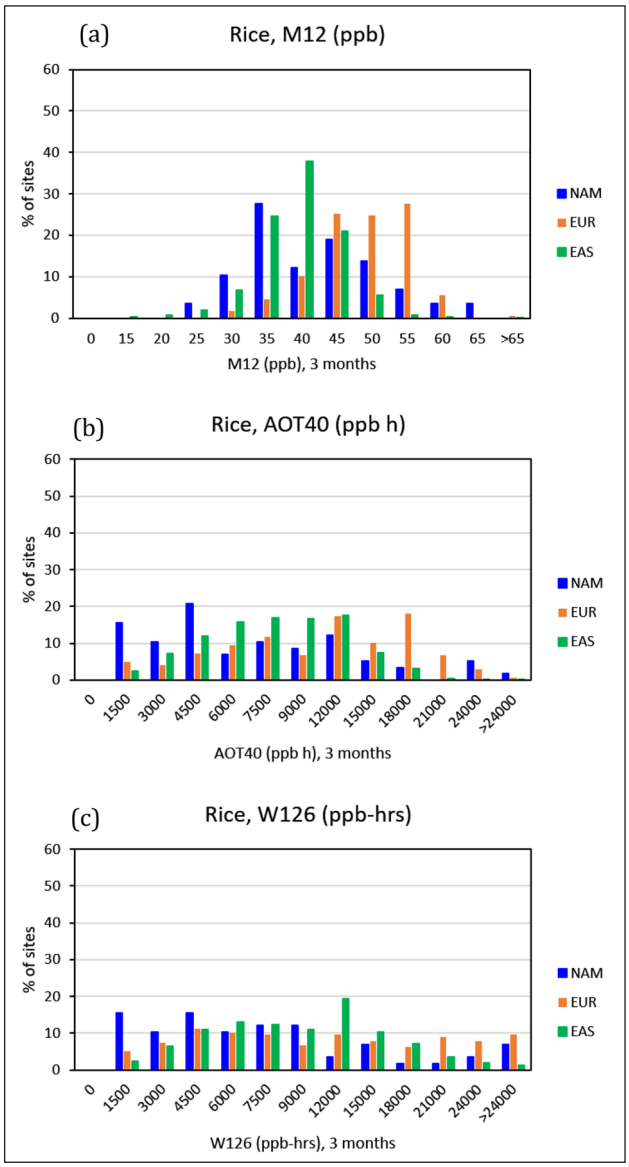

Figure 10: Frequency distributions for mean M12, AOT40 and W126 for the rice 3-month period, 2010–2014. Presented for sites in North America (NAM), Europe (EUR) and East Asia (EAS). DOI: https://doi.org/10.1525/elementa.302.f10

Interesting differences emerged in the distribution of AOT40 between climatic zones (Table S-6). In NAM, the mean values are highest in warm temperate dry climates at a mean of 11386 ppb h (N = 26), and are considerably higher than in warm temperate moist (7508 ppb h, 6 sites) and tropical moist climates (2709 ppb h, N = 25). In contrast, in EUR, mean values are higher in warm temperate moist climates (15725 ppb h, N = 44) than in warm temperate dry climates (9296 ppb h, N = 121), whilst almost all sites in SEA are in warm temperate moist climates where the mean AOT40 was 7381 ppb h (N = 723). Given that rice is usually irrigated in both climates when needed, it is likely that stomatal uptake is not limited by soil moisture. Therefore, the results of this analysis, based on metrics of ambient ozone observations, suggest that the highest impacts on rice yield are likely in the warm temperate moist climates of EUR and warm temperate dry climates of NAM.

3.2.3.3. W126 for rice

Regional mean W126 values in EUR (11578 +/– 8291 ppb-hrs, N = 178) are higher than those in EAS (9077 +/– 5578 ppb-hrs, N = 734) and NAM (8155 +/– 8135 ppb-hrs, N = 58), but as for M12 and AOT40 are not statistically significantly different (Text S-3). Overall, 17.2% of rice sites have W126 values in excess of the NAAQS_Crops (15000 ppb-hrs) (**Table 6**, **Figure 13**). The spatial distribution of this metric is similar to that for AOT40, with highest values found in N Italy, W Spain, W USA and central parts of Japan and the Republic of Korea (**Figure 13**).

3.2.4. Three-month W126 values for vegetation

Although outside the original remit of *TOAR-Vegetation*, we briefly consider the wheat W126 distribution (**Table 4, Figure 9**) in the context of other impacts considered in establishing the US EPA secondary ozone standard for vegetation. It should first be noted that in TOAR, W126 is calculated for a 3-month growing season for wheat averaged over 5 years, whilst the EPA calculates the metric for the three consecutive months with the highest W126 values and averaged over three years. The 3-month time-period for all vegetation including trees in the NAAQS values is also different to the 6-month accumulation period used for perennial vegetation in the CLRTAP_CLs. Thus, we apply here the 3-month W126 values for wheat to all vegetation types in the context of exceedance of the NAAQS.

The percentage of TOAR sites that exceeded NAAQS_Ecosystems, NAAQS_Injury and NAAQS_Trees are 1.1%, 11.3% and 26.9%, respectively. For the most stringent of these limits (NAAQS_Trees), the percentage of sites exceeding 7000 ppb-hrs is 22.2 % in NAM, 21.1% in EUR and 86.8% in EAS, suggesting that the highest risk to tree biomass is in EAS. The less stringent NAAQS_Injury is exceeded at sites in, for example, central and W USA, India, and southern Europe including Spain, France, Italy and other sites around the Mediterranean basin.

3.2.5. Correlations between metrics

The data from wheat and rice growing areas were explored for patterns in the correlation between metrics (**Figure 14**). For both vegetation types, AOT40 and W126 are strongly correlated (r^2 = 0.94 and 0.96 for wheat and rice, respectively, polynomial function), with W126 becoming increasingly higher at the highest AOT40 values, reflecting the weighting aspect of the metric. Both W126 and AOT40 are >0 at M12 values above approximately 20 ppb, with values increasing rapidly at M12 values above 40 ppb. Using these relationships, it can be seen that the CLRTAP_CL_Crops(AOT40 of 3000 ppb h) is equivalent to a W126 of 2578 ppb-hrs. Similarly, a W126 of 17000 ppb-hrs for NAAQS_Ecosystems, is equivalent to an AOT40 of 15695 ppb h; a W126 of 15000 ppb-hrs for NAAQS_Crops is equivalent to an AOT40 of 14181 ppb h; a W126 of 10000 ppb-hrs for NAAQS_Injury is equivalent to an AOT40 of 10079 ppb h; and a W126 of 7000 ppb-hrs for NAAQS_Trees is equivalent to an AOT40 of 7400 ppb h.

The correlations between metrics for perennial vegetation are provided in Figure S-2.

3.2.6. Effect of monitoring inlet height on metric value

AOT40 is calculated from ozone observations at canopy height (1 m for crops and grassland, 20 m for forests) after adjustment for monitoring inlet height (methods provided in CLRTAP, 2017). In contrast, W126 is calculated from the ozone values at the monitoring inlet height, which can vary from site to site (e.g. it varies across the USA from ≤5 m through to ≥ 10 m, as described earlier). As inlet height was not included in the TOAR database, it has not been possible to standardise for the effect of this variation across sites. To illustrate the uncertainty introduced by measurement height, 3- and 6-month M12, AOT40 and W126 were calculated for a range of heights using a tabulated gradient for an "artificial" crop and tree species (CLRTAP, 2017). This example uses a hypothetical daily

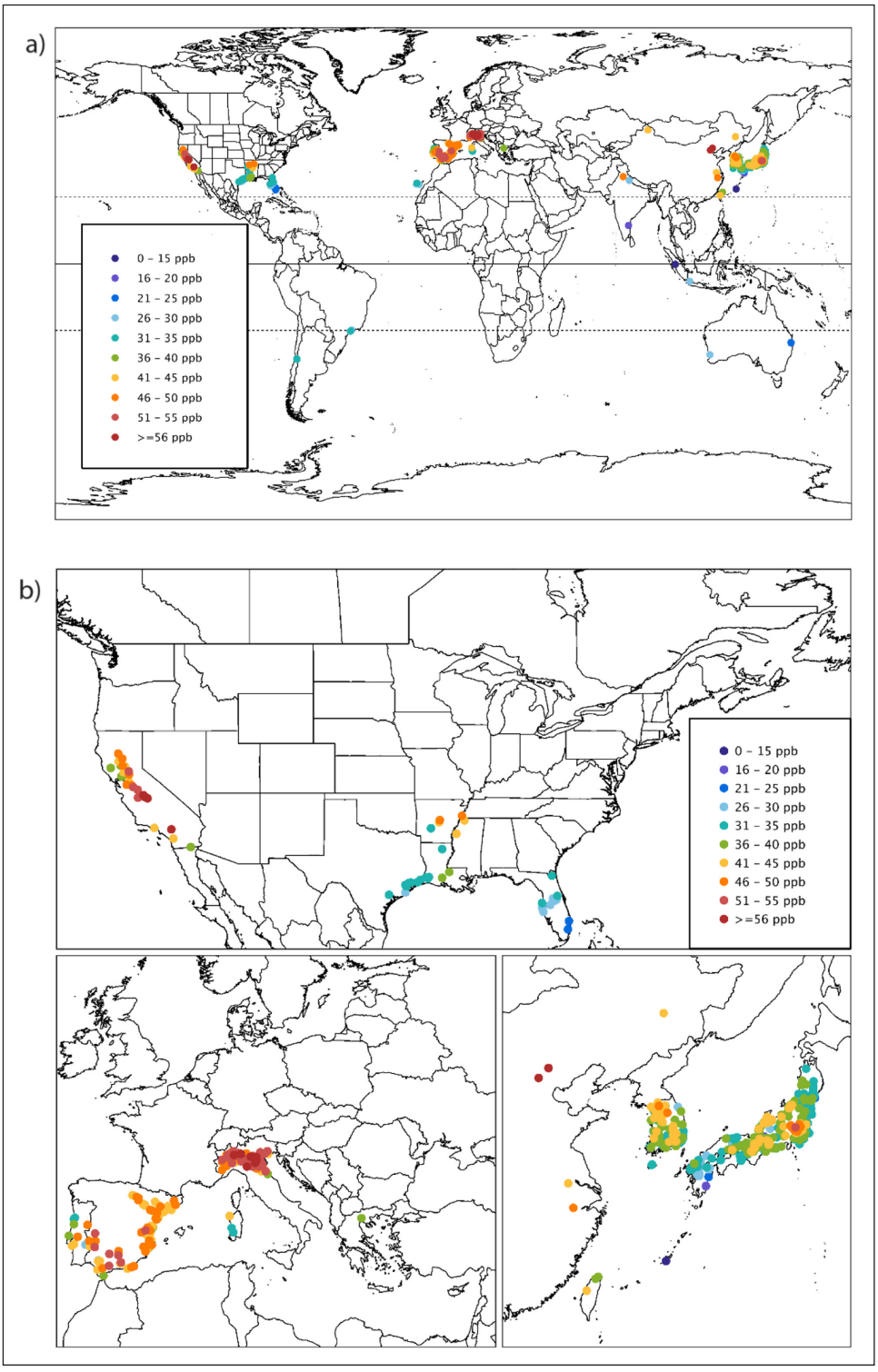

Figure 11: (a) Global and (b) regional distribution of the mean M12, 2010–2014, for rice (3-months). DOI: https://doi.org/10.1525/elementa.302.f11

Table 5: The present-day mean and standard deviation (SD) for M12, AOT40 and W126 for wheat for 3-months (2010–2014), presented by HTAP region. Note: The mean and SD for each country are provided in Table S-3. DOI: https://doi.org/10.1525/elementa.302.t5

HTAP region	N	M12 (ppb)		AOT40 (ppb h)		W126 (ppb-hrs)	
		Mean	SD	Mean	SD	Mean	SD
NAM	532	41.0	4.9	6013	2821	5403	2772
EUR	1418	39.0	5.4	5324	2884	4798	2886
SAS	3	41.4	13.6	9057	6595	10582	8747
EAS	275	45.8	4.2	10373	3142	11355	4489
PAN	16	26.4	3.1	320	357	520	355
MDE	7	41.2	8.2	6623	5940	6306	6820
MCA	4	39.2	9.7	7033	8399	8733	12776
SAM	11	22.1	1.7	1145	587	1090	648
RBU	2	49.5	4.2	10625	5261	7576	4256
Global	**2268**	**40.2**	**5.9**	**6066**	**3401**	**5719**	**3857**

Table 6: The present-day mean and standard deviation (SD) for M12, AOT40 and W126 for rice for 3-months (2010–2014), presented by HTAP region. Note: The mean and SD for each country are provided in Table S-5. DOI: https://doi.org/10.1525/elementa.302.t6

HTAP region	N	M12 (ppb)		AOT40 (ppb h)		W126 (ppb-hrs)	
		Mean	SD	Mean	SD	Mean	SD
NAM	58	39.3	9.4	7112	5954	8155	8135
EUR	178	46.3	6.8	10502	5780	11578	8291
SAS	3	30.7	14.0	4920	6041	6772	8746
EAS	734	36.9	5.9	7454	3774	9077	5578
SEA	5	19.2	4.5	901	693	1091	973
PAN	3	23.3	3.4	705	467	787	512
MCA	1	40.0		6985		6974	
SAM	9	28.6	9.6	3357	1488	3429	1671
Global	**991**	**38.5**	**7.6**	**7883**	**4547**	**9347**	**6423**

ozone profile that at 1 m peaked at 55 ppb between 10:00 and 17:00 repeated each day over 90 or 180 d, Figure S-3 and Table S-7). For "crops", conversion of observed ozone value from a monitoring inlet height of 5 m to a canopy height of 1 m decreases the 90 d M12 from 55.1 ppb to 50 ppb, the 90 d AOT40 from 16323 to 10800 ppb h and the W126 from 806 to 390 ppb-hrs. Differences between 5 m and 10 m are less pronounced, with values at 10 m being an M12 of 56.3 ppb, a 3-month AOT40 of 17550 ppb h and a W126 of 934 ppb-hrs (Table S-7). In contrast, for a 20 m "tree", the observed ozone at 5 m would underestimate the ozone value at the top of the 20 m canopy. Using the stylised ozone profile, M12 is 52.7 ppb, 53.8 ppb and 54.3 ppb at 5 m, 10 m and 20 m respectively, the 180 d AOT40 is 27470 ppb h at 5 m, 29817 ppb h at 10 m and 30991 ppb h at 20 m, and the 180 d W126 is 1162 ppb-hrs at 5m, 1352 at 10 m and 1456 ppb-hrs at 20 m. The implications of using the inlet height versus the canopy height on metric values are considered in the discussion.

3.3. Global long-term trends (over 15 and 20 years)

3.3.1. Trends in metrics for perennial vegetation

Across the three perennials metrics, a statistically significant decrease is the most common pattern of change globally between 1995 and 2014 (**Figures 15–18**). Globally there are more sites with statistically significant decreasing trends (33%, 45% and 50%, for M12, AOT40 and W126 respectively) compared to those in other categories (**Figure 15**); in contrast, only 9%, 4%, and 4% of sites have statistically significant increasing trends, respectively.

Figures 16–18 show that there is a substantially larger proportion of sites with statistically significant decreasing trends in NAM than in EUR over the period 1995–2014. Indeed, over 70% of sites have statistically significant decreasing trends in NAM for AOT40 (median rate: –730 ppb h y^{-1}) and W126 (median rate: –1065 ppb-hrs y^{-1}), with 54% significantly decreasing for M12 (median rate: –0.42 ppb y^{-1}). The equivalent figures for EUR are 28% of sites for AOT40 (median rate: –351 ppb h y^{-1}), 32% for W126 (median rate: –396 ppb-hrs y^{-1}) and 17% for M12 (median rate: –0.25 ppb y^{-1}). The EUR sites with significant decreases are accompanied by an additional one third of sites showing an indication of a decrease, or a weak indication of decrease for AOT40 and W126, but only 21% of sites for M12 (**Figure 15**). In both NAM and EUR, less than 2% of sites have statistically significant increases in AOT40 and W126, with a slightly higher proportion having significant increases in M12 (3% for NAM and 5% EUR).

In contrast, the predominant EAS trend, where all but 3 of the sites included in the 1995–2014 analysis are in Japan, is a statistically significant ozone increase at approximately 25% of sites for AOT40 (median rate: +618 ppb h y^{-1}), 24% of sites for W126 (median rate: +748 ppb-hrs y^{-1}), and 37% of sites for M12 (median rate: +0.52 ppb y^{-1}, **Figures 15–18**). For the 2000–2014 analysis, 58 sites from the Republic of Korea are also included (Figure S-4), 40–50% of which have significant increasing trends across all three metrics (spatial distributions are not presented for 2000–2014 trends). Interestingly, the proportion of sites with statistically significant increasing trends in Japan for 2000–2014 is substantially lower than for 1995–2014 (Figure S-4 compared to **Figure 15**). For example, only 17% of sites in Japan have statistically significant increasing trends for M12 between 2000 and 2014, as opposed to 36% of sites for the 1995–2014 period.

In other HTAP regions, there are substantially fewer sites to characterise trends and insufficient in number to generalize across an entire region. Across the 18 sites in PAN (all in Australia), conclusions about changing perennial vegetation ozone exposure during 1995–2014 vary depending on the metric used. For AOT40, two sites exhibit an

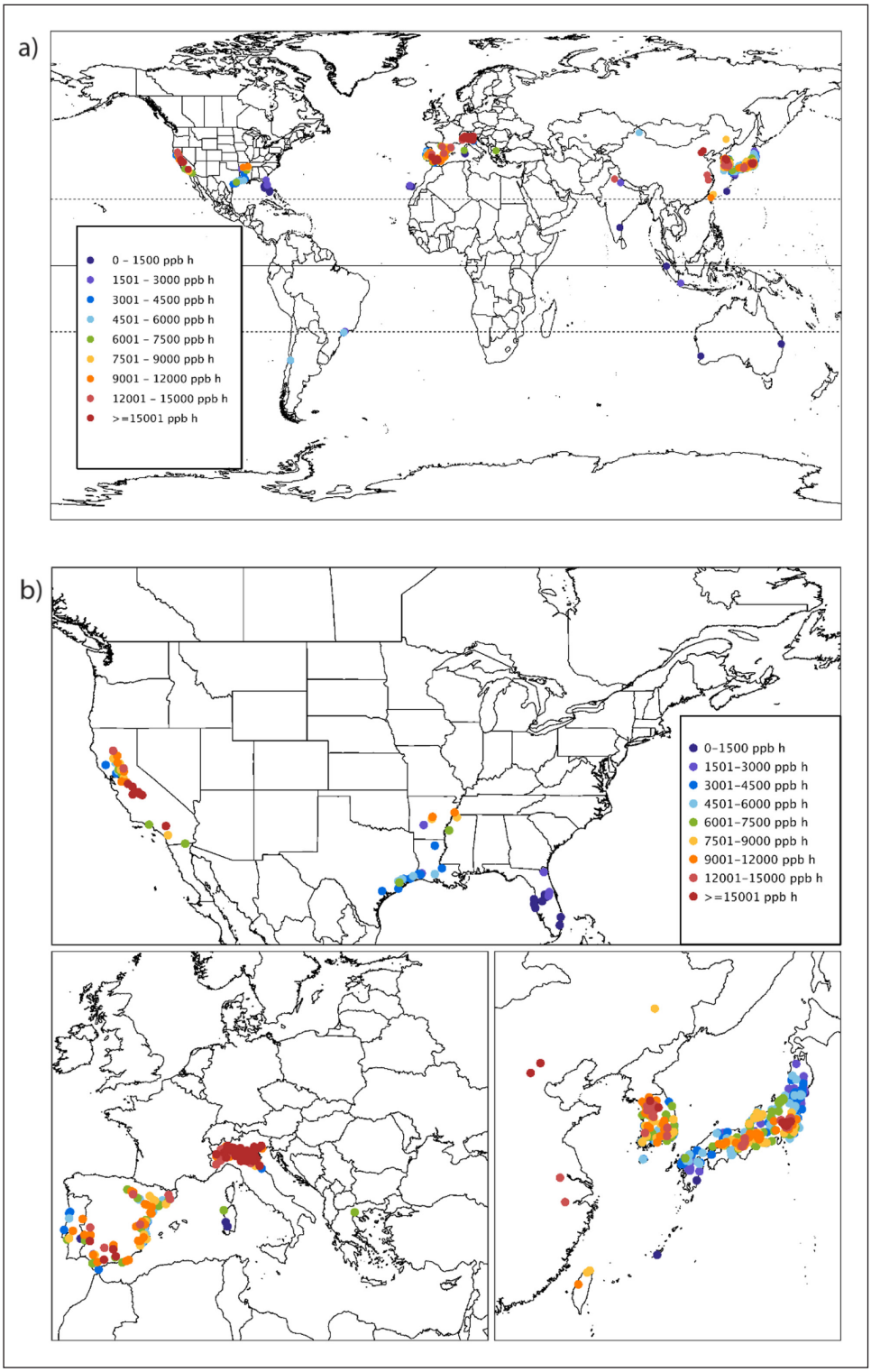

Figure 12: (a) Global and (b) regional distribution of the mean AOT40, 2010–2014, for rice (3-months). DOI: https://doi.org/10.1525/elementa.302.f12

indication of a decrease, and three exhibit a weak indication of a decrease. For W126, two sites show a statistically significant decrease, but for M12, the predominant pattern of change is an increase (5 sites have a significant increase, 2 sites an indication of increase, and 7 sites a weak indication of increase). During 2000–2014, a substantially greater proportion of the 24 available PAN sites exhibit a statistically significant decrease in AOT40 and W126, and no site has a significant increase in M12. Only 5 perennial vegetation sites from MCA and SAM span 1995–2014, with 8 sites having sufficient data spanning 2000–2014. During both periods, more sites have significant decreasing trends for all three metrics than an increasing trend (**Figures 15** and S-4). In Africa, only one perennial vegetation site has sufficient data, Cape Point in South Africa. At this site, AOT40 and W126 are very low and remained stable at 150 ppb h and 2 ppb-hrs respectively, while M12 has a statistically significant increase from 22 ppb at a rate of 0.09 ppb y^{-1}. Similar shifts are observed for perennial metrics at PAN sites, when comparing 1995–2014 and

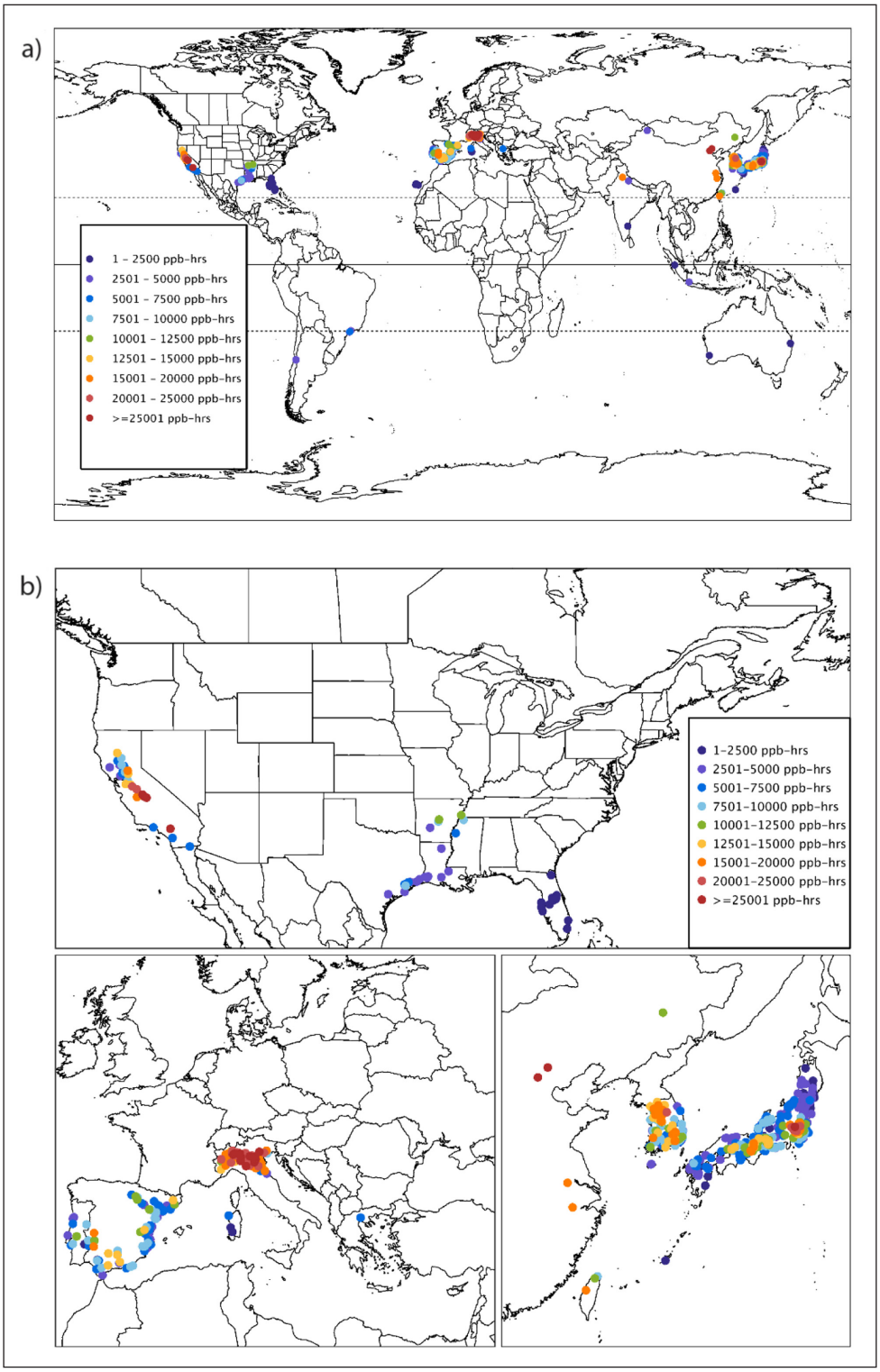

Figure 13: (a) Global and (b) regional distribution of the mean W126, 2010–2014, for rice (3-months). DOI: https://doi.org/10.1525/elementa.302.f13

2000–2014. Here, the dominant trend is an increase in M12 and no change in AOT40 and W126 for 1995–2014, and no significant change for 2000–2014.

3.3.2. Trends in metrics for wheat

There are 691 sites in wheat-producing regions with sufficient data to characterise 1995–2014 trends (**Figures 19–22**). Only 7%, 13% and 20% of sites globally have statistically significant decreasing trends in M12, AOT40 and W126, respectively during the 3-month wheat-growing season, which is a substantially lower percentage of sites compared to the 6-month perennial time-period. These differences result from i) a lower proportion of sites in NAM and EUR with decreasing trends, and ii) a larger proportion of sites in EAS with increasing trends for the wheat-growing season metrics compared with the 6-month perennial growing season.

In NAM and EUR, the proportion of sites with statistically significant decreases in the three metrics during the wheat-growing season (1995–2014) is less than half

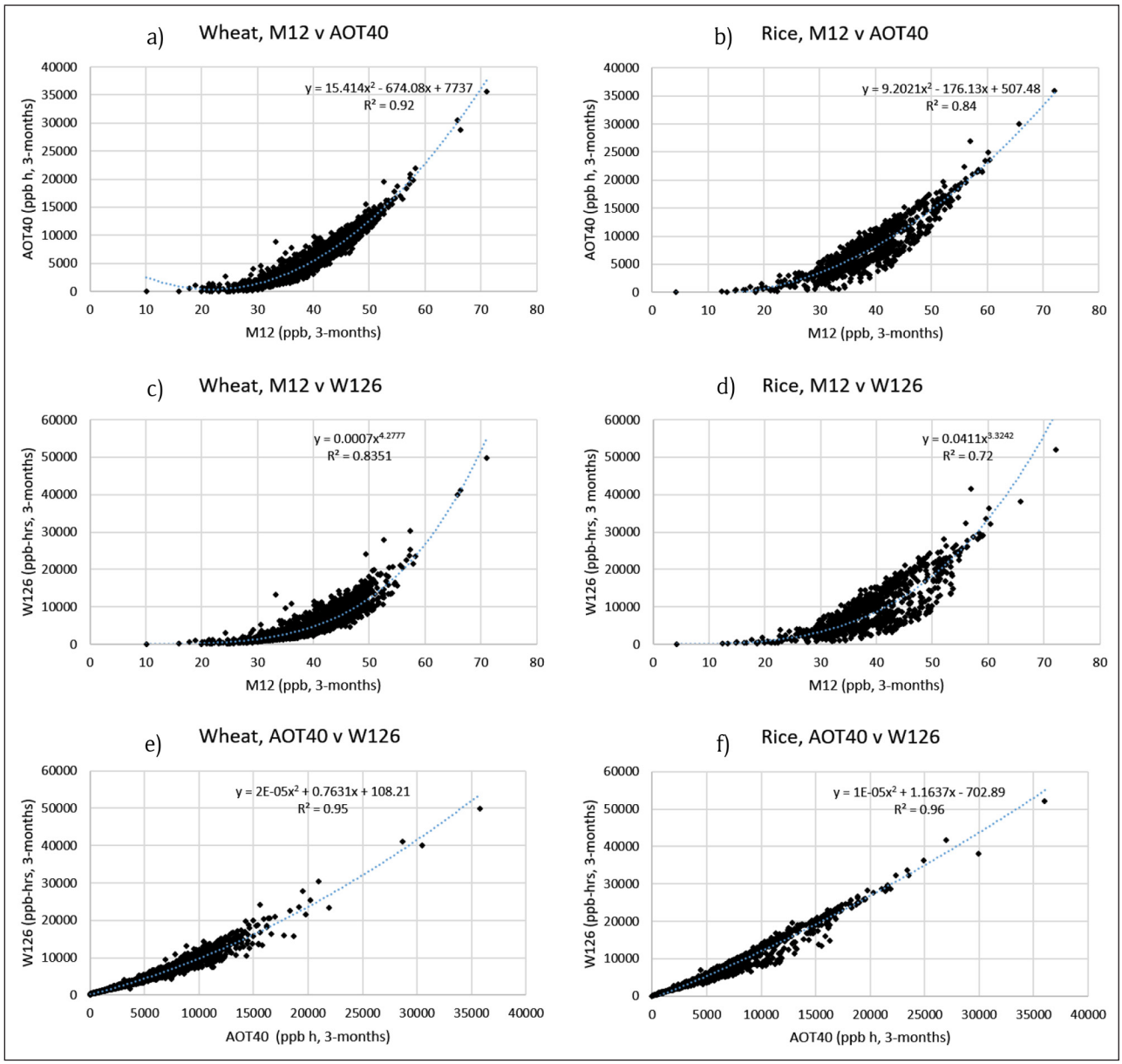

Figure 14: Correlations between metrics for wheat (a) to (c) and rice (d) to (f). Data presented are for all sites with these vegetation types. DOI: https://doi.org/10.1525/elementa.302.f14

of those for the 6-month perennial-growing season. For wheat, 11%, 26% and 39% of sites in NAM have statistically significant decreasing trends in M12, AOT40 and W126, respectively, whilst 6%, 11% and 6% of sites have such trends, respectively, in EUR (**Figure 19**). Over the 15-year period (2000–2014), these proportions are reduced further to 7% of sites (M12), 17% of sites (AOT40) and 25% (W126) for NAM, but increased to 10% (M12), 10% (AOT40) and 13% (W126) for EUR. Of the three metrics, more than three times as many sites show an increase in M12 compared to increases in AOT40 or W126 in NAM and EUR (**Figures 19–22**) and this is much more pronounced than for perennial metrics. Overall, there is a larger proportion of sites with no indication of change during the wheat-growing season across all three metrics compared with the 6-month perennial season.

As for metrics for perennial vegetation, a different pattern emerged for trends in EAS compared to NAM and EUR for the wheat metrics. In Japan (where all wheat-relevant sites in EAS were located), 55%, 45% and 42% of sites had statistically significant increasing trends in M12, AOT40 and W126, respectively (1995–2014, **Figure 19**). Consistent with the results for the perennial vegetation metrics, there is a reduction in the proportion of increasing trends in Japan in 2000–2014 compared to 1995–2014 (Figure S-5 compared with **Figure 19**), with only 29%, 18% and 14% of sites with statistically significant increasing trends in M12, AOT40 and W126, respectively.

As with trends for the 6-month perennial period, the distribution of trends for wheat over 3-months varies for the different metrics. In NAM and EUR, there is a greater proportion of sites with statistically significant decreasing trends in AOT40 and W126 compared with M12, and in SEA, a larger proportion of sites have statistically significant increasing trends in M12 compared to AOT40 and W126.

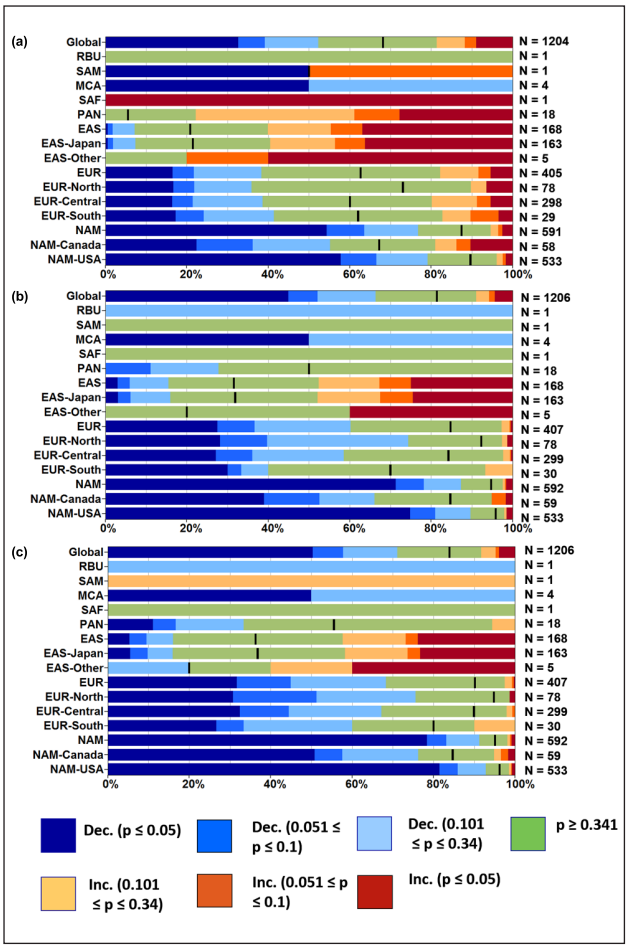

Figure 15: Trends in perennials (a) M12, (b) AOT40 and (c) W126 for 1995–2014. Data are for changes in the 6-month period relevant for perennials, and are presented as the proportion of non-urban monitoring sites in different regions and countries with trends that: are significantly increasing or decreasing ($p \leq 0.05$); show an indication of an increase/decrease ($0.05 < p \leq 0.1$); have a weak indication of an increase/decrease ($0.1 < p \leq 0.34$), or no change ($p > 0.34$). Blue colours indicate decreasing trends, green colours no trend and red colours indicate decreasing trends. Colours have been selected to match the arrows in Figures 16–18. DOI: https://doi.org/10.1525/elementa.302.f15

3.3.3. Trends in metrics for rice

Globally, 217 monitoring sites in rice-growing regions have sufficient time series data for inclusion in the 1995–2014 trend analysis (**Figures 23–26**). As discussed above, of the world's top ten rice producing countries, only Japan has sufficient data to allow meaningful trend analysis.

The rice-growing regions of NAM show consistent decreases across all three metrics during 1995–2014 (61%, 79% and 84%, of sites have statistically significant decreases in M12, AOT40 and W126, respectively, **Figures 23–26**). In EUR, there is a relatively large number of sites with no indication of change (56%, 22% and 56% of sites for M12, AOT40 and W126, respectively), and the majority of the other sites have decreasing trends. The proportion of sites with significant decreases is greater for the 2000–2014 period, largely due to the inclusion of more sites in rural areas in EUR rice-growing regions. Also for 2000–2014, 8 SAM and MCA sites are included in the trend analysis, with decreases being the dominant pattern of change.

Across the Japanese sites, all metrics indicate an increasing pattern of change in rice-relevant time-periods, with a larger proportion of sites having increasing M12, compared with AOT40 and W126. This is consistent with the trend pattern identified in Japan for the perennial and wheat-relevant time-periods. Also consistent is the substantial fall in the proportion of increasing trends during 2000–2014 compared to 1995–2014. During 1995–2014, 38%, 19% and 15% of sites have significant increasing trends in M12, AOT40 and W126, respectively, while only 9%, 2% and 1% of sites have statistically significant increases in the three metrics during 2000–2014. The distribution of trends at the 99 sites in the Republic of Korea during 2000–2014 indicates that 63%, 47% and 47% of these sites have statistically significant increasing trends in M12, AOT40 and W126, respectively (Figure S-6).

4. Discussion

4.1. Spatial representativeness of analysis

TOAR-Vegetation provides the first major attempt to use observations rather than modelling data to assess the ozone exposure of vegetation on a global scale. Sites meeting the criteria for inclusion for perennial vegetation, wheat, and/or rice metrics were most abundant in NAM, EUR and EAS, allowing detailed assessments of present-day ozone distributions and long-term trends for these regions. Thus, much of the ozone data are from the NH mid-high latitudes of the developed world (20 to 60° N), with very limited data available for rapidly developing countries of Africa, South America, and parts of SAS/SEA. TOAR has strong representation in areas of NAM and EUR predicted to have high ozone impacts on crops (Avnery et al., 2011; Van Dingenen et al., 2009; Mills et al., submitted) and biodiversity (Fuhrer et al., 2016) such as central states of the USA and Mediterranean areas. However, other areas predicted from modelling to have high impacts of ozone on vegetation such as northern areas of India and the northern plains of China (e.g. Burney and Ramanathan, 2014; Ghude et al., 2014; Tang et al., 2013) are poorly -represented in TOAR. As there is field evidence of ozone impacts on vegetation in these regions (Emberson et al., 2009; Feng et al., 2014; Harmens and Mills, 2014) and high crop yield losses predicted from locally observed ozone (Sinha et al., 2015), more publically available monitoring data are urgently needed.

To provide a broad overview of ozone concentrations relevant to crops, we have only included data for sites where two of the world's most important staple crops, wheat and rice are grown. These two crops are mainly grown under different climatic conditions and together represent a substantial proportion of the global crop growing regions (Figure S-1). Whilst four of the top 10 wheat producing countries (USA, France, Canada and Germany, FAOSTAT mean production from 2010–14) are well represented in TOAR (83–450 sites per country, total 1060 sites), only Japan represents the top 10 rice

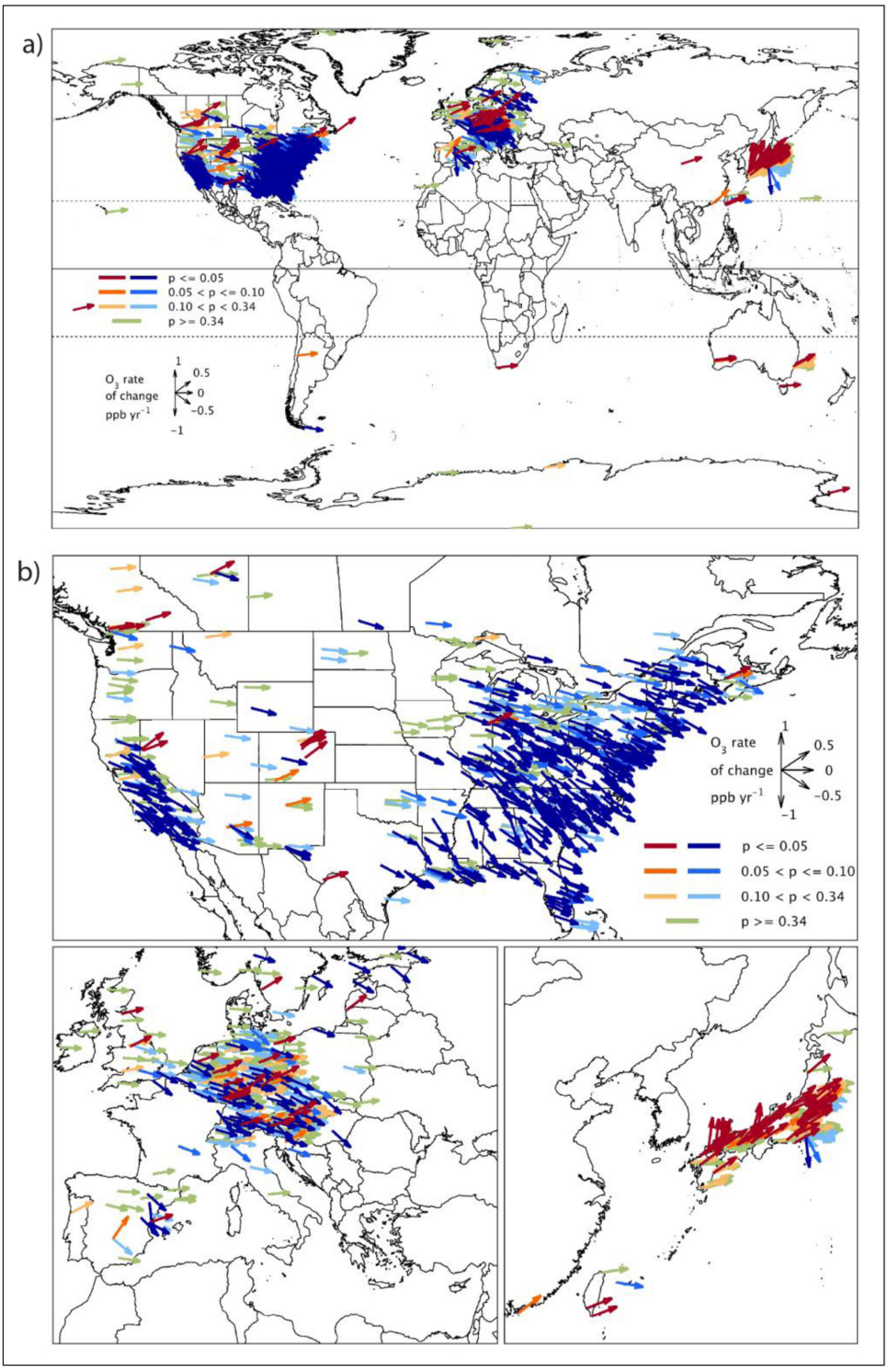

Figure 16: (a) Global and (b) regional trends in M12 (Perennial vegetation, 6-months), 1995–2014, non-urban sites. DOI: https://doi.org/10.1525/elementa.302.f16

producing countries in the database (535 sites), with the Republic of Korea, ranked 14th also being well represented (190 sites). There are only 25 other sites included in TOAR in the remaining 6 highest wheat producing countries and 19 sites in the remaining 9 highest rice producing countries within the TOAR dataset. It is notable that data from only a handful of sites was available for TOAR from India (3 sites) and China (9 sites), the highest wheat and rice producing countries in the world. Other under-represented crop growing areas include parts of SEA, SSA and SAM where crops such as soybean and maize are also commonly grown. Expanding the analysis to include these two crops could have added <5 extra sites for SAM and SAF and 2 for SEA. As there are no vegetation standards that have been developed specifically for these two crops and the response function for maize is only based on data for three cultivars, exposed to ozone in the USA in the 1980s and early 1990s (Mills et al., submitted), soybean and maize were not included in the *TOAR-Vegetation* analysis. It is also important to note that of the other top 10

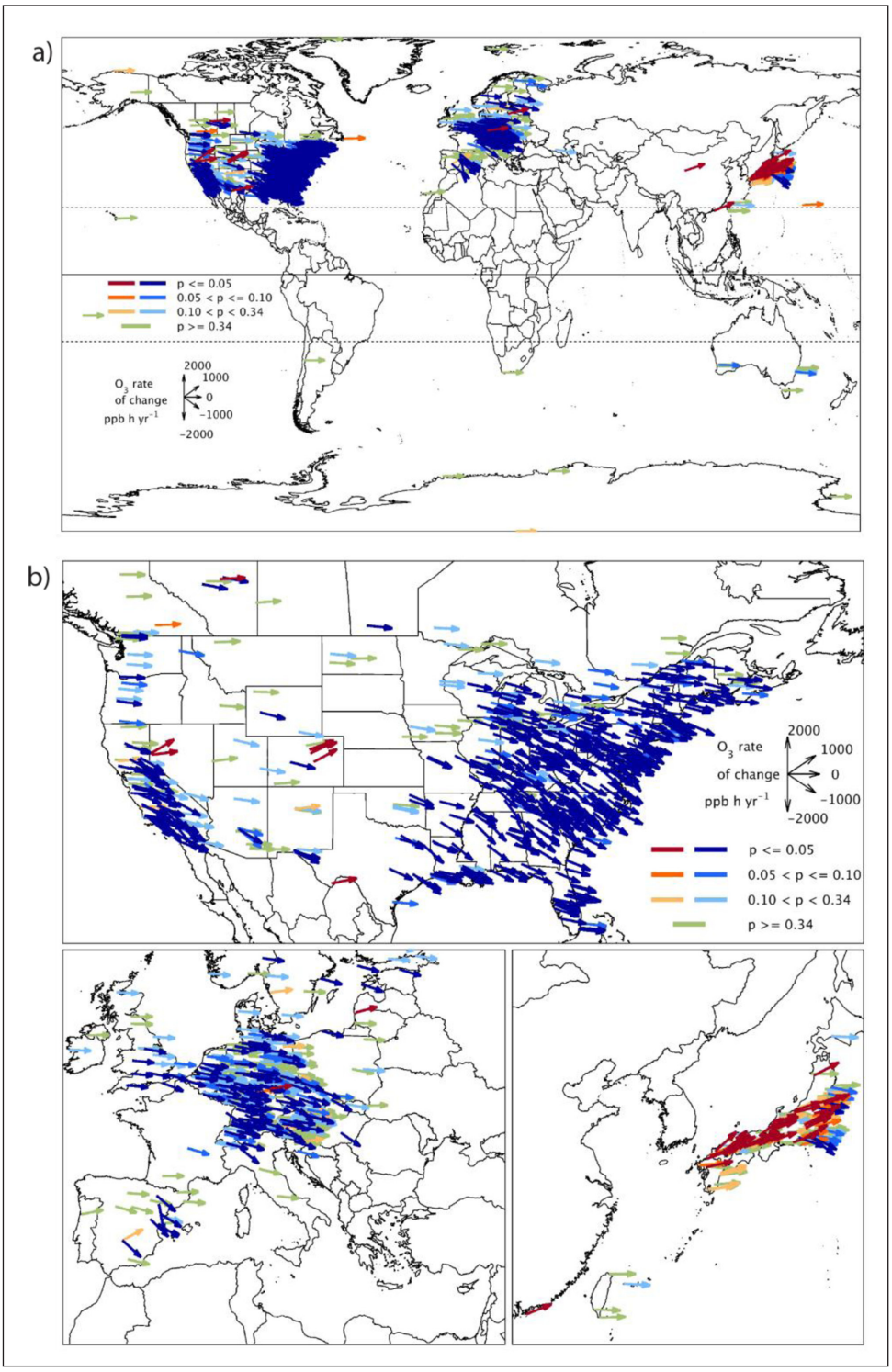

Figure 17: (a) Global and (b) regional trends in AOT40 (Perennial vegetation, 6-months), 1995–2014, non-urban sites. DOI: https://doi.org/10.1525/elementa.302.f17

global staple food crops (FAOSTAT), only potato has been extensively studied for ozone response and is considered moderately sensitive (Mills and Harmens, 2011a/b). One study has indicated that sweet potato is sensitive to ozone while very little/no information exists on the sensitivity of cassava, sorghum, yams and plantain. Although potato is usually harvested a little later in the season than wheat, we considered that the overlap in growing areas for the two crops was sufficient to use wheat in *TOAR-Vegetation* as an indicator of ozone risk to temperate annual crops. Overall, due to the shortage of ozone monitoring data in some major crop growing areas, together with a lack of information on ozone sensitivity of many staple food crops, we were unable to fully meet the first aim of this study, which was to conduct a global analysis of crop-relevant metrics. However, we were able to meet the third aim of identifying those areas of the world where more ozone data are required. Currently, an assessment of the global impacts of ozone on crop yield that covers all growing regions remains reliant on modelling, based on

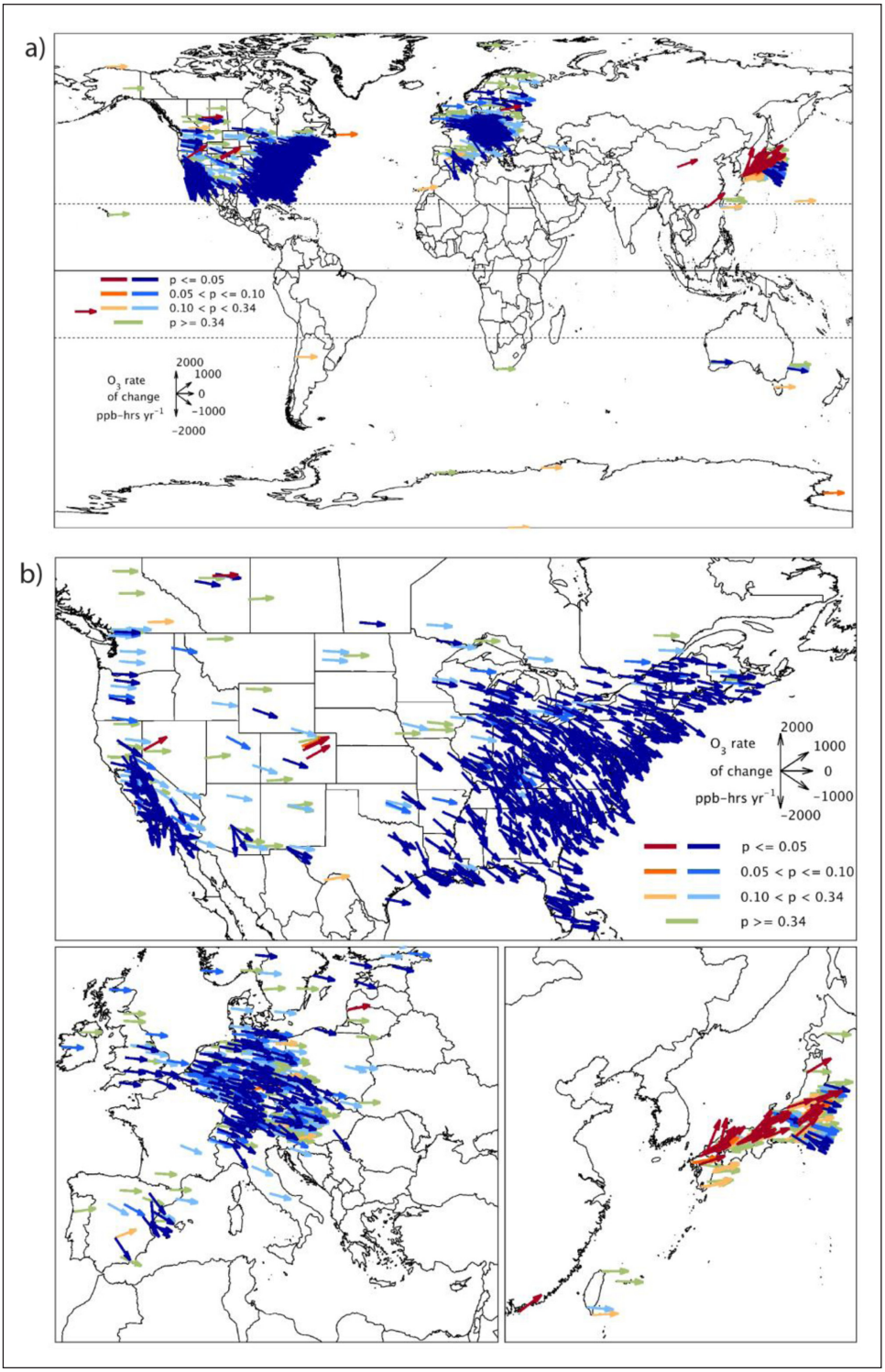

Figure 18: (a) Global and (b) regional trends in W126 (Perennial vegetation, 6-months), 1995–2014, non-urban sites. DOI: https://doi.org/10.1525/elementa.302.f18

either ozone concentration (e.g. Avnery et al., 2011; Van Dingenen et al., 2009) or stomatal ozone uptake (e.g. Mills et al., 2018; Mills et al., submitted).

For perennial vegetation, there is good representation of data in mid-latitudes of the Northern Hemisphere where grassland and forested areas provide grazing, harvestable biomass and other ecosystem services. However, many areas of globally important perennial vegetation are under-represented in the dataset, particularly those that are likely to have high conservation value. A recent analysis of current ozone risks to global terrestrial biodiversity and ecosystem processes based on modelled M12, indicated that about 40% of the Global 200 (G200) terrestrial ecoregions are exposed to ozone above thresholds for ecological risks (Fuhrer et al., 2016). The *TOAR-Vegetation* data cover many of the (G200) Ecoregions in NAM and EUR identified by Fuhrer et al. (2016) as having the highest risk of ozone effects such as temperate broad-leaf and mixed forests and Mediterranean forests, woodlands and shrubs. However, there is very poor/no representation in

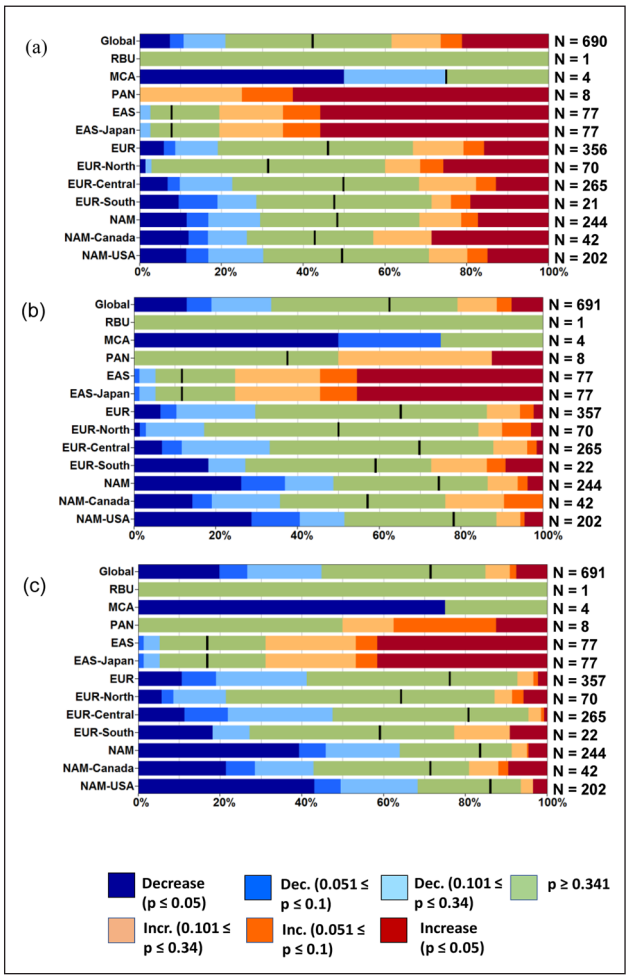

Figure 19: Trends in wheat (a) M12, (b) AOT40 and (c) W126, for 1995–2014. Data are presented as the proportion of monitoring sites in wheat-growing areas of the different regions and countries with trends in 3-month metrics that: are significantly increasing or decreasing ($p \leq 0.05$); show an indication of an increase/decrease ($0.05 < p \leq 0.1$); have a weak indication of an increase/decrease ($0.1 < p \leq 0.34$), or no change ($p > 0.34$). Blue colours indicate decreasing trends, green colours no trend and red colours indicate decreasing trends. Colours have been selected to match the arrows in Figures 20–22. DOI: https://doi.org/10.1525/elementa.302.f19

TOAR-Vegetation of other major forested areas of the world such as the Amazon and northern European/Asian forests of the Caucasus region, alpine meadows, topical and subtropical grasslands and savannas also identified by Fuhrer et al. (2016) as being potentially at high risk of effects of ozone. The sparsity of monitoring sites in these locations again limits our current ability to assess the global extent of risk based on measured values of ozone.

After consideration of data availability for vegetation-relevant metrics, TOAR-Vegetation makes three recommendations for increased monitoring of ozone (**Table 7**). Recommendation (1) is that improved scientific understanding of the impacts of ozone on vegetation in vulnerable and developing regions would require increased ozone monitoring at rural sites in SEA, SAS, SAM and Africa, especially in areas at high risk of ozone exposure. Low-cost sensors could be considered for potential deployment in such areas, providing adequate quality control and accuracy can be achieved (Lewis et al., 2018). Current satellite products and ozonesondes cannot, as yet, provide the hourly data at vegetation heights needed to calculate concentration-based vegetation-metrics for ozone (see *TOAR-Climate* for further details). In defining crop growing areas based on production data, *TOAR-Vegetation* identified that crops are often produced in urban-rural fringes (see discussion of uncertainties in Section 4.6). In many such areas, peri-urban agriculture can be of large importance, especially for people living on a low income. These areas may experience very high ozone exposure. *TOAR-Vegetation* Recommendation (2) is that impacts on peri-urban agriculture should be specifically considered with respect to ozone effects on food security in future investigations. Mountain/upland areas often experience higher ozone levels than adjacent areas at low altitude and are important conservation areas. *TOAR-Vegetation* Recommendation (3) is that future design of monitoring networks and assessments of ozone effects of vegetation should consider the special conditions of mountains and the underrepresentation of high elevation areas in current monitoring.

4.2. Present-day distribution of ozone metrics of relevance to vegetation

Across all three metrics, the highest exposure of vegetation to ozone is in areas where high emissions and climatic conditions together promote ozone formation. These are primarily in the following mid-latitude areas of the NH: S USA; S Europe including parts of Spain, Italy, France and Greece; N India; NW and E China; Republic of Korea and Japan. Conversely, the lowest ozone metric values are in Australia and New Zealand, southern parts of SAM, and northern areas of EUR and Canada. For most SH sites, the metric values are considerably lower than in the NH, although SH sites are under-represented in the database. Ozone metric values in some coastal regions, e.g. the Pacific coast of the USA, Atlantic coast of Europe and some coastal areas of Japan are frequently lower than in adjacent inland sites.

A statistical analysis of differences was only conducted for the three regions with the greatest data representation (NAM, EUR and SEA) because of the large variation in the number and spatial distribution of the monitoring sites. This analysis showed that despite variation in the means, there were no significant differences between regions for any of the rice metrics. Potentially this reflects the fact that rice tends to be grown during the hottest months when ozone levels might be the highest. For wheat, AOT40 and W126 are significantly lower in EUR and NAM than in EAS, whilst for perennials this was only the case for W126 for EUR vs EAS. Differences between regions were only significant for M12 for EUR vs SEA in wheat growing areas. Thus, differences between metrics are more pronounced for those metrics that accumulate medium and higher ozone values (AOT40 and W126) than those based on daytime means.

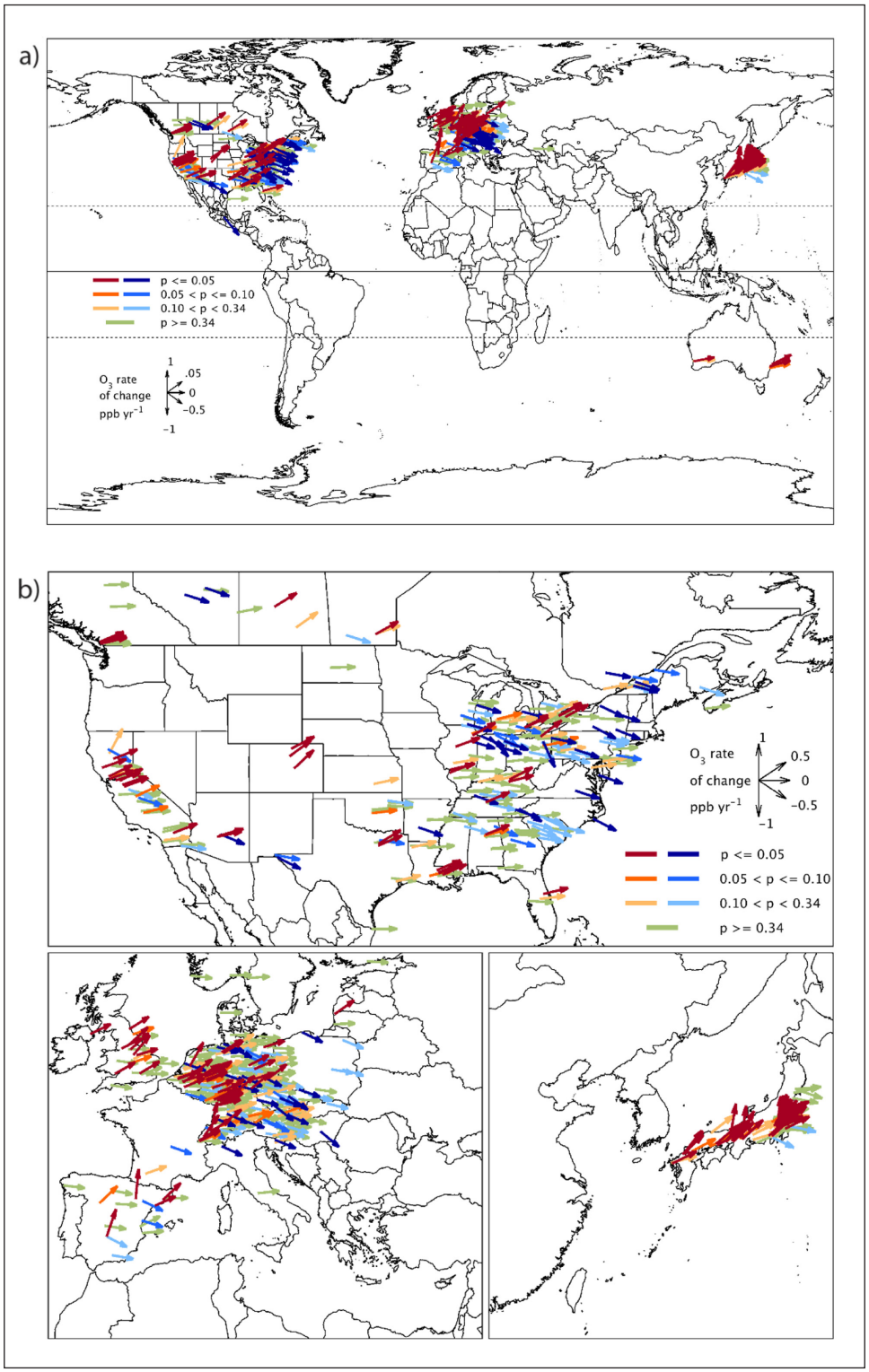

Figure 20: (a) Global and (b) regional trends in M12 (wheat, 3-months), 1995–2014, wheat-growing sites.
DOI: https://doi.org/10.1525/elementa.302.f20

TOAR-Vegetation shows that ozone metric values can be high in both moist and dry climates as well as in cool or warm climates; the lowest values are associated with tropical conditions although such sites are under-represented in the database. Globally, the largest range of values is for W126 where the stronger weighting for the highest ozone levels makes the areas with the highest W126 values stand out from those with lower values. A similar, but less pronounced pattern is shown for AOT40, with M12 showing proportionately less spatial variation across the sites, especially in the NH. Inclusion of M12 is particularly useful, however, for showing ozone level gradations at the low ozone sites where 40 ppb is rarely exceeded. For example, the M12 values for perennials sites are <20 ppb in Brazil, 16–20 ppb in New Zealand and 16–30 ppb at most Australian sites; these sites have zero or minimal AOT40 and W126.

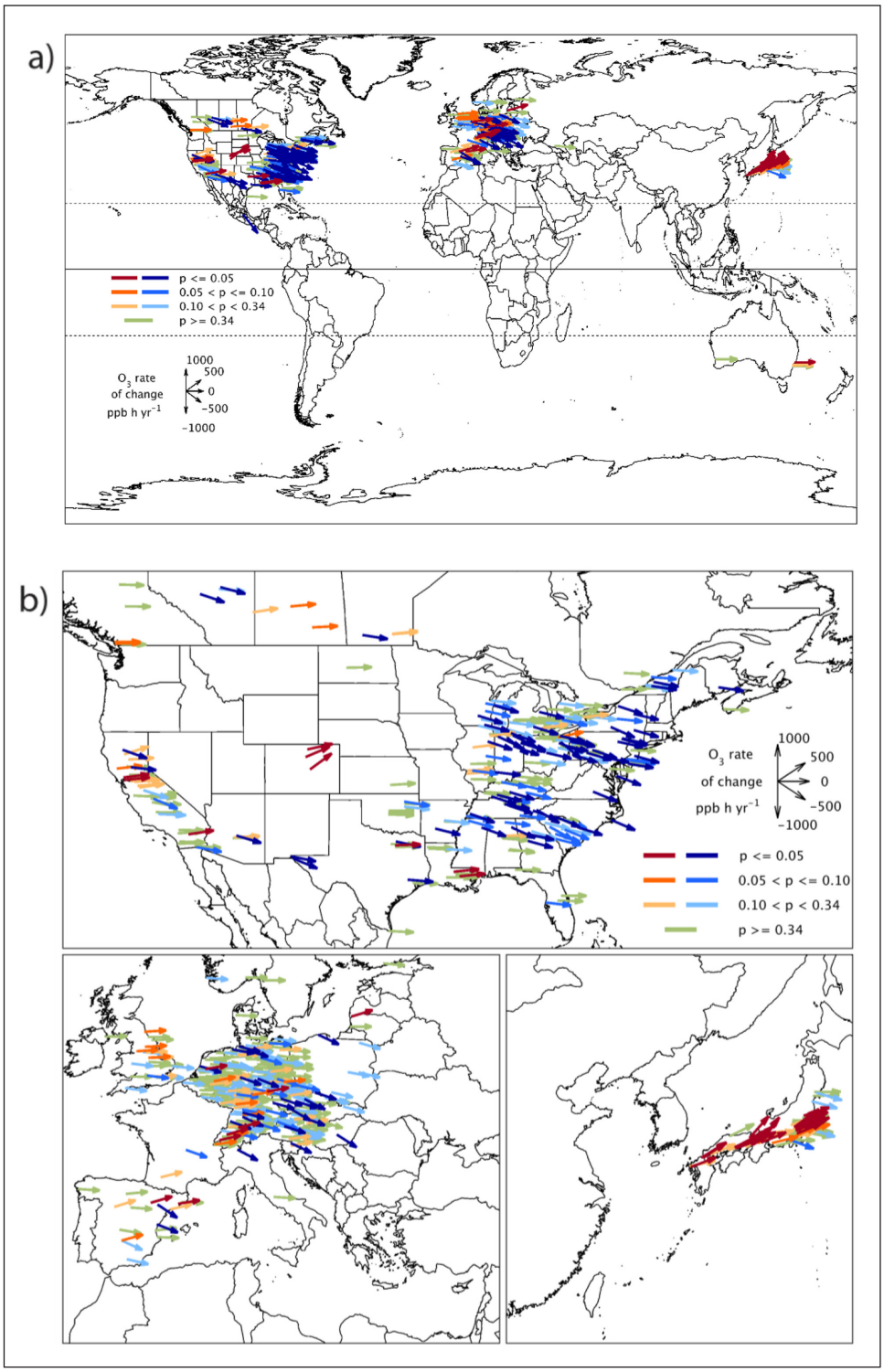

Figure 21: (a) Global and (b) regional trends in AOT40 (wheat, 3-months), 1995–2014 wheat-growing sites.
DOI: https://doi.org/10.1525/elementa.302.f21

Some of the highest M12, AOT40 and W126 values are in areas that have dry climates with low air and soil humidity, which will limit stomatal conductance and thus ozone uptake (Pleijel et al., 2007). This is an important consideration since ozone uptake will represent the phytotoxic dose more accurately than a metric solely calculated from the ambient ozone surrounding the plants. In situations where irrigation is used to overcome soil moisture deficits in dry climates, ozone uptake is likely to be higher and effects are more likely to be similar to those predicted by M12, AOT40 and W126 if other factors such as temperature do not limit ozone uptake.

4.3. Exceedance of air quality standards for vegetation

TOAR-Vegetation has identified the areas of the world where existing air quality standards relevant to vegetation are currently exceeded, based on the CLRTAP metric AOT40 and the levels of concern developed by the US EPA for W126. Whilst these two metrics are strongly correlated within the dataset (**Figure 14**), the CLRTAP_CL_Crops

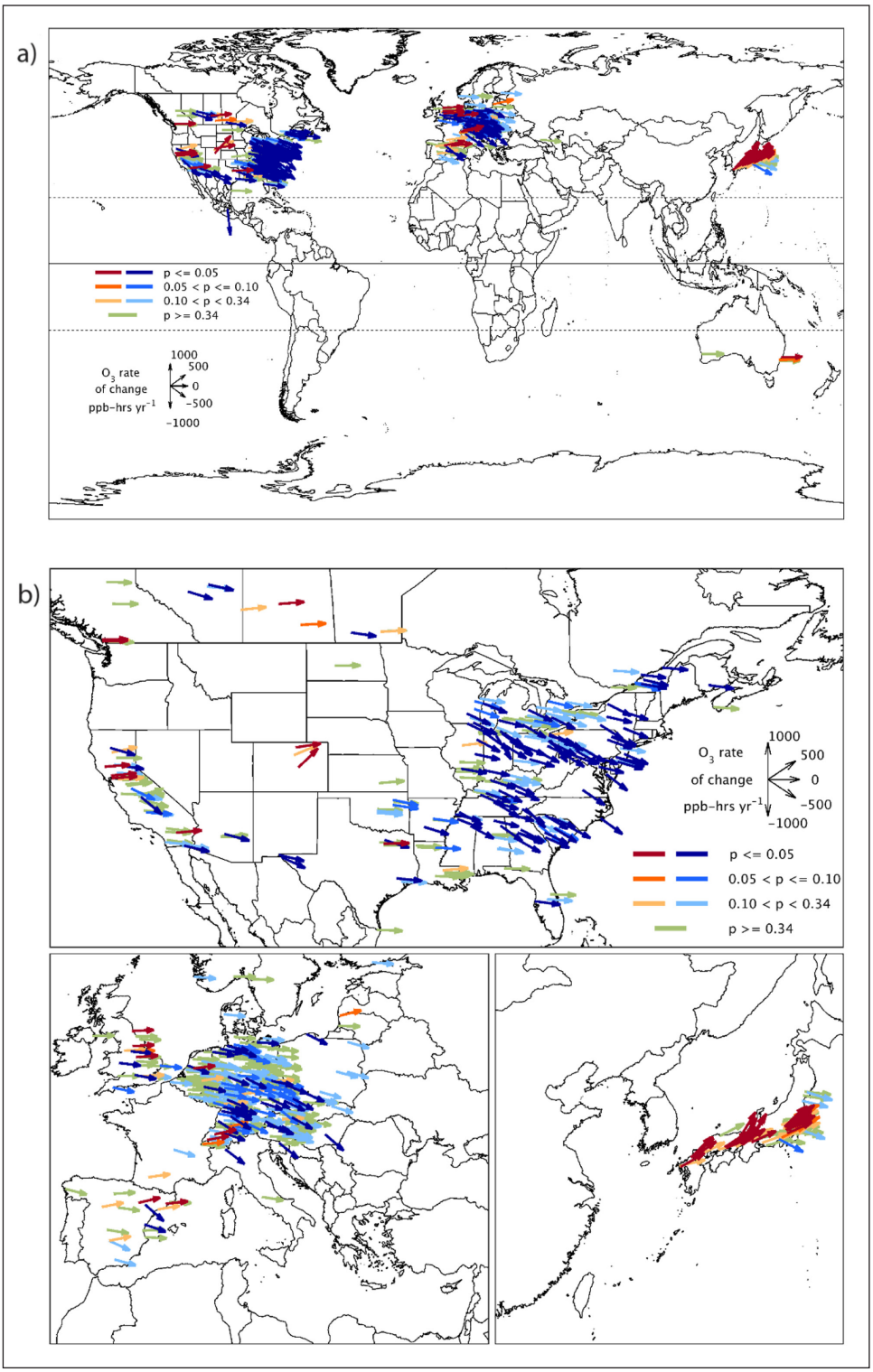

Figure 22: (a) Global and (b) regional trends in W126 (wheat, 3-months), 1995–2014 wheat-growing sites.
DOI: https://doi.org/10.1525/elementa.302.f22

appears to be much more extensively exceeded globally (82.2% of sites) than the NAAQS_Crops (2.1% of sites), even though both are set to protect crops against a 5% yield loss. Thus, the CLRTAP_CL_Crops (AOT40 of 3000 ppb h) appears to be more stringent than the NAAQS_Crops, which from the functions in **Figure 14** based on the wheat dataset, is equivalent to an AOT40 of 14181 ppb h. This finding is in agreement with a comparison of exceedance of air quality standards for central Italy, where the CLRTAP_CL_Crops was exceeded at 98% of monitoring sites in durum wheat-growing areas whilst the NAAQS_Crops was exceeded at only 33% of sites (determined from Figure 2 of De Marco et al., 2010).

The disparity between the sensitivity of CLRTAP CLs and NAAQS may in part reflect differences in their development. The CLRTAP established the AOT40-based CL for crops from a linear relationship between AOT40 and effect on wheat yield using data from field-based open

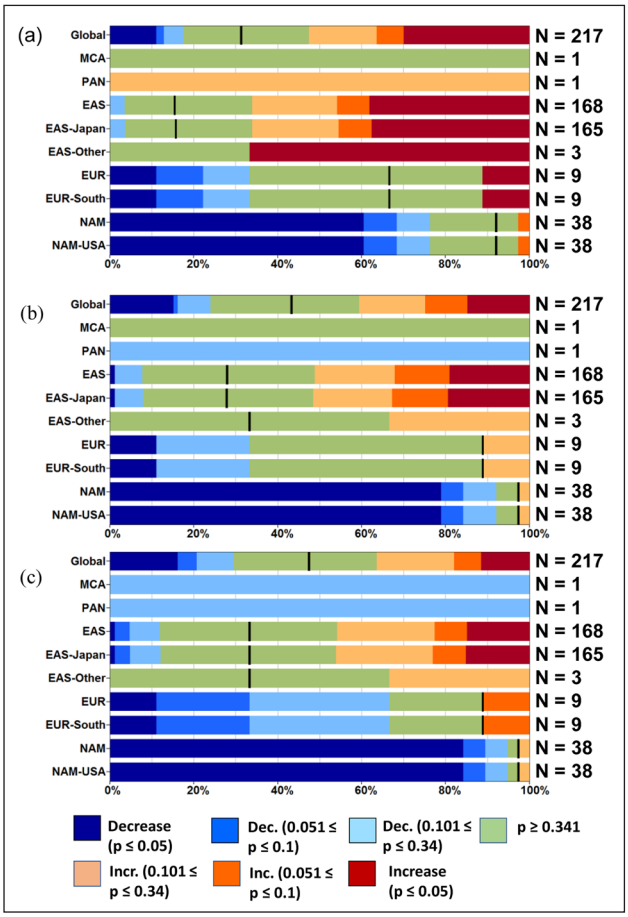

Figure 23: Trends in rice (a) M12 (b) AOT40 and (c) W126, for 1995–2014. Data are presented as the proportion of monitoring sites in rice-growing areas of the different regions and countries with trends in 3-month metrics that: are significantly increasing or decreasing ($p \leq 0.05$); show an indication of an increase/decrease ($0.05 < p \leq 0.1$); have a weak indication of an increase/decrease ($0.1 < p \leq 0.34$), or a weak or no change ($p > 0.34$). Blue colours indicate decreasing trends, green colours no trend and red colours indicate decreasing trends. Colours have been selected to match the arrows in Figures 24–26. DOI: https://doi.org/10.1525/elementa.302.f23

top chamber experiments conducted in Belgium, Finland, Italy and Sweden with 9 cultivars ($r^2 = 0.89$, $p < 0.001$, Mills et al., 2007a). Wheat was selected for deriving the CL as it is: (i) the most relevant crop for agricultural areas in Europe of those identified as ozone sensitive (Mills et al., 2007a); (ii) the most extensively grown crop in Europe (26 million ha in EU28 in 2016, EUROSTAT); (iii) data are included in the response function from experiments covering Mediterranean through to northern climates; and (iv) wheat has the strongest linear relationship with AOT40 compared to other crops (with the exception of watermelon, Mills et al., 2007a). In contrast, the US EPA has found that a non-linear Weibull function fits experimental data from open-top chamber experiments conducted for 10 representative crops in the USA (Heagle, 1989; US Federal Register, 2015). When considering all of the response functions, the 5% yield loss level was set for wheat, a crop of average sensitivity to ozone, with potato, kidney bean, soybean and cotton being more sensitive than wheat, and peanut, sorghum and barley being less sensitive than wheat at 15000 ppb-hrs. As the shape of the fitted response function varies per crop, the relative sensitivity changes as W126 increases, with kidney bean and wheat being the most sensitive crops at higher W126 values, particularly those in excess of 30000 ppb-hrs. As discussed later (Section 4.6), the effect of measurement height may also partially explain these differences as the CLRTAP CL considers canopy height ozone (e.g. 1 m for crops) whilst the W126 values of concern are calculated at ozone monitor inlet height.

The AOT40-based CLs for crops and perennial vegetation are extensively exceeded across the USA, with the highest exceedances of more than three times the CLs occurring in central and western states. This CL is also exceeded by up to three times in parts of Canada, particularly in S Ontario and in the southern Prairies. Vegetation is least at risk along western coastal areas of NAM, in southern parts of Florida, western areas along the Canada-USA border and northern provinces of Canada. Exceedance of the NAAQS_Crops (W126 of 15000 ppb-hrs over 3-months) is very limited in NAM, with occasional exceedances occurring in the central state of Colorado and inland areas of California. In EUR, the areas of AOT40 CL exceedance for crops and perennials fall roughly below a line starting along the N coast of France, Belgium and Germany and extending into southern Sweden. AOT40 values are four or more times the CLs in central and southern areas of Spain, southern France, most areas of northern Italy and at monitoring sites in countries such as Slovakia, Slovenia, Croatia, and Greece. The area of high exceedance extends throughout the Mediterranean basin and includes sites in Malta, Israel and Macedonia, indicating high potential risk to vegetation especially if irrigation is used. Exceedance of the NAAQS_Crops occurs occasionally in the areas with the highest AOT40 values.

There are currently no policy-related thresholds in use for vegetation in EAS or SEA, with air pollution reduction initiatives being focussed only on health impacts (see *TOAR-Health*). Nevertheless, *TOAR-Vegetation* shows extensive exceedance of the CLRTAP_CL_Perennials in Japan and the Republic of Korea, often by more than three times, with similar levels of exceedance occurring at monitoring sites in mainland China, N India and Taiwan. The potential risk to wheat in the Republic of Korea was not included as the GAEZ dataset indicated no production of the crop in 2000, the most recent year available for crop distribution data. This is supported by FAO (Food and Agriculture Organisation) statistics showing that wheat production in this country was very low in 2000 at 2,339 tonnes, although production had increased to 39,116 tonnes by 2010 (FAOSTAT). The risk of ozone damage to wheat is potentially large for Japan with values frequently four times the CL and it is highly likely that a similar level of risk occurs in the current wheat-growing areas of the Republic of Korea. In both the Republic of Korea and Japan, rice is by far a more important crop than wheat, being grown on 71 and 8 times the area of

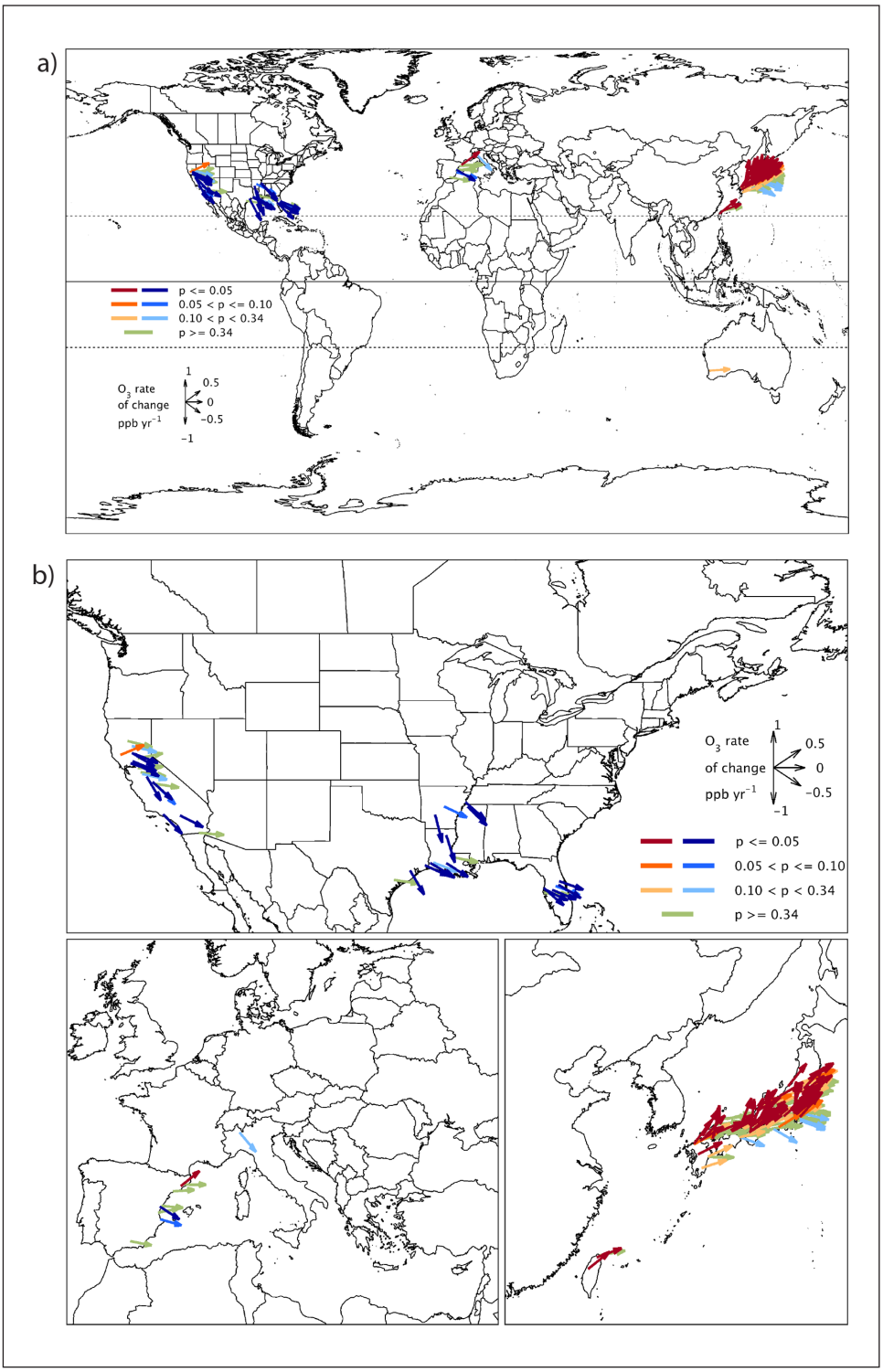

Figure 24: (a) Global and (b) regional trends in M12 (rice, 3-months), 1995–2014, rice growing sites. DOI: https://doi.org/10.1525/elementa.302.f24

wheat in the two countries, respectively (2010, FAOSTAT). *TOAR-Vegetation* shows that the 5% effect threshold of an AOT40 of 12800 ppb h (Mills et al., 2007a) is exceeded in a higher proportion of sites in Japan than in the Republic of Korea (24.7 compared to 3.7%). An assessment of yield losses in rice in Japan based on monitoring data suggested that losses of 9% may have occurred in 2005 (Amin, 2014), and losses could be even higher now. Exceedance of an AOT40 of 12800 ppb h also occurs at several of the sites in the other rice-growing countries, including in 3 of the 6 rice-growing sites in China. Given the extensive exceedance of AOT40-based CLs for vegetation in parts of Asia, there is a growing need to quantify effects using region-specific thresholds and metrics. For some countries, such as China (Feng et al., 2012, 2014; Hu et al., 2015), a large body of suitable evidence is emerging from experimental studies that could be used in such an analysis.

Countries of Eastern Europe, Caucasus and Central Asia (EECCA, http://www.oecd.org/env/outreach/listofeeccacountries.htm) are poorly represented in TOAR, limited

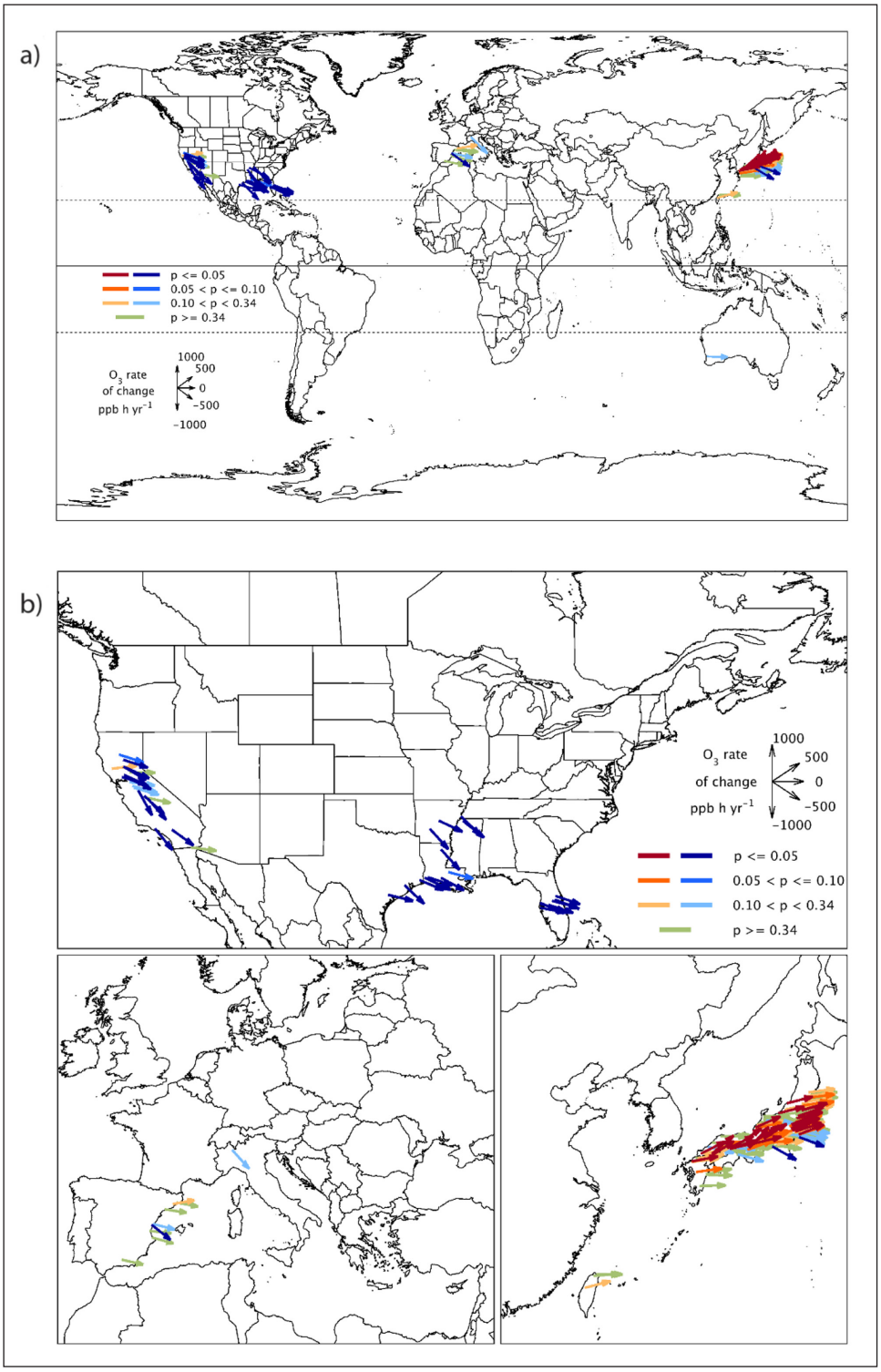

Figure 25: (a) Global and (b) regional trends in AOT40 (rice, 3-months), 1995–2014, rice growing sites. DOI: https://doi.org/10.1525/elementa.302.f25

to one high elevation site (>2000 m) each in Armenia and the Russian Federation and none in the other 10 countries. The site in Armenia has the greatest potential threat from ozone to perennial vegetation having a 6-month AOT40 of 31231ppb h, with lower risk of effects at the site in the Russian Federation (e.g. a 6-month AOT40 of 12868 ppb h). As these are both high elevation sites, they are unlikely to be representative of the ozone conditions in all areas with perennial vegetation in each country. Of the very few sites south of the equator, almost all showed small exceedance of the CL for effects of ozone on perennials. As discussed earlier, where trees are taller than measurement height, the risk of ozone damage could be higher than indicated in *TOAR-Vegetation*, whilst lower effects might be expected for shorter perennial vegetation such as some grassland types. For wheat, the only SH sites were in Chile, Australia and New Zealand, where the AOT40-based CL or the W126 limit is not exceeded, suggesting that there

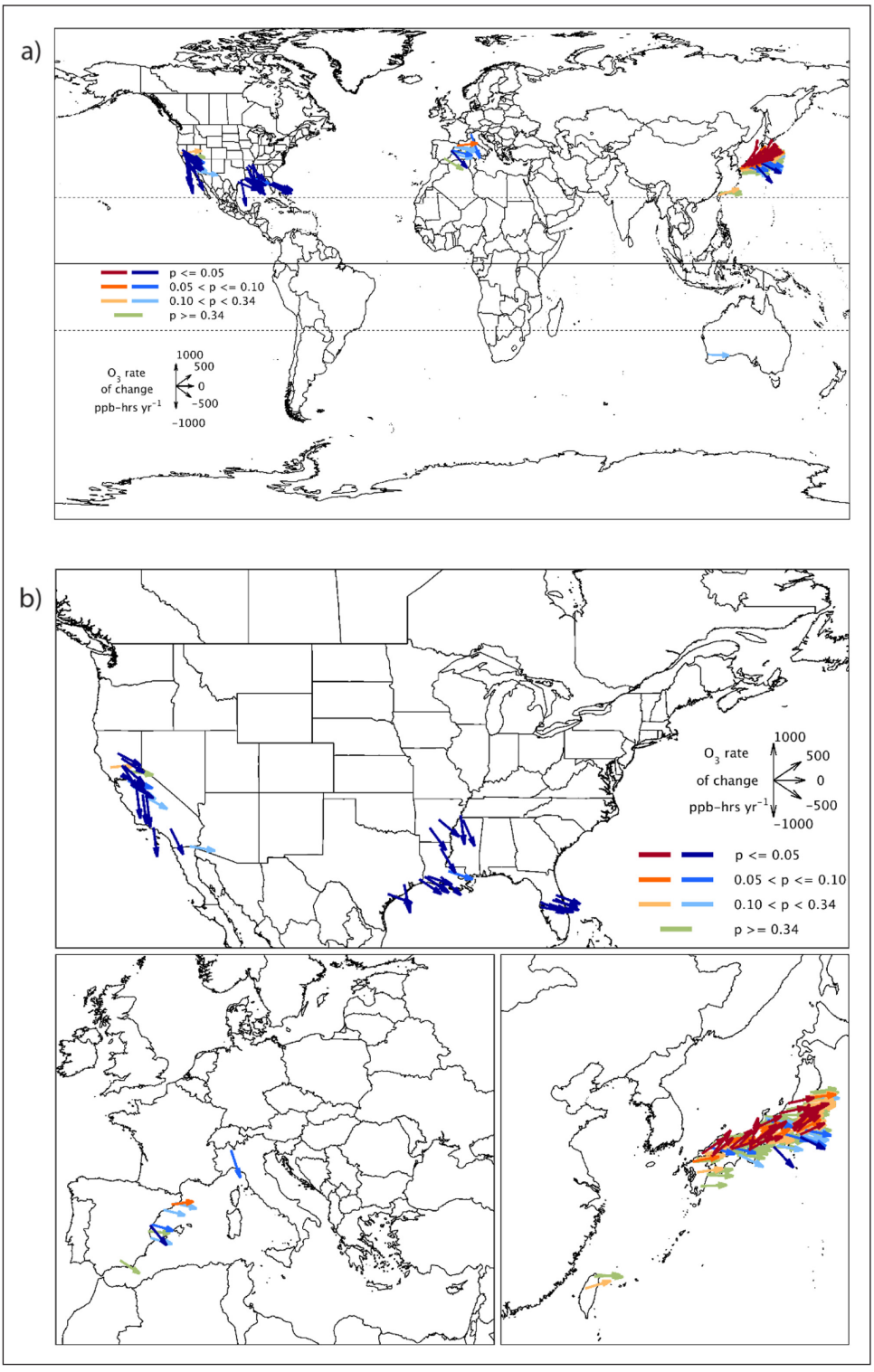

Figure 26: (a) Global and (b) regional trends in W126 (rice, 3-months), 1995–2014, rice growing sites. DOI: https://doi.org/10.1525/elementa.302.f26

is currently no risk of yield loss due to ozone. Similarly, the few SH rice-growing sites did not have AOT40 values above the 5% yield loss threshold (Mills et al., 2007a).

Thus, *TOAR-Vegetation* Recommendation (4) is that, especially in countries and regions where these are not already available, the development of policy-relevant indicators or thresholds would facilitate a scientifically sound assessment of the extent of current impacts of ozone on vegetation that is either monitoring or modelling based. Continued development of such thresholds is also recommended for countries and regions where they already exist to reflect new scientific developments (**Table 7**).

4.4. Comparison with modelled distributions of ozone

At the coarsest resolution, the distribution of areas identified in *TOAR-Vegetation* as having vegetation at low or high risk of damage from ozone largely matches that predicted

Table 7: Recommendations from *TOAR-Vegetation*. DOI: https://doi.org/10.1525/elementa.302.t7

1. Improved scientific understanding of the impacts of ozone on vegetation in vulnerable and developing regions would require increased ozone monitoring at rural sites in South and East Asia, South America and Africa, especially in areas at high risk of ozone exposure.
2. In many such areas, peri-urban agriculture can also be of large importance, especially for people living on a low income. These areas may experience very high ozone exposure and should be specifically considered with respect to ozone effects on food security in future investigations.
3. Mountain/upland areas are known to experience higher ozone levels than adjacent areas at low altitude. Future design of monitoring networks and assessments of ozone effects on vegetation should consider the special conditions of mountains and the underrepresentation of high elevation areas in current monitoring.
4. In countries and regions where these are not already available, the development of policy-relevant indicators or thresholds could facilitate a scientifically sound assessment of the extent of current impacts of ozone on vegetation that is either monitoring or modelling based. Continuing development of such thresholds is also recommended for countries and regions where they already exist to reflect new scientific developments.
5. Improved scientific understanding of the impact of ozone on vegetation across broad spatial scales and over long time-periods (decadal or more) would require the development of new vegetation monitoring networks and the strengthening of existing networks.
6. Height of the monitoring inlet should be included in the next phase of TOAR to facilitate conversion of ozone metrics to canopy height to add further certainty to the risks identified.
7. The TOAR community should consider how to include stomatal uptake-based indicators in the next phase of work for the programme, including collation of additional meteorological and NO_x data within the database.
8. A more complete global assessment of ozone impacts on vegetation should be conducted in the future, using an expanded TOAR dataset and an innovative integration of observations and modelling, including stomatal uptake of ozone.

by global modelling of M12, AOT40 or W126 (Avnery et al., 2011; Chuwah et al., 2015; Fuhrer et al., 2016; Hollaway et al., 2012; Van Dingenen et al., 2009;). However, the high values for ozone metrics in *TOAR-Vegetation* at SEA sites tend to be underestimated in modelling studies. It is more difficult though to align measurements included in *TOAR-Vegetation* with modelled data due to uncertainties introduced by comparing site-specific data with grid square values presented at resolutions of 2.8° × 2.8° (Avnery et al., 2011; Hollaway et al., 2012) or 3° × 2° (Chuwah et al., 2015). Differences in the years used also confound detailed comparisons as the global modelling studies tend to have used earlier years such as 2000 (Avnery et al., 2011; Fuhrer et al., 2016; Hollaway et al., 2012) or 2005 (Chuwah et al., 2015) whilst *TOAR-Vegetation* provides 5-year means for the period 2010–2014.

To gain some impression of how well global or regional modelling represents the current measured ozone distribution, we focus on AOT40 for wheat in southern EUR. Here, the TOAR dataset indicates that values are frequently in the range 9000–15000 ppb h, and occasionally > 15000 ppb h. Whereas there are differences in the spatial patterns of measured and modelled values, modelled AOT40 values were in a similar range in southern France and Italy to the TOAR observations in two studies (10000–15000 ppb h, Avnery et al., 2011, and 7000–15000 ppb h, Chuwah et al., 2015). In another global study, however, little spatial variation in AOT40 was predicted over Europe, with crop AOT40 values approximately in the range 2000–4500 ppb h (Hollaway et al., 2012). At the regional scale, predictions using the EMEP MSC-W model (Simpson et al., 2012) for 3 m height (more closely aligned with the data in the TOAR database than canopy height ozone usually used by EMEP when using the CLRTAP recommendations for AOT40) provide better spatial agreement with the TOAR dataset for EUR (Simpson et al., 2007). This latter modelling study predicted AOT40 values in southern Europe in the year 2000 to be mostly in the range 6000–12000 ppb h, rising to 12000–18000 ppb h in N Italy. From a model validation perspective, it would be useful for the next phase of TOAR to include canopy height measurements, and data from simultaneous measurements of NO_x and meteorological factors affecting ozone deposition. NO_x data would provide valuable data for untangling the role of local NO_X emissions in controlling ozone concentrations. Whilst simultaneous measurement data may not be available for all sites, such data are typically available from sites around the world where carbon fluxes are routinely measured.

4.5. Long-term trends in vegetation metrics for ozone

TOAR-Vegetation also provides a unique opportunity to examine trends in ozone metrics over 15- and 20-year periods (see Chang et al., 2017 and *TOAR-Metrics* for sources of uncertainty in the trends analysis). A full analysis of regional trends in the TOAR data in NAM, EUR and EAS is provided in Chang et al. (2017). From a vegetation impacts perspective, it is most striking from all of the vector maps and bar charts included here, that the dominant trends are region-specific over the period 1995–2014. In NAM, the dominant trend is for a significant decrease in ozone, whilst in EUR there is no change and in EAS there is a significant increase in ozone. For example, the more than halving of AOT40 in the eastern USA, including an annual decrease of 500–1000 ppb h per year over the period 1995–2014 indicates a substantial reduction in the potential risk of damage to perennial vegetation due to ozone. These falling peak ozone levels are associated with reductions in the occurrence of visible ozone injury on the leaves of native plants growing in undisturbed openings in forests during 1994–2009 (Smith, 2012). It has not been possible to match changes in ozone metrics detected in *TOAR-Vegetation* with other ozone injury

surveys conducted elsewhere as these have been more spatially and temporally sporadic and/or for shorter time periods. Nevertheless, collation of field evidence does have an important role to play in showing where there is damage in areas predicted to have a risk of effects (e.g. Fuhrer et al., 2016; Mills et al., 2011a; Braun et al., 2014) or in areas where monitoring data are limited (e.g. Emberson et al., 2009). *TOAR-Vegetation* Recommendation (5) is that improved scientific understanding of the impact of ozone on vegetation across broad spatial scales and over long time-periods (decadal or more) would require the development of new vegetation monitoring networks and the strengthening of existing networks (**Table 7**).

At a substantial number of sites, there is a discrepancy between trends in the three metrics, due to each metric focusing on different ranges of the observed ozone distribution. For example, in NAM and EUR, where regional ozone precursor emissions decreased substantially during 1995–2014 due to national, EU and CLRTAP pollution control policies (CLRTAP, 2016), for all vegetation types, far more sites have decreasing trends in AOT40 and W126 than M12. Indeed, some rural areas show increasing M12, particularly when averaged over 3-months for rice (10–20% of rice-growing sites), which tend to capture the highest ozone periods of the year. AOT40 and particularly W126 are determined to a greater extent by high ozone during pollution episodes compared with the M12 metric, and therefore their reductions reflect the decreases in regional precursor emissions (see *TOAR-Metrics* for further details). Changes in M12, on the other hand, are more indicative of changes across the full ozone distribution, including increases in lower ozone levels linked to regional decreases of NO_x emissions across EUR and NAM resulting from successful abatement strategies (Chang et al., 2017; CLRTAP, 2016; Paoletti et al., 2014; Simon et al., 2015; *TOAR-Climate*; *TOAR-Metrics*). The consequences of this shift in ozone profile for vegetation require further study as almost all published experimental studies have exposed plants to simulated high peak, low background diurnal profiles. Where the effects of different profiles have been studied, increased background profiles had a similar effect on biomass to low background/medium peak treatments in grassland species (Hayes et al., 2010) and yield in wheat (Harmens et al., 2018), with the latter study showing a strong correlation between crop loss and accumulated stomatal flux of ozone, regardless of ozone profile.

Globally, positive ozone trends are most prevalent in EAS across all three metrics. Data availability in *TOAR-Vegetation* is almost exclusively from Japan for the longest time-period, with sufficient data from the Republic of Korea available for the 2000–2014 trend assessments. Ozone effects on crops and trees have been observed during this time-period in Japan, either from field observations of visible injury or by showing the beneficial effect of reducing ambient ozone levels in open-top chambers (Watanabe et al., 2016; Yonekura and Izuta, 2016). Both studies highlight the need to consider the stomatal flux of ozone in risk assessment for all types of vegetation in Japan, as high vapour pressure deficit (i.e. low humidity) and low soil moisture in some regions may mean that effects are not as high in rain-fed vegetation as indicated by increasing ozone metrics based on ambient observations. The only other trends data available for 1995–2014 for EAS were for one site each in NW mainland China and Hong Kong and for two sites in Taiwan, all indicating increasing risk of damage to perennial vegetation. Model projections of surface ozone mixing ratios in 2030 indicate that if emissions continue to increase, generally following the RCP8.5 scenario, then annual mean surface ozone will increase by 2–5 ppb across most of South and East Asia, with even greater increases across India (Wild et al., 2012; Young et al., 2013). Given that the monitoring data available in *TOAR Vegetation* indicates that some of the highest vegetation ozone exposures globally currently occur in these regions, such model projections suggest that the most severe ozone exposures in the future (through 2030) will most likely occur in these region.

Over the 15- and 20- year time-periods included in *TOAR-Vegetation*, data availability was limited for SH trends analysis. In Australia, small increases in M12 were evident at several sites with the perennials W126 decreasing at some sites. M12 was also increasing in South Africa and had a weak indication of an increase in Chile. The implications of these small changes for vegetation are difficult to ascertain.

4.6. Sources of uncertainty in the TOAR-Vegetation analysis

After a comprehensive global effort, the TOAR dataset includes all currently available ozone monitoring data in vegetated areas around the world. Sources of systematic errors and uncertainty associated with the dataset are described in detail in *TOAR-Surface Ozone Database*. Whilst preparing the data for the vegetation metrics presented in this paper, we made several assumptions and used selection criteria that have some influence on the conclusions drawn.

An important source of uncertainty for the vegetation metrics arises from the fact that the ozone monitor inlets are not always at the ideal height for different types of vegetation and that this height varies from site to site and is not documented in TOAR. Ozone levels near the ground exhibit a significant logarithmic gradient as a function of height, especially over vegetation surfaces with low roughness such as crops (Pleijel et al., 1995; Sofiev and Tuovinen, 2001). This gradient has particularly marked effects on accumulated metrics such as AOT40 and W126 where a consistent small change in ozone can have a magnified effect on the final value (Pleijel et al., 1995; Sofiev and Tuovinen, 2001). For trees, the difference between the measured ozone level at a monitoring station over grassland and the level at the top of a 30m tree canopy varies according to atmospheric stability, time of day and growing season (Gerosa et al., 2017). As we did not know the measurement height at the TOAR sites, we could not correct all data to one height per vegetation type using standard methods (e.g. CLRTAP, 2017) and could not quantify how much of an impact this source of uncertainty has on the data presented here. It is likely

that at measurement heights of 3–10 m, metrics for crops and low-growing grassland are overestimating the risk of effects at canopy height, whilst those for trees are underestimating risk. Because of this unquantifiable uncertainty, *TOAR-Vegetation* Recommendation (6) is that the height of the monitoring inlet should be included in the next phase of TOAR to facilitate conversion of ozone metrics to canopy height to add further certainty to the risks identified (**Table 7**).

In mapping exceedance of CLRTAP CLs and US NAAQS for vegetation, the assumption is made that all vegetation of a specified type or species is equally sensitive to ozone and that the accumulation or averaging periods are the same in all areas of the world. Collation of field evidence of effects (Emberson et al., 2009) and comparison of response functions (Osborne et al., 2016) indicate that crop varieties grown in Asia may have greater sensitivity to ozone. However, both studies acknowledged that other factors such as local environmental conditions and other pollutants may have an as yet, unquantifiable impact on such conclusions. Vegetation responses in any specific location will also be influenced by variation in ozone sensitivity between cultivars of crops (e.g. Mills et al., 2007a) as well as within and between species of trees (e.g. Büker et al., 2015; Hu et al., 2015; Xu et al., 2017) and grasslands (e.g. Calvete-Sogo et al., 2016; Hayes et al., 2007).

By necessity, we have standardised the accumulation or averaging period for each site to 3- or 6-months depending on vegetation type. In warmer regions, crop growth cycles are completed more quickly and therefore a shorter time period would be more appropriate, e.g. 75 rather than 90 days has been used for wheat and rice in India and China (Tang et al., 2013). Similarly for trees, use of hemispheric-specific 6-month periods is simplistic and does not reflect the spatially varying start and end of growing season with latitude, altitude and aspect (Anav et al., 2017). Our selection criteria for site inclusion for each vegetation type may have also introduced some uncertainty. Use of all non-urban categories for perennial vegetation also includes some sites that are "unclassified" within TOAR that could be considered urban (see *TOAR-Surface Ozone Database*). For crop production data, we used the GAEZ dataset for the year 2000, whilst present-day ozone values are averaged for the period 2010–2014. As discussed in Section 4.3, this meant that no wheat sites were included for the Republic of Korea. Where there has been urban spread since the year 2000, this approach may also have introduced some sites into the crop datasets that are in urban fringes that could be strongly influenced by local emissions. For example, some of the sites in Japan with high rice production fall into the urban category as defined in *TOAR-Surface Ozone Database*.

A further source of uncertainty in interpreting the maps presented here is that *TOAR-Vegetation* only includes measured concentration-based metrics. These give an indication of the maximum risk to vegetation assuming all climate, soil and plant factors that might influence the uptake of the pollutant through the stomatal pores are non-limiting. Thus, concentration-based metrics only provide the most reliable estimates of vegetation risk in climatic conditions where stomatal uptake is likely to be optimal during the main parts of the growing season such as in moist climates where rainfall is sufficient, or drier climates where irrigation is used to supplement rainfall. An analysis of field evidence of ozone damage to vegetation (visible injury, growth and yield effects) in 17 European countries showed that effects were better correlated with modelled stomatal flux than AOT40 (Mills et al., 2011a). In particular, stomatal flux provides a better indication of ozone effects in the northern third of Europe where moderate ozone concentrations coincided with conditions highly conducive to ozone uptake and the AOT40-based CL was not exceeded. In the *TOAR-Vegetation* dataset, the highest AOT40 and W126 values were found in warm temperate dry climates in NAM (e.g. mean of 21470 ppb h and 22987 ppb-hrs for perennials, respectively) and EUR (e.g. mean of 15888 ppb h and 14814 ppb-hrs for perennials, respectively). Here, the highest risk would be to irrigated crops whilst non-irrigated crops and perennial species might have reduced risk in these climates due to partial stomatal closure. In SEA, almost all of the perennial sites are in warm temperate moist climates where there might be less restriction on ozone uptake for several months of the growing season, and mean AOT40 and W126 values of 16073 ppb h and 18609 ppb-hrs, respectively for the perennial metrics might provide a good indication of potential risk.

These sources of uncertainty should be considered in the next phase of TOAR with the aim of progressing beyond quantifying the extent of exceedance of CLs/values of concern to quantifying the magnitude of effects predicted for each site. To achieve this, *TOAR Vegetation* has two further recommendations (**Table 7**). *TOAR-Vegetation* Recommendation (7) is for the TOAR community to consider how to include stomatal uptake-based indicators in the next phase of the programme, including collation of additional meteorological and NO_x data within the database. Such an approach would require additional stomatal conductance measurements to be made in some regions of the world to provide regional or local flux model parameterisation. *TOAR-Vegetation* recommendation (8) is that a more complete global assessment of ozone impacts on vegetation should be conducted in the future, using an expanded TOAR dataset and an innovative integration of observations and modelling, including the stomatal uptake of ozone.

5. Summary and conclusions

TOAR-Vegetation reports on the present-day global distribution of ozone at over 3300 vegetated sites across the world and long-term trends at nearly 1200 sites. As such, the TOAR database provides a unique opportunity to assess the potential threat from ozone pollution to vegetation based on measurements rather than modelling. The highest values for ozone metrics related to vegetation are in mid-latitudes of the NH where the density of ozone monitoring has also been greatest, reflecting long-standing national concerns about the potential impacts of the pollutant. Some countries of the NH such as China and India where modelling has indicated an impact of ozone on vegetation, have only been able to provide limited ozone monitoring

data to TOAR for rural areas. SH data availability is also very sparse, limiting the regional scope of any conclusions drawn for this hemisphere. Nevertheless, *TOAR-Vegetation* has provided a unique insight into current knowledge of the exposure of vegetation to ozone pollution around the world based on actual monitoring data.

We have shown that ozone CLs for vegetation implemented in the 51 signatory countries of the CLRTAP are extensively exceeded in many regions of NAM, EUR and EAS. The highest CL exceedance is in S USA, in countries around the Mediterranean basin, N India, NW and E China, the Republic of Korea and Japan. The lowest values for vegetation-specific metrics tend to be in Australia and New Zealand, southern parts of South America and northern areas of Europe, Canada and the USA. Whilst W126 and AOT40 have been decreasing at many sites in NAM and EUR, at some sites in these regions the M12 values have been increasing. Further research is needed to understand the basis of these changes in relation to hemispheric transport of precursors (Gaudel et al., 2018) and changes in NO titration of ozone, as well as the consequences for vegetation.

A series of recommendations have been made based on the findings of *TOAR-Vegetation* (**Table 7**) to facilitate a more complete global assessment of ozone impacts on vegetation in the future. Of particular relevance for rapidly developing regions would be an increase in monitoring of ozone, especially in rural, upland and peri-urban areas, establishment of region specific thresholds and indicators of damage, and a coordinated effort to collate field evidence to understand how vegetation is responding to changing air quality. We also recommend that for assessment of risk of damage to vegetation it is important to know the canopy height ozone level and have access to other information such as NO_x observations and meteorological conditions, where available. Lastly, keeping in mind that many plant and environmental factors influence the uptake and thus effect of ozone, *TOAR-Vegetation* recommends considering how to incorporate stomatal-flux based metrics within the TOAR database in the future.

Data Accessibility Statement

General access to TOAR data is free and unrestricted through the JOIN web interface (https://join.fz-juelich.de/) and its associated REST service (see documentation at https://join.fz-juelich.de/services/rest/surfacedata/). In addition, all of the database metrics and figures have been uploaded to the PANGAEA data publisher, where the products are permanently archived. The URL is https://doi.org/10.1594/PANGAEA.876108. All use of TOAR surface ozone data should include a reference to *TOAR-Surface Ozone Database*.

Supplemental Files

The supplemental files for this article can be found as follows:

- **Figure S-1.** Climatic zones in the (a) wheat and (b) rice growing areas of the world. DOI: https://doi.org/10.1525/elementa.302.s1
- **Figure S-2.** Correlations between metrics for perennial vegetation. DOI: https://doi.org/10.1525/elementa.302.s1
- **Figure S-3.** Stylised 24 h mean ozone profile to illustrate the effect of measurement height on ozone value. DOI: https://doi.org/10.1525/elementa.302.s1
- **Figure S-4.** Trends in (a) M12, (b) AOT40 and (c) W126 over a 6-month growing season for perennials at all non-urban sites for the period 2000–2014. DOI: https://doi.org/10.1525/elementa.302.s1
- **Figure S-5.** Trends in (a) M12 (b) AOT40 and (c) W126 over a 3-month wheat growing season at wheat growing sites for the period 2000–2014. DOI: https://doi.org/10.1525/elementa.302.s1
- **Figure S-6.** Trends in (a) M12 (b) AOT40 and (c) W126 over a 3-month rice growing season at rice growing sites for the period 2000–2014. DOI: https://doi.org/10.1525/elementa.302.s1
- **Table S-1.** Mean and standard deviation (SD) for M12, AOT40 and W126 for the 6-month summer period (2010–2014), by country. DOI: https://doi.org/10.1525/elementa.302.s1
- **Table S-2.** Present-day perennial vegetation metrics, by climatic zone for North America (NAM), Europe (EUR) and East Asia (EAS), presented as 6-month values, mean and standard deviation (SD) for 2010–2014). DOI: https://doi.org/10.1525/elementa.302.s1
- **Table S-3.** Mean and standard deviation (SD) for M12, AOT40 and W126 for the 3-month wheat period (2010–2014), by country. DOI: https://doi.org/10.1525/elementa.302.s1
- **Table S-4.** Present-day wheat metrics, by climatic zone for North America (NAM), Europe (EUR) and East Asia (EAS) (3-month values mean and standard deviation (SD) for 2010–2014). DOI: https://doi.org/10.1525/elementa.302.s1
- **Table S-5.** Mean and standard deviation (SD) for M12, AOT40 and W126 for the 3-month rice period (2010–2014), by country. DOI: https://doi.org/10.1525/elementa.302.s1
- **Table S-6.** Present-day rice metrics, by climatic zone for North America (NAM), Europe (EUR) and East Asia (EAS) (3-month values mean and standard deviation (SD) for 2010–2014). DOI: https://doi.org/10.1525/elementa.302.s1
- **Table S-7.** The effect of change in measurement height on 3-month and 6-month AOT40, calculated using the conversion factors in CLRTAP (2017) for a representative ozone gradient over a 1m high crop or 20m high tree. DOI: https://doi.org/10.1525/elementa.302.s1
- **Text S-1.** Analysis of the statistical differences between the NAM, EUR and EAS regions for perennial metrics. DOI: https://doi.org/10.1525/elementa.302.s1
- **Text S-2.** Analysis of the statistical differences between the NAM, EUR and EAS regions for wheat metrics. DOI: https://doi.org/10.1525/elementa.302.s1
- **Text S-3.** Analysis of the statistical differences between the NAM, EUR and EAS regions for rice metrics. DOI: DOI: https://doi.org/10.1525/elementa.302.s1

Acknowledgements and Funding information

This work is part of the Tropospheric Ozone Assessment Report (TOAR) which has been supported by the International Global Atmospheric Chemistry (IGAC) project, the National Oceanic and Atmospheric Administration (NOAA), Forschungszentrum Jülich, and the World Meteorological Organization (WMO). GM, KS and HH acknowledge the Natural Environment Research Council (NERC project NEC06476) and GM thanks the Adlerbertska Foundation for supporting this study by funding her Guest Professorship at the University of Gothenburg (NERC project NEC05831). EP acknowledges the LIFE15 project MOTTLES (ENV/IT/000183). FZZ acknowledges Key Research Program of Frontier Sciences, CAS (QYZDB-SSW-DQC019). HP acknowledges support from the BECC Strategic Research Area (http://www.becc.lu.se/).

Competing interests

The authors have no competing interests to declare.

Author contributions

- Substantial contributions to conception and design: GM, ORC, MGS, CM, HP, DS, HN, EP, BS, ZF
- Acquisition of data: MGS, VS, XX, KS
- Analysis and interpretation of data: GM, HP, ORC, CM, VS, BS, DS, EP, HN, KS
- Drafting the article or revising it critically for important intellectual content: all
- Final approval of the version to be published: all

References

Ainsworth, EA. 2016. Understanding and improving global crop response to ozone pollution. *The Plant Journal* **90**: 886–897. DOI: https://doi.org/10.1111/tpj.13298

Ainsworth, EA, Yendrek, CR, Sitch, S, Collins, WJ and **Emberson, LD.** 2012. The effects of tropospheric ozone on net primary productivity and implications for climate change. *Annu Rev Plant Biol* **63**: 637–661. DOI: https://doi.org/10.1146/annurev-arplant-042110-103829

Amin, N. 2014. Effect of ozone on the relative yield of rice crop in Japan evaluated based on monitored concentrations. *Water Air Soil Poll* **225**: 1797–1806. DOI: https://doi.org/10.1007/s11270-013-1797-5

Anav, A, Liu, Q, De Marco, A, Proietti, C, Savi, F, Paoletti, E and **Pia, S.** 2017. The role of plant phenology in stomatal ozone flux modelling. *Glob Change Biol*. DOI: https://doi.org/10.1111/gcb.13823

Ashmore, MR. 2005. Assessing the future global impacts of ozone on vegetation. *Plant Cell Environ* **28**: 949–964. DOI: https://doi.org/10.1111/j.1365-3040.2005.01341.x

Avnery, S, Mauzerall, DL, Liu, J and **Horowitz, LW.** 2011. Global crop yield reductions due to surface ozone exposure: 1. Year 2000 crop production losses and economic damage. *Atmos Environ* **45**: 2284–2296. DOI: https://doi.org/10.1016/j.atmosenv.2010.11.045

Bassin, S, Volk, M and **Fuhrer, J.** 2007. Factors affecting the ozone sensitivity of temperate European grasslands: An overview. *Environ Poll* **146**: 678–691. DOI: https://doi.org/10.1016/j.envpol.2006.06.010

Bates, D, Maechler, M, Bolker, B and **Walker, S.** 2015. Fitting Linear Mixed-Effects Models Using lme4. *Journal of Statistical Software* **67**(1): 1–48. DOI: https://doi.org/10.18637/jss.v067.i01

Braun, S, Schindler, C and **Rihm, B.** 2014. Growth losses in Swiss forests caused by ozone: Epidemiological data analysis of stem increment of *Fagus sylvatica* L. and *Picea abies* Karst. *Environ Pollut* **192**: 129–138. DOI: https://doi.org/10.1016/j.envpol.2014.05.016

Büker, P, Feng, Z, Uddling, J, Briolat, A, Alonso, R, et al. 2015. New flux based dose-response relationships for ozone for European forest tree species. *Environ Pollut* **206**: 163–174. DOI: https://doi.org/10.1016/j.envpol.2015.06.033

Burney, J and **Ramanathan, V.** 2014. Recent climate and air pollution impacts on Indian agriculture. *Proc Nat Acad Sci* **111**: 16319–16324. DOI: https://doi.org/10.1073/pnas.1317275111

Calvete-Sogo, H, Gonzalez-Fernandez, I, Sanz, J and **Elvira, S.** 2016. Heterogeneous responses to ozone and nitrogen alter the species composition of Mediterranean annual pastures. *Oecologia* **181**: 1055–1067. DOI: https://doi.org/10.1007/s00442-016-3628-z

Chang, K-L, Petropavlovskikh, I, Cooper, OR, Schultz, MG and **Wang, T.** 2017. Regional trend analysis of surface ozone observations from monitoring networks in eastern North America, Europe and East Asia. *Elem Sci Anth.* DOI: https://doi.org/10.1525/elementa.243

Chuwah, C, van Noije, T, van Vuuren, DP, Stehfest, E and **Hazeleger, W.** 2015. Global impacts of surface ozone changes on crop yields and land use. *Atmos Environ* **106**: 11–23. DOI: https://doi.org/10.1016/j.atmosenv.2015.01.062

CLRTAP. 2016. Towards Cleaner Air. Scientific Assessment Report 2016. Maas, R and Grennfelt, P (eds.), *EMEP Steering Body and Working Group on Effects of the Convention on Long-Range Transboundary Air Pollution*, 50. Oslo.

CLRTAP. 2017. Manual on methodologies and criteria for modelling and mapping critical loads and levels and air pollution effects, risks and trends. Chapter 3: Mapping critical levels for vegetation. http://icpvegetation.ac.uk (accessed on 30 October, 2017).

Cooper, OR, Gao, RS, Tarasick, D, Leblanc, T and **Sweeney, C.** 2012. Long-term ozone trends at rural ozone monitoring sites across the United States, 1990–2010. *J Geophys Res Atmos* **117**(D22). DOI: https://doi.org/10.1029/2012JD018261

Cooper, OR, Parrish, DD, Ziemke, J, Balashov, NV, Cupeiro, M, et al. 2014. Global distribution and trends of tropospheric ozone: An observation-based review. *Elem Sci Anth* **2**. DOI: https://doi.org/10.12952/journal.elementa.000029

De Marco, A, Screpanti, A and **Paoletti, E.** 2010. Geostatistics as a validation tool for setting ozone standards for durum wheat. *Environ Pollut* **158**: 536–542. DOI: https://doi.org/10.1016/j.envpol.2009.08.006

Dentener, F and **Guizzardi, D.** 2013. TDHTAP Work Package 2.1. Common set of regions. Available at: http://iek8wikis.iek.fz-juelich.de/HTAPWiki/WP2.1?action=AttachFile&do=view&target=_region_definition_document_v4.docx. Accessed 11 August, 2016.

Derwent, RG, Witham, CS, Utembe, SR, Jenkin, ME and **Passant, NR.** 2010. Ozone in Central England: the impact of 20 years of precursor emission controls in Europe. *Environ Sci Policy* **13**: 195–204. DOI: https://doi.org/10.1016/j.envsci.2010.02.001

EC. 2008. European Council Directive 2008/50/EC of the European Parliament and of the Council of 21 May 2008 on ambient air quality and cleaner air for Europe. *Official Journal of the European Union*, 11.6.2008, L152/1-44.

EC. 2016. European Council Directive (EU) 2016/2284 of the European Parliament and of the Council of 14 December 2016 on the reduction of national emissions of certain atmospheric pollutants, amending Directive 2003/35/EC and repealing Directive 2001/81/EC. http://eur-lex.europa.eu/legal-content/EN/TXT/HTML/?uri=CELEX:32016L2284&from=EN. Accessed 30 October, 2017.

EUSOILS. 2015. The climatic zone layer. http://eusoils.jrc.ec.europa.eu/projects/RenewableEnergy/. Accessed 1 June, 2015.

Emberson, LD, Ashmore, MR, Cambridge, HM, Simpson, D and **Tuovinen, JP.** 2000. Modelling stomatal ozone flux across Europe. *Environ Pollut* **109**: 403–413. DOI: https://doi.org/10.1016/S0269-7491(00)00043-9

Emberson, LD, Büker, P, Ashmore, MR, Mills, G, Jackson, L, et al. 2009. A comparison of North American and Asian exposure-response data for ozone effects on yield. *Environ Pollut* **43**: 1945–1953. DOI: https://doi.org/10.1016/j.atmosenv.2009.01.005

FAOSTAT. www.faostat.fao.org. Accessed October, 2017.

Feng, Z, Sun, J, Wan, W, Hu, E and **Calatayud, V.** 2014. Evidence of widespread ozone-induced visible injury on plants in Beijing, China. *Environ Pollut* **193**: 296–301. DOI: https://doi.org/10.1016/j.envpol.2014.06.004

Feng, Z, Tang, H, Uddling, J, Pleijel, H, Kobayashi, K, et al. 2012. A stomatal ozone flux–response relationship to assess ozone-induced yield loss of winter wheat in subtropical China. *Environ Pollut* **164**: 16–23. DOI: https://doi.org/10.1016/j.envpol.2012.01.014

Fishman, J, Creilson, JK, Parker, PA, Ainsworth, EA, Vining, GG, et al. 2010. An investigation of widespread ozone damage to the soybean crop in the upper Midwest determined from ground-based and satellite measurements. *Atmos Environ* **44**: 2248–2256. DOI: https://doi.org/10.1016/j.atmosenv.2010.01.015

Fleming, ZL, Doherty, RM, von Schneidemesser, E, Malley, CS, Cooper, OR, et al. 2017. Tropospheric Ozone Assessment Report: Present-day ozone distribution and trends relevant to human health. *Elem Sci Anth.* 2018. DOI: https://doi.org/10.1525/elementa.273

Fuhrer, J, Val Martin, M, Mills, G, Heald, CL, Harmens, H, et al. 2016. Current and future ozone risks to global terrestrial biodiversity and ecosystem processes. *Ecol Evol* **6**(24): 8785–8799. DOI: https://doi.org/10.1002/ece3.2568

Fumagalli, I, Gimeno, BS, Velissariou, D, De Temmerman, L and **Mills, G.** 2001. Evidence of ozone-induced adverse effects on crops in the Mediterranean region. *Atmos Environ* **35**: 2583–2587. DOI: https://doi.org/10.1016/S1352-2310(00)00468-4

GAEZ. 2015. Global Agro-ecological Zones v3.0. http://www.gaez.iiasa.ac.at/ (accessed, October 2015).

Galbally, IE, Schultz, MG, Buchmann, B, Gilge, S, Guenther, F, et al. 2013. Guidelines for Continuous Measurement of Ozone in the Troposphere, GAW Report No 209, Publication WMO-No. 1110, ISBN: 978-92-63-11110-4, WMO, Geneva.

Gaudel, A, Cooper, OR, Ancellet, G, Barret, B, Boynard, A, et al. 2017. Tropospheric Ozone Assessment Report: Present-day distribution and trends of tropospheric ozone relevant to climate and global atmospheric chemistry model evaluation. *Elem Sci Anth.* 2018. DOI: https://doi.org/10.1525/elementa.291

Gerosa, G, Marzouli, R, Monteleone, B, Chiesa, M and **Finco, A.** 2017. Vertical ozone gradients above forests. Comparison of different calculation options with direct ozone measurements above a mature forest and consequences for ozone risk assessment. *Forests* **8**: 337. DOI: https://doi.org/10.3390/f8090337

Ghude, SD, Jena, C, Chate, DM, Beig, G, Pfister, GG, et al. 2014. Reductions in India's crop yield due to ozone. *Geophys Res Let* **41**: 5685–5691. DOI: https://doi.org/10.1002/2014GL060930

Granier, C, Bessagnet, B, Bond, T, D'Angiola, A, van der Gon, HD, et al. 2011. Evolution of anthropogenic and biomass burning emissions of air pollutants at global and regional scales during the 1980–2010 period. *Climatic Change* **109**: 163–190. DOI: https://doi.org/10.1007/s10584-011-0154-1

Grünhage, L, Pleijel, H, Mills, G, Bender, J, Danielsson, H, et al. 2012. Updated stomatal flux and flux-effect models for wheat for quantifying effects of ozone on grain yield, grain mass and protein yield. *Environ Pollut* **165**: 147–157. DOI: https://doi.org/10.1016/j.envpol.2012.02.026

Harmens, H, Hayes, F, Mills, G, Sharps, K, Osborne, S, et al. 2018. Wheat yield responses to stomatal uptake of ozone: Peak vs rising background ozone conditions. *Atmos Environ* **173**: 1–5. DOI: https://doi.org/10.1016/j.atmosenv.2017.10.059

Harmens, H and **Mills, G.** 2012. Ozone pollution: Impacts on carbon sequestration in Europe. *Centre*

for Ecology & Hydrogogy. Bangor, UK. ISBN: 978-1-906698-31-7. http://icpvegetation.ceh.ac.uk/. Accessed 30 October, 2017.

Harmens, H and **Mills, G.** 2014. Air Pollution: Deposition to and impacts on vegetation in (South-) East Europe, Caucasus, Central Asia (EECCA/SEE) and South-East Asia. ICP Vegetation Programme Coordination Centre, Centre for Ecology and Hydrology, Bangor, UK. ISBN: 978-1-906698-48-5. http://icpvegetation.ceh.ac.uk/. Accessed 30 October, 2017.

Hayes, F, Mills, G, Jones, L and **Ashmore, M.** 2007. Meta-analysis of the relative sensitivity of semi-natural vegetation species to ozone. *Environ Pollut* **146**: 754–762. DOI: https://doi.org/10.1016/j.envpol.2006.06.011

Hayes, F, Mills, G, Jones, L and **Ashmore, M.** 2010. Does a simulated upland grassland community respond to increasing background, peak or accumulated exposure of ozone? *Atmos Environ* **44**: 4155–4164. DOI: https://doi.org/10.1016/j.atmosenv.2010.07.037

Heagle, AS. 1989. Ozone and crop yield. *Annu Rev Phytopathol* **27**: 397–423. DOI: https://doi.org/10.1146/annurev.py.27.090189.002145

Hollaway, MJ, Arnold, SR, Challinor, AJ and **Emberson, LD.** 2012. Intercontinental trans-boundary contributions to ozone-induced crop yield losses in the Northern Hemisphere. *Biogeosciences* **9**: 271–292. DOI: https://doi.org/10.5194/bg-9-271-2012

Hoshika, Y, Katata, G, Deushi, M, Watanabe, M, Koike, T, et al. 2015. Ozone-induced stomatal sluggishness changes carbon and water balance of temperate deciduous forests. *Scientific Reports* **5**. DOI: https://doi.org/10.1038/srep09871

Hothorn, T, Bretz, F and **Westfall, P.** 2008. Simultaneous inference in general parametric models. *Biometrical Journal* **50**(3): 346–363. DOI: https://doi.org/10.1002/bimj.200810425

Hu, EZ, Gao, F, Xin, Y, Jia, HX, Li, KH, et al. 2015. Concentration- and flux-based ozone dose-response relationships for five poplar clones grown in North China. *Environ Pollut* **207**: 21–30. DOI: https://doi.org/10.1016/j.envpol.2015.08.034

IPCC. 2006. Intergovernmental Panel on Climate Change Guidelines for National Greenhouse Gas Inventories **4**. http://www.ipcc-nggip.iges.or.jp/public/2006gl/vol4.html. Accessed 1 June, 2015.

Karlsson, PE, Braun, S, Broadmeadow, M, Elvira, S, Emberson, L, et al. 2007a. Risk assessments for forest trees – the performance of the ozone flux versus the AOT concepts. *Environ Pollut* **146**: 608–616. DOI: https://doi.org/10.1016/j.envpol.2006.06.012

Karlsson, PE, Klingberg, J, Engardt, M, Andersson, C, Langner, J, et al. 2017. Past, present and future concentrations of ground-level ozone and potential impacts on ecosystems and human health in northern Europe. *Sci Total Environ* **576**: 22–35. DOI: https://doi.org/10.1016/j.scitotenv.2016.10.061

Karlsson, PE, Tang, L, Sundberg, J, Chen, D, Lindskog, A, et al. 2007b. Increasing risk for negative ozone impacts on vegetation in northern Sweden. *Environ Pollut* **150**: 96–106. DOI: https://doi.org/10.1016/j.envpol.2007.06.016

Lal, S, Venkataramani, S, Naja, M, Kuniyal, JC, Mandal, TK, et al. 2017. Loss of crop yields in India due to surface ozone: an estimation based on a network of observations. *Environ Sci Pollut Res* **24**: 20972–20981. DOI: https://doi.org/10.1007/s11356-017-9729-3

Lefohn, AS, Lawrence, JA and **Kohut, RJ.** 1988. A comparison of indices that describe the relationship between exposure to ozone and reduction in the yield of agricultural crops. *Atmos Environ* **22**: 1229–1240. DOI: https://doi.org/10.1016/0004-6981(88)90353-8

Lefohn, AS, Malley, CS, Simon, H, Wells, B, Xu, X, et al. 2017. Responses of human health and vegetation exposure metrics to changes in ozone concentration distributions in the European Union, United States, and China. *Atmos Environ* **152**: 123–145. DOI: https://doi.org/10.1016/j.atmosenv.2016.12.025

Lefohn, AS, Malley, CS, Smith, L, Wells, B and **Hazucha, M.** 2018. Tropospheric Ozone Assessment Report: Global ozone metrics for climate change, human health, and crop/ecosystem research. *Elem Sci Anth.* DOI: https://doi.org/10.1525/elementa.279

Lewis, AC, von Schneidemesser, E and **Peltier, R.** 2018. Low-cost sensors for the measurement of atmospheric composition: Overview of topic and future applications. World Meteorological Organization. https://www.wmo.int/pages/prog/arep/gaw/documents/Draft_low_cost_sensors.pdf.

Malley, CS, Heal, MR, Mills, G and **Braban, CF.** 2015. Trends and drivers of ozone human health and vegetation impact metrics from UK EMEP supersite measurements (1990–2013). *Atmos Chem Phys* **15**: 4025–4042.

Matyssek, R, Gunthardt-Goerg, MS, Maurer, S and **Keller, T.** 1995. Nighttime exposure to ozone reduces whole-plant production in *Betula pendula*. *Tree Physiol.* **15**: 159–165. DOI: https://doi.org/10.1093/treephys/15.3.159

McLaughlin, SB, Nosal, M, Wullschleger, SD and **Sun, G.** 2007. Interactive effects of ozone and climate on tree growth and water use in a southern Appalachian forest in the USA. *New Phytol* **174**: 109–124. DOI: https://doi.org/10.1111/j.1469-8137.2007.02018.x

Mills, G, Buse, A, Gimeno, B, Bemejo, V, Holland, M, et al. 2007a. A synthesis of AOT40-based response functions and critical levels of ozone for agricultural and horticultural crops. *Atmos Environ* **41**: 2630–2643. DOI: https://doi.org/10.1016/j.atmosenv.2006.11.016

Mills, G and **Harmens, H.** 2011. Ozone pollution: A hidden threat to food security. *Centre for Ecology & Hydrogogy*. Bangor, UK. ISBN: 978-1-906698-27-0. http://icpvegetation.ceh.ac.uk/. Accessed 30 October, 2017.

Mills, G, Hayes, F, Jones, MLM and **Cinderby, S.** 2007b. Identifying ozone-sensitive communities of (semi-) natural vegetation suitable for mapping exceedance

of critical levels. *Environ Pollut* **146**: 736–743. DOI: https://doi.org/10.1016/j.envpol.2006.04.005

Mills, G, Hayes, F, Simpson, D, Emberson, L, Norris, D, et al. 2011a. Evidence of widespread effects of ozone on crops and (semi-) natural vegetation in Europe (1990–2006) in relation to AOT40-and flux-based risk maps. *Global Change Biol* **17**: 592–613. DOI: https://doi.org/10.1111/j.1365-2486.2010.02217.x

Mills, G, Pleijel, H, Braun, S, Büker, P, Bermejo, V, et al. 2011b. New stomatal flux-based critical levels for ozone effects on vegetation. *Atmos Environ* **45**: 5064–5068. DOI: https://doi.org/10.1016/j.atmosenv.2011.06.009

Mills, G, Sharps, K, Simpson, D, Pleijel, H, Broberg, M, et al. 2018. Ozone pollution will compromise efforts to increase global wheat production. *Global Change Biology*. https://onlinelibrary.wiley.com/doi/10.1111/gcb.14157.

Mills, G, Sharps, K, Simpson, D, Pleijel, H, Frei, M, et al. Submitted. Closing the global ozone yield gap: Quantification and co-benefits for multi-stress tolerance. *Submitted to Global Change Biology*.

Mills, G, Wagg, S and **Harmens, H.** 2013. Ozone pollution: Impacts on ecosystem services and biodiversity. ICP Vegetation Programme Coordination Centre, CEH, Bangor, UK. ISBN: 978-1-906698-39-3. http://icpvegetation.ceh.ac.uk/. Accessed 30 October, 2017.

Monks, PS, Archibald, AT, Colette, A, Cooper, O, Coyle, M, et al. 2015. Tropospheric ozone and its precursors from the urban to the global scale from air quality to short-lived climate forcer. *Atmos Chem Phys* **15**(15): 8889–8973. DOI: https://doi.org/10.5194/acp-15-8889-2015

Musselman, RC, Lefohn, AS, Massman, WJ and **Heath, RL.** 2006. A critical review and analysis of the use of exposure- and flux-based ozone indices for predicting vegetation effects. *Atmos Environ* **40**: 1869–1888. DOI: https://doi.org/10.1016/j.atmosenv.2005.10.064

MWCACP. USDA Major World Crop Areas and Climate Profiles. http://www.usda.gov/oce/weather/pubs/Other/MWCACP/index.htm. Accessed 1 June, 2015.

Osborne, SA, Mills, G, Hayes, F, Ainsworth, EA, Büker, P and **Emberson, L.** 2016. Has the sensitivity of soybean cultivars to ozone pollution increased with time? An analysis of published dose–response data. *Global Change Biol* **22**: 3097–3111. DOI: https://doi.org/10.1111/gcb.13318

Paoletti, E, De Marco, A, Beddows, DCS, Harrison, RM and **Manning, WJ.** 2014. Ozone levels in European and USA cities are increasing more than at rural sites, while peak values are decreasing. *Environ Pollut* **192**: 295–299. DOI: https://doi.org/10.1016/j.envpol.2014.04.040

Pleijel, H. 2011. Reduced ozone by air filtration consistently improved grain yield in wheat. *Environ Pollut* **159**: 897–902. DOI: https://doi.org/10.1016/j.envpol.2010.12.020

Pleijel, H, Broberg, MC, Uddling, J and **Mills, G.** 2018. Current surface ozone concentrations significantly decrease wheat growth, yield and quality. *Sci Total Environ* **613–614**: 687–692. DOI: https://doi.org/10.1016/j.scitotenv.2017.09.111

Pleijel, H, Danielsson, H, Emberson, L, Ashmore, M and **Mills, G.** 2007. Ozone risk assessment for agricultural crops in Europe: Further development of stomatal flux and flux–response relationships for European wheat and potato. *Atmos Environ* **4**: 3022–3040. DOI: https://doi.org/10.1016/j.atmosenv.2006.12.002

Pleijel, H, Wallin, G, Karlsson, P, Skärby, L and **Selldén, G.** 1995. Gradients of ozone at a forest site and over a field crop – consequences for the AOT40 concept of critical level. *Water Air Soil Poll* **85**: 2033–2038. DOI: https://doi.org/10.1007/BF01186133

R Core Team. 2018. R: A language and environment for statistical computing. R Foundation for Statistical Computing, Vienna, Austria. URL: https://www.R-project.org/.

REVIHAAP. 2013. Review of evidence on health aspects of air pollution – REVIHAAP Project technical report. World Health Organization (WHO) Regional Office for Europe. Bonn. Available at: http://www.euro.who.int/data/assets/pdf_file/0004/193108/REVIHAAP-Final-technical-report-final-version.pdf. Accessed on 30 October, 2017.

Sacks, WJ, Deryng, D, Foley, JA and **Ramankutty, N.** 2010. Crop planting dates: an analysis of global patterns. *Global Ecol Biogeogr* **19**: 607–620. DOI: https://doi.org/10.1111/j.1466-8238.2010.00551.x

Schultz, MG, Schröder, S, Lyapina, O, Cooper, O, Galbally, I, et al. 2017. Tropospheric Ozone Assessment Report: Database and metrics data of global surface ozone observations. *Elem Sci Anth*. DOI: https://doi.org/10.1525/elementa.244

Simon, H, Reff, A, Wells, B, Xing, J and **Frank, N.** 2015. Ozone trends across the United States over a period of decreasing NO_x and VOC emissions. *Environ. Sci. Technol.* **49**: 186–195. DOI: https://doi.org/10.1021/es504514z

Simpson, D, Benedictow, A, Berge, H, Bergström, R, Emberson, LD, et al. 2012. The EMEP MSC-W chemical transport model – technical description. *Atmos Chem Phys* **12**: 7825–7865. DOI: https://doi.org/10.5194/acp-12-7825-2012

Simpson, D, Emberson, L, Ashmore, M and **Tuovinen, J-P.** 2007. A comparison of two different approaches for mapping potential ozone damage to vegetation: A model study. *Environ Pollut* **146**: 715–725. DOI: https://doi.org/10.1016/j.envpol.2006.04.013

Sinha, B, Sangwan, KS, Maurya, Y, Kumar, V, Sarka, C, et al. 2015. Assessment of crop yield losses in Punjab and Haryana using two years of continuous in-situ ozone measurements. *Atmos Chem Phys* **15**: 9555–9576. DOI: https://doi.org/10.5194/acp-15-9555-2015

Sitch, S, Cox, PM, Collins, WJ and **Huntingford, C.** 2007. Indirect radiative forcing of climate change through

ozone effects on the land-carbon sink. *Nature* **448**: 791–794. DOI: https://doi.org/10.1038/nature06059

Smith, G. 2012. Ambient ozone injury to forest plants in Northeast and North Central USA: 16 years of biomonitoring. *Environ Monit Assess* **184**: 4049–4065. DOI: https://doi.org/10.1007/s10661-011-2243-z

Sofiev, M and **Tuovinen, J-P.** 2001. Factors determining the robustness of AOT40 and other ozone exposure indices. *Atmos Environ* **35**: 3521–3528. DOI: https://doi.org/10.1016/S1352-2310(01)00086-3

Soja, G, Barnes, JD, Posch, M, Vandermeiren, K, **Pleijel, H,** et al. 2000. Phenological weighting of ozone exposures in the calculation of critical levels for wheat, bean and plantain. *Environ Pollut* **109**: 517–524. DOI: https://doi.org/10.1016/S0269-7491(00)00055-5

Sun, G, McLaughlin, SB, Porter, JH, Uddling, J, Mulholland, PJ, et al. 2012. Interactive influences of ozone and climate on streamflow of forested watersheds. *Global Change Biol* **18**: 3395–3409. DOI: https://doi.org/10.1111/j.1365-2486.2012.02787.x

Tang, H, Takigawa, M, Liu, G, Zhu, J and **Kobayashi, K.** 2013. A projection of ozone-induced wheat production loss in China and India for the years 2000 and 2020 with exposure-based and flux-based approaches. *Global Change Biol* **19**: 2739–2752. DOI: https://doi.org/10.1111/gcb.12252

TOAR-Climate. See Gaudel, et al. 2017.

TOAR-Health. See Fleming, et al. 2017.

TOAR-Metrics. See Lefohn, et al. 2017.

TOAR-Surface Ozone Database. See Schultz, et al. 2017.

US EPA. 2013. Integrated Science Assessment of Ozone and Related Photochemical Oxidants (Final Report). EPA/600/R-10/076F. Research Triangle Park, NC: Environmental Protection Agency. Available at: https://cfpub.epa.gov/ncea/isa/recordisplay.cfm?deid=247492 (accessed on 30 October 2017).

US Federal Register. 2015. National Ambient Air Quality Standards for Ozone, 40 CFR Part 50, 51, 52, 53, and 58, 65292–65468.

Van Dingenen, R, Dentener, FJ, Raes, F, Krol, MC, Emberson, L, et al. 2009. The global impact of ozone on agricultural crop yields under current and future air quality legislation. *Atmos Environ* **43**: 604–618. DOI: https://doi.org/10.1016/j.atmosenv.2008.10.033

Watanabe, M, Hoshika, Y, Koike, T and **Izuta, T.** 2016. Effects of ozone on Japanese trees. In: *"Air Pollution Impacts on Plants in East Asia"*, Izuta, T (ed.), 57–72. Springer. ISBN: 978-4-431-56436-2. DOI: https://doi.org/10.1007/978-4-431-56438-6

Wild, O, Fiore, AM, Shindell, DT, Doherty, RM, Collins, WJ, et al. 2012. Modelling future changes in surface ozone: a parameterized approach. *Atmos Chem Phys* **12**: 2037–2054. DOI: https://doi.org/10.5194/acp-12-2037-2012

Wittig, VE, Ainsworth, EA, Naidu, SL, Karnosky, DF and **Long, SP.** 2009. Quantifying the impact of current and future tropospheric ozone on tree biomass, growth, physiology and biochemistry: a quantitative meta-analysis. *Global Change Biol* **15**: 396–424. DOI: https://doi.org/10.1111/j.1365-2486.2008.01774.x

Xu, YS, Shang, B, Yuan, XY, Feng, ZZ and **Calatayud, V.** 2017. Relationships of CO_2 assimilation rates with exposure- and flux-based O_3 metrics in three urban tree species. *Sci Total Environ,* 613–614; 233–239. DOI: https://doi.org/10.1016/j.scitotenv.2017.09.058

Yonekura, T and **Izuta, T.** 2016. Effects of ozone on Japanese agricultural crops. In: *"Air Pollution Impacts on Plants in East Asia"*, Izuta, T (ed.), 57–72. Springer. ISBN: 978-4-431-56436-2. DOI: https://doi.org/10.1007/978-4-431-56438-6

Young, PJ, Archibald, AT, Bowman, KW, Lamarque, J-F, Naik, V, et al. 2013. Pre-industrial to end 21st century projections of tropospheric ozone from the Atmospheric Chemistry and Climate Model Intercomparison Project (ACCMIP). *Atmos Chem Phys* **13**: 2063–2090.

Yue, X and **Unger, N.** 2014. Ozone vegetation damage effects on gross primary productivity in the United States. *Atmos Chem Phys* **14**: 9137–9153. DOI: https://doi.org/10.5194/acp-14-9137-2014

Zhang, Y, Cooper, OR, Gaudel, A, Thompson, AM and **Nédélec, P.** 2016. Tropospheric ozone change from 1980 to 2010 dominated by equatorward redistribution of emissions. *Nature Geoscience* **9**: 875–87s9.

How to cite this article: Mills, G, Pleijel, H, Malley, CS, Sinha, B, Cooper, OR, Schultz, MG, Neufeld, HS, Simpson, D, Sharps, K, Feng, Z, Gerosa, G, Harmens, H, Kobayashi, K, Saxena, P, Paoletti, E, Sinha, V and Xu, X. 2018. Tropospheric Ozone Assessment Report: Present-day tropospheric ozone distribution and trends relevant to vegetation. *Elem Sci Anth,* 6: 47. DOI: https://doi.org/10.1525/elementa.302

Domain Editor-in-Chief: Detlev Helmig, Ph.D., Institute of Alpine and Arctic Research, University of Colorado Boulder, US

Associate Editor: Alastair Lewis, National Centre for Atmospheric Science, University of York, UK

Knowledge Domain: Atmospheric Science

Part of an *Elementa* Special Feature: Tropospheric Ozone Assessment Report (TOAR): GLOBAL METRICS FOR CLIMATE CHANGE, HUMAN HEALTH AND CROP/ECOSYSTEM RESEARCH

Submitted: 15 January 2018 **Accepted:** 17 May 2018 **Published:** 28 June 2018

ELEMENTA Science of the Anthropocene

Elem Sci Anth is a peer-reviewed open access journal published by University of California Press.

OPEN ACCESS